THE CHARACTERIZATION AND SIGNIFICANCE OF THE COMPLEMENT SYSTEM ACTIVATED BY PHOTODYNAMIC THERAPY IN THE TREATMENT OF SOLID TUMORS

by

Ivana Katarina Cecic

B.Sc., The University of British Columbia, 1995
M.Sc., The University of British Columbia, 1999

A THESIS SUBMITTED IN PARTIAL FULFILMENT OF THE REQUIREMENTS

FOR THE DEGREE OF

DOCTOR OF PHILOSOPHY

in

THE FACULTY OF GRADUATE STUDIES
(Department of Pathology and Laboratory Medicine)

We accept this thesis as conforming to the required standard

THE UNIVERSITY OF BRITISH COLUMBIA
January, 2004

ABSTRACT

Photodynamic therapy (PDT) is approved by health agencies throughout the developed world for the treatment of a variety of diseases, and continues to gain recognition as a treatment for neoplastic lesions. During PDT a light-sensitive drug (photosensitizer) is excited locally in tissue with light of appropriate wavelength. The transfer of energy from the excited photosensitizer to molecular oxygen (O_2) results in the production of reactive oxygen species (ROS) that inflict damage to various cell components resulting in the disruption of tissue homeostasis. The aim of this project was to ascertain whether the complement (C) system is engaged in a PDT-treated solid tumor and if this plays a role in overall tumor response to treatment. The following summarizes the findings of this dissertation.

C activation in response to PDT-inflicted tumor injury proceeds via the antibody-independent alternative pathway and results in significantly elevated levels of the fluid phase C protein C3 in both serum and Lewis lung carcinoma tumors. Other indications of C activity are the presence of the C3 breakdown fragment C3b and assembly of the membrane-inserted complex containing proteins C5b through C9.

In mice bearing PDT-treated EMT6 tumors, a multitude of signals are released from the treated lesion into circulation to promote immune cell trafficking. Although a variety of inflammatory mediators such as IL-1β, IL-6, TNF-α, and histamine promote neutrophilia in mice following PDT the most significant effect was demonstrated by C. Blocking C activity prior to PDT also resulted in a significant decrease in tumor cures.

A C3 knockout model (C3 k.o.) was employed to address the impact of the loss of C function on the long-term control of Lewis lung carcinoma tumors by PDT. Results suggest that the relevance of C activity may depend on the mechanism of action of the photosensitizer of choice and subsequent levels of tumor oxygen during light activation. Enhanced tumor O_2 levels during treatment theoretically increased the probability of ROS production.

Understanding the mechanism of how the C system responds to PDT-induced injury could lead to methods of improving the overall therapeutic benefit of treatment and gain wider acceptance for clinical applications.

TABLE OF CONTENTS

LIST OF TABLES

LIST OF FIGURES

ACKNOWLEDGMENTS

I dedicate this thesis to all those who were involved from the inception of my very first experiment. I thank the members of the departments of Cancer Imaging, Medical Biophysics, and Advanced Therapeutics at the BC Cancer Research Centre, for their friendship and support in particular to Ms. Denise McDougal for flow cytometry assistance. It was a pleasure to have had the opportunity to work with Dr. Katherine Serrano and Dr. Maria Issa of the Devine Lab at UBC whose guidance and enthusiasm will always be appreciated. Thanks to Dr.Van Niekirk at the BC Cancer Agency for assistance in digital imaging. Members of my supervisory committee were beacons of advice, support, and encouragement. My supervisor Dr. Korbelik has taught me the virtue of perseverance and devotion to the pursuit of science. Thank you for your trust and confidence. To my family and dearest friends, your unconditional love and support I will treasure in my heart always.

The work in this thesis was supported by the Michael Smith Foundation for Health Research.

ABBREVIATIONS

AA	Arachidonic acid
ALA	Aminolevulinic acid
AMD	Age-related macular degeneration
ATP	Adenosine triphosphate
BCG	Bacillus Calmette-Geurin
BPD	Benzoporphyrin derivative monoacid ring A
Ca	Calcium
CO_2	Carbon dioxide
CTL	Cytotoxic T cell
CVF	Cobra venom factor
D_5W	5% dextrose in water
DAB	diaminobenzidine substrate
DPBS	Dulbecco's phosphate buffered saline
EDTA	Ethylenediaminetetraacetic acid
EGTA	Ethylene glycol-bis(2-aminoethyl)-N,N,N',N'-tetraacetic acid
ELISA	Enzyme-linked immunosorbent assay
FBS	Fetal bovine serum
FITC	Fluorescein isothiocyanate
TNFα	Tumor necrosis factor alpha
G-CSF	Granulocyte colony stimulating factor
H_2O_2	Hydrogen peroxide
H_2SO_4	Sulphuric acid
HBSS	Hanks buffered saline solution
HpD	Hematoporphyrin derivative
HUVEC	Human umbilical vein endothelial cells
IgG	Immunoglobulin G
IL-1β	Interleukin-1 beta
IL-2	Interleukin-2
IL-6	Interleukin-6
IL-10	Interleukin-10
INF-α	Interferon alpha
INF-γ	Interferon gamma
i.p.	intra-peritoneum
I/R	Ischemia reperfusion
i.v.	intravenous
HSP70	Heat shock protein 70
ICAM-1	Intracellular adhesion molecule –1
LLC	Lewis lung carcinoma
MAC	Membrane attack complex
MCP-1	Monocyte chemotactic protein 1
mCRP	Membrane-bound complement regulatory protein
MEM	Minimal essential medium

Mg	Magnesium
$MgCl_2$	Magnesium chloride
MHC	Major histocompatibility complex
mTHPC	Tetrametahydroxyphenyl chlorine
N_2	Nitrogen
NAAGA	N-acetyl-L-aspartyl glutamic acid
NaN_3	sodium azide
Na_4EDTA	Tetrasodium ethylenediaminetetraacetic acid
NFκb	Nuclear factor kappa b
NH_4Cl	Ammonium chloride
NK	Natural killer cell
OPD	o-Phenylenediamine
PAF	Platelet activating factor
PARP	Poly ADP-ribose polymerase
PBS	Phosphate-buffered saline
PDT	Photodynamic therapy
PE	phycoerythrin
pO_2	partial pressure of oxygen
ROS	Reactive oxygen species
SCCVII	Squamous cell carcinoma VII
SDS	Sodium dodecyl sulphate
SEM	Standard error of the mean
SPG	schizophyllan
TAM	Tumor-associated macrophages
$TPPS_{2a}$	Tetraphenylporphine sulfonate
XO	xanthine oxidase
Z-DEVD	Z-Asp(OME)-Glu(OME)-Val-Asp(OME)

GENERAL INTRODUCTION TO PHOTODYNAMIC THERAPY

Photodynamic therapy (PDT) involves three key components to induce cell death: the administration of a photosensitive drug, light of appropriate wavelength, and molecular oxygen [Dougherty *et al*, 1998]. Following selective retention of drug in cancerous tissue, the tumor is illuminated with light of appropriate tissue-penetrating wavelength for absorption by the respective sensitizer used. Upon absorption of light, the photosensitizer, now in an excited, triplet state, can undergo two types of reactions designated as Type I and Type II photosensitization [Henderson and Dougherty, 1992; Oleinick, 1998]. The Type I reaction occurs when the activated drug reacts directly with a substrate by a mechanism involving hydrogen or electron transfer to form radicals which, in the presence of oxygen, can form oxygenated products. The Type II reaction results in the formation of singlet oxygen ($^1O_2$) by the transfer of energy from the excited triplet state of the drug to molecular oxygen, resulting in electron rearrangement. Singlet oxygen can then react with substrates causing oxidative damage to cell components such as plasma membranes, lysosomes, and mitochondria. The Type II reaction is generally accepted to predominate in PDT with singlet oxygen acting as the major oxidant formed inducing tumor cell death by oxidative damage to various cell components.

I. History of PDT

PDT is a modality in use for the treatment of a variety of both oncological and non-oncological diseases. Documentation for the practice of combining light and photosensitive dyes for medicinal use can be traced back several thousand years. In the ancient cultures of India and Egypt, the skin condition vitiligo was treated using a combination of plants, carrying light-sensitive properties, and sunlight [Pathak MA *et al*, 1974]. Photochemical sensitization with the intent to induce cell death was found during the time of ancient Greece when the Greek scholar Herodotus described the healing power of light [Daniel MD *et al*, 1991]. The development of modern-day PDT was inspired by the graduate studies of Raab, from the turn of the 20^{th} century [Raab, 1900]. Raab noted that certain wavelengths of light were lethal to *Paramecia* exposed to acridine and other dyes. Use of PDT for the treatment of neoplastic lesions followed. In 1903, Von Tappeiner and Jesionek reported treating skin cancer by combining eosin and light [Jesionek, 1903].

To date, the most explored group of dyes is the porphyrins. In 1913, Meyer-Betz investigated the accumulation of hematoporphyrin in rat tumors and PDT effects following systemic administration of the drug [Meyer-Betz, 1913]. Later, Lipson and Baldes established that an impurity of hematoporphyrin localizes in tumors and not the parent compound [Lipson RL and Baldes EJ, 1960]. These findings led to the preparation of hematoporphyrin derivative (HpD), a mixture of porphyrin monomers, dimers and oligomers, produced by the acid treatment of hematoporphyrin.

An expansion of studies and applications of PDT began in the 1970s and-80s initiated by Dougherty and co-workers , who began to study the use of HpD in combination with light for the treatment of different animal neoplastic lesions [Dougherty, 1974, 1975, 1978, 1984, 1987]. This work instigated the development of the most widely used photosensitizer to date, Photofrin, with the approval of Photofrin-based PDT for clinical use in 1993.

II. Clinical applications of PDT

The effectiveness of PDT depends on numerous parameters including drug and light dose administered, the mode of light delivery, and the depth of light penetration, combinations of which differ according to the type and site of disease. With advances in the design of light delivery systems PDT has been applied to virtually all sites in/on a body. State approval has been gained for the use of Photofrin-mediated PDT in the treatment of early- and late-stage endobronchial non-small-cell lung cancer in patients who cannot tolerate surgery or radiotherapy due to poor cardiopulmonary function or multifocal cancer [Dougherty 2002; Lam *et al*, 1998; Pass HI, 1992]. In addition, Photofrin-mediated PDT has been approved for palliative treatment of advanced cancer of the esophagus, if the esophagus is totally or partially obstructed and the lesions are unsuitable for thermal laser therapy [Dougherty 2002; Lam *et al*, 1998; Pass HI, 1992]. In 2003 FDA approval was attained for treatment of high-grade dysplasia associated with Barrett's esophagus. Clinical trials at present include those for Photofrin-based PDT in the treatment of non-melanoma skin cancers, and in conjunction with surgery for brain

and intrathoracic tumors (pleural mesothelioma) [Biel M, 1998; Fan *et al*, 1997; Muller 1995, 1996; Popovic *et al*, 1996; Pass *et al*, 1994].

Basal and squamous cell carcinomas of skin, malignant melanomas, mycosis fungoides, recurrent metastatic breast carcinoma, and AIDS-related Kaposi's sarcoma, are among the numerous cutaneous and subcutaneous malignancies treated with Photofrin-based PDT to date [Dougherty, 1986; Santoro *et al*, 1990; Waldow, 1987]. Complete responses lasting up to 4 years with a response rate of 80% in managing basal cell carcinomas have been achieved.

PDT may play an important role as therapy for certain head and neck cancers. Long-term control of ear, lip, nose, and throat carcinoma *in situ* has been reported with a 70% response rate [Gluckman, 1986]. As of 1993 PDT has been effective in eradicating papillomas of an animal model, therefore, the treatment of laryngeal papillomatosis by PDT is being evaluated clinically [Shikowitz MJ *et al*, 1986].

Photofrin-based PDT was originally approved for palliative care to relieve suffering associated with endobronchial obstruction. In 1998, FDA approval was obtained for early-stage non-small cell lung cancer [Dougherty *et al*, 1998]. Photodynamic techniques have also been studied as potential devices for detecting small carcinomas (*in situ* lesions) or superficial lung tumors covering a large endobronchial area [Lam *et al*, 1990]. The treatment of advanced non-small cell lung cancer with PDT has been compared with ablation using Nd-YAG laser therapy alone [Dougherty *et al*, 1998]. In addition, encouraging results favoring the combined use of PDT plus radiotherapy versus radiotherapy alone for the opening of obstructed airways has been reported [Lam *et al*, 1991].

Clinical trials for the use of PDT in the treatment of gastrointestinal malignancies, colon cancer, and gynecologic and intra-abdominal malignancies are underway. Results are encouraging and suggest that PDT could be developed as palliation, an alternative to surgery, or an intraoperative procedure, respectively [Hayata *et al*, 1985, Barr *et al*, 1990, Rettenmaier *et al*, 1984, Sindelar *et al*, 1991]. Bladder tumors have been candidates for treatment by PDT although some side effects such as whole organ contraction and irritation have been reported [Nseyo *et al*, 1998]. However, advantages include that in murine and human cases the sensitizer is selectively retained in bladder tumors at higher levels compared to normal bladder tissue, decreasing the probability of normal tissue damage [Hisazumi *et al*, 1983]. Successful destruction of superficial transitional cell cancers not involving the muscularis using PDT have been documented [Benson *et al*, 1982].

Advantages of PDT over other standard cancer treatments such as chemotherapy and radiotherapy include that PDT does not induce resistance and is generally tolerated well by patients. Few unwanted side effects are associated with this treatment modality, with the exception of skin photosensitivity [Pass, 1993]. Quick recovery and cosmetic healing, thereby healing of normal tissue is favorable, and this therapy can be used where other more conventional therapies have failed [Fisher *et al*, 1995]. One disadvantage of PDT compared to radiotherapy is that the dosimetry for PDT is not as precise, but efforts toward improvement are underway.

III. Second-generation photosensitizers

All of the studies mentioned thus far have been conducted using the FDA approved Photofrin-based PDT. Other sensitizers referred to as "second generation" sensitizers have come on the scene with many encouraging results. Tin Etiopurpurin (SnET2) is in phase II trials for the treatment of cutaneous metastatic breast cancer and Kaposi's sarcoma [Razum, 1996]. Lutetium Texaphrin (Lu-tex) is in a phase II/III trial for skin lesions [Dougherty *et al*, 1998]. Problems can arise in applying PDT for the treatment of melanomas, since melanin absorbs light efficiently, however, exciting progress in the use of Lu-tex-based PDT against this disease has been documented [Woodburn *et al*, 1998]. Benzoporphyrin derivative mono-acid (BPD-MA), marketed as Verteporfin or Visudyne from QLT, Inc., is in ongoing trials for the treatment of skin cancer and psoriasis, but most recently received regulatory approval for use in the treatment of age-related macular degeneration (AMD) [Leung, 1994]. One main advantage of BPD-MA based PDT in the treatment of AMD over the use of thermal lasers for example, is that BPD-PDT avoids damage of overlying retina, and close to 50% of patients treated experience improved vision [Gragoudas *et al*, 1997]. The most potent sensitizer to date, tetrametahydroxyphenyl chlorin (mTHPC), shows promise in the treatment of head and neck cancers and also pancreatic cancers [Grosjean *et al*, 1993]. Lastly, aminolevulinic acid (ALA) is in use to treat a number of non-cancerous, pre-malignant, and malignant lesions. ALA does not act directly in PDT. In the mitochondria of tumor cells, ALA engages in the biosynthetic pathway for heme, leading to the production and accumulation of the photosensitizer protoporphyrin IX (precursor

of heme) which acts as the active photosensitizer [Hasan and Parrish, 1997; Gabeler *et al*, 2003]. Topical application of ALA followed by light illumination has been employed for treating human papilloma virus-associated skin diseases, acne vulgaris, epithelial tumors and basal cell carcinomas [Zeitouni *et al*, 2003]. ALA-PDT is favored by many clinicians since ALA can be topically applied to skin lesions eliminating generalized photosensitivity.

IV. Mechanism of PDT-induced cell death

PDT results in the production of singlet oxygen ($^1O_2$), a reactive non-radical oxygen species. $^1O_2$ has a short half-life (estimated to be 10^{-6} to 10^{-5} seconds) and a very short radius of action (<0.02 μm). $^1O_2$ can interact with target molecules either by transferring its excitation energy or by chemical combination, such as combining with fatty acids leading to lipid peroxidation [Hasan and Parrish, 1997; Ochsner, 1997]. Preferential targets for chemical reactions are double bonds such as those found in polyunsaturated fatty acids or guanine bases in DNA. Korbelik and Krosl [1994b] showed that direct killing of PDT occurs mostly on tumor cells near vessels. The authors concluded that the further cells are removed from vessels the less they are exposed to oxygen and cellular levels of sensitizer are far less.

Uptake of the photosensitizer by cells prior to light treatment is critical for effective PDT [Korbelik and Krosl, 1994b]. Photosensitizers are usually retained in neoplastic cells/tissue in amounts greater than in surrounding normal tissues, although the

ratio between tumor and peritumoral amounts are not very high [Bellnier *et al*, 1989; Ma *et al*, 1992; Tralau et al, 1990; Belliner and Henderson, 1992]. The mechanism by which this occurs is still being debated and may differ with different sensitizers. Since lipoproteins in blood are the major transporters of porphyrin-containing photosensitizers it has been proposed that low-density lipoproteins (LDL) are responsible for delivering such compounds to tumor cells [Barel *et al*, 1986; Jori, 1989; Kessel and Luo, 16; Maziere *et al*, 1991; Kessel, 1986b]. Porphyrin compounds that associate with LDL are taken up by cells via the apoB-E receptor, and this receptor-mediated uptake then targets LDL for lysosomal degradation [Goldstein and Brown, 1977]. One LDL receptor that has been shown to be critical in Photofrin-PDT killing of mouse tumor cells is the α-Macroglobulin Receptor/Low Density Lipoprotein Receptor [Luna *et al*, 1995]. This may enhance binding and entry of circulating lipoproteins carrying lipophilic porphyrins, such as BPD-MA [Allison *et al*, 1990]. The low pH environment in tumors may enhance tumor retention of hydrophobic photosensitizers that become more water-soluble as pH is decreased. Poor lymphatic drainage may result in the build-up of porphyrins in the interstitial space [Henderson and Dougherty, 1992]. Rapidly dividing tumor cells may have an increased ability to phagocytose porphyrin aggregates [Hasan and Parrish, 1997]. Recent studies indicate that stromal elements of a tumor retain photosensitizer more selectively than do malignant cells. Korbelik and Krosl [1996] showed that tumor-associated macrophages (TAM) collect a large amount of photosensitizer within malignant tissue. Interestingly, the cellular content of experimental tumors can contain up to 80% TAM and human tumors comprise 20-50% [Milas *et al*, 1987].

Specific cellular localization varies among photosensitizers, depending on their lipophilic or hydrophobic nature. To date it is well accepted that most sensitizers do not accumulate in nuclei, minimizing the potential for DNA damage and/or mutations to occur. Some damage to DNA has been reported including strand breaks and chromosomal aberrations, however recovery can occur, suggesting that this effect may not be lethal [Oleinick and Evans, 1998; Evenson and Moan, 1982]. Damage can be targeted to various sites in a cell such as plasma membrane, lysosomes, and/or mitochondria, depending on the localization of the drug thereby initiating different forms of cell injury and death [Dougherty *et al*, 1998; Berg and Moan, 1994].

Damage by HpD-based PDT for example seems to concentrate to the plasma membrane [Christensen *et al*, 1985]. Porphyrin uptake begins with binding at the level of plasma membrane then migrates with time to other cellular components [Kessel, 1986]. Many reports have described the damage induced by PDT on plasma membranes. Observations include swelling, bleb formations, shedding of vesicles containing plasma membrane marker enzymes, cytosol and lysosomal enzymes [Moan *et al*, 1979; Volden *et al*, 1981]. Membrane transport is also affected. There is a reduction of active transport, depolarization, and increased permeability to lactate dehydrogenase [Moan *et al*, 1983; Specht and Rodgers, 1990; Moan and Christensen, 1981, Henderson and Donovan, 1989]. Other effects include inhibition of the activity of numerous plasma membrane enzymes, up- and down-regulation of surface antigens, and lipid peroxidation [Ocshner, 1997; Joshi *et al*, 1994; Davies *et al*, 1986; Thomas and Girotti, 1989]. The cumulative effect is a halt in cell division, followed by cell lysis [Pass, 1993].

PDT damage can be inflicted on membranes of mitochondria, Golgi apparatus, lysosomes, and the endoplasmic reticulum. Aggregated and also hydrophobic sensitizers, such as $TPPS_{2a}$, are likely to enter a cell by pinocytosis and endocytosis thereby accumulating in lysosomes and endosomes [Dougherty *et al*, 1998]. Membrane permeability of these vesicles increases upon light exposure, resulting in the release of hydrolytic enzymes into the cytosol [Berg and Moan, 1994]. Photofrin and ALA-derived protoporphyrin localize in mitochondria. Characteristics of PDT damage to these organelles has been described as aberrations in functional oxidative phosphorylation and electron transport chain activity, in addition to a decrease in cellular adenosine triphosphate (ATP) levels [Hilf *et al*, 1994; Hilf *et al*, 1996]. In cells that have accumulated these photosensitizers in mitochondria, photo-illumination initiates a rapid release of cytochrome c into the cytoplasm. Cytochrome c migrates toward the nucleus where it binds with the transcription factor APAF-1 activating caspases, driving the process of cell death by apoptosis [Oleinick, 1998]. Furthermore, mitochondrial damage induced by singlet oxygen that leads to apoptosis has been shown to be mediated by oxidation of Bcl-2 [Xue *et al*, 2001; Kessel and Castelli, 2001].

V. Secondary effects of PDT

It is generally described that the anti-tumor effect of PDT combines both direct and indirect cell death [Dougherty *et al*, 1998; Korbelik, 1996]. The direct lethal effect is a result of irreparable photooxidative injury of vital cellular structures, damaging parenchymal neoplastic cells, host immune cell populations, vessels, and extracellular

matrix. The indirect killing of cancer cells results from a series of events following initial phototoxicity. Collapsed vasculature starves a tumor of oxygen supply and nutrients, and the host immune response is initiated against a PDT-treated tumor. The complex interplay of secondary anti-tumor effects induced by PDT is dominated by three major responses: the breakdown of tumor vasculature, an inflammatory reaction, and an immune response. The induction of a strong, acute inflammatory response is in part mediated by the combined local release of histamine and serotonin, as well as lipid degradation products, and metabolites of arachidonic acid from photooxidative lesions of lipids [Fingar, 1996]. A series of events that lead up to secondary cell kill include ischemic death from PDT-mediated vascular damage and blood flow stasis, ischemia-reperfusion injury, cell death mediated by resident and infiltrating cells (namely neutrophils), and a tumor specific immune reaction [Korbelik and Cecic, 1998, 2002].

Knowledge gained in describing the host immune response to PDT-induced tumor cell death has led to the development of cancer vaccines using photodynamic therapy as a vaccine preparation. Korbelik [1996] has shown that T-cell mediated tumor-specific immune memory can be induced by PDT. Based on these findings, research has led to the use of generating cancer vaccines using PDT categorized in two sub-types, PDT-treated cell lysates or whole-cell vaccines [Gollnick *et al*, 2002; Korbelik and Sun, 2003]. By administering these PDT-generated cancer vaccines, protection against tumor re-challenge or significant slowdown in tumor growth rate os murine tumor systems is significantly better compared to vaccines prepared by UV, gamma-irradiation or freeze-thaw generated cell lysates.

The compilation of data comprising this thesis continues to shed light on the PDT-induced host response with particular focus on the impact of the complement system in mediating PDT-induced inflammation. Furthermore, it has become increasingly clear that neutrophil chemotaxis and activation in the realm of PDT rely on the activity of the complement system. The following work leads to a description of the activation of the complement system in the response of tumors to PDT and that complement activation significantly affects the anti-cancer activity of PDT.

HYPOTHESIS

Photodynamic therapy (PDT) applied in the treatment of solid tumors induces an acute inflammatory reaction initiated and driven by systemic and tumor-localized complement activation. The activated complement system participates in the events that determine the efficacy of PDT-mediated eradication of solid tumors.

SPECIFIC AIMS

1. Define the pro-inflammatory signals that specifically mediate the rise in circulating neutrophil numbers in response to PDT applied in the treatment of solid tumors, and the role of complement in this phenomenon.

2. Characterize complement activation following PDT-treatment *in vitro* and *in vivo*.

3. Investigate the impact of complement activation on the effectiveness of PDT against tumors growing in complement-proficient and complement-deficient mice.

Chapter 1

Complement is a key mediator of PDT-induced neutrophil sequestration

1.1 INTRODUCTION

1.1.1 PDT-INDUCED INFLAMMATION

PDT applied in the treatment of cancer results in direct tumor cell cytotoxicity, damage to tissue microvasculature, and engagement of a host immune response. The significance of vascular damage and amplification of an immune response in overall tumor cures was demonstrated in a clonogenicity assay in which no difference was observed between tumor cells isolated immediately after light treatment and those isolated from untreated controls [Henderson *et al*, 1985]. However, if tumors were excised between two and twenty-four hours following treatment a significant drop in tumor cell survival was documented. The authors therefore concluded that tumor cytotoxicity was a result of what has now been characterized as secondary mechanisms, not direct tumor cytotoxicity by the photodynamic process.

Damage inflicted on tumors by photodynamic therapy results in the production and release of a multitude of pro-inflammatory signals. Inflammation is described as the response to infection or physical injury that has evolved to eliminate microorganisms and promote repair of damaged tissue. Four classical signs of inflammation include redness and heat which occur as a response to vascular dilatation, swelling due to increased vascular permeability to plasma and leukocytes, and also pain [Janeway and Travers, 1996]. The inflammatory process is potentially dangerous since it can cause indiscriminate damage to tissues. Cells and plasma proteins that are potentially the source of injury normally exist in a quiescent, non-active state. However, at the site of an

inciting stimulus, such as PDT-induced damage, the inflammatory process is initiated with local activation of inflammatory cells and plasma proteins creating a pro-inflammatory environment. Increased vascular permeability, for example, allows plasma proteins, such as those of the complement system, that are precursors of inflammatory mediators to leak out into tissues, where they become activated locally by proteolytic cleavage. By the same token, leukocytes are quiescent until they encounter mediators at a site of inflammation that then prime them and/or activate them for a variety of functions such as enhanced phagocytic activity and killing.

The induction of pro-inflammatory damage triggers an almost instantaneous release of various chemotactic factors that promote, along a path of their increasing concentration, the migration of inflammatory cells from the bloodstream to an inflamed site. Neutrophils are the first cells engaged in an inflammatory response and their chemotaxis is mediated by a multitude of pro-inflammatory mediators [Janeway and Travers, 1996; Warren *et al*, 1990; Lehrer et al, 1988]. Among these mediators are components of the complement system, acute phase proteins, proteinases, peroxidases, radicals, leukocyte chemoattractants, cytokines, growth factors, and other immune regulators [Ochsner, 1997; Fingar, 1996]. Vasoactive agents released include eicosanoids, clotting factors, and histamine [Ben-Hur *et al*, 1988; Fingar *et al*, 1990; Henderson and Donovan, 1989; Kerdel *et al*, 1987; Evans *et al*, 1990]. The main cytokine mediating the acute phase response is interleukin (IL)-6 and it has been shown that IL-6 levels rise in EMT6 tumor bed and also in spleens following Photofrin-based PDT [Gollnick *et al*, 1997; Gollnick *et al*, 2003]. In addition to IL-6, PDT induces the production of the cytokines IL-1beta (β), IL-2, tumor necrosis factor alpha (TNF-α), G-

CSF, and the chemokines, MIP-1α and KC. In an attempt to maintain homeostasis, the immune suppressing cytokine IL-10 is expressed in normal tissues, such as skin, following PDT; however, tumor IL-10 levels decrease following PDT [Gollnick *et al*, 1997; Gollnick *et al*, 2001]. Increased macrophage activity was demonstrated following PDT *in vitro* and *in vivo* [Yamamoto *et al*, 1991; Krosl and Korbelik, 1995]. It was also reported that activated macrophages release TNF-α following PDT treatment [Evans *et al*, 1990], and preferentially destroy PDT-treated tumor cell targets [Korbelik and Krosl, 1994a]. The underlying molecular biology behind the expression of most cytokines following PDT is the involvement of transcription factors, such as AP-1 and NF-κb. Cell surface and organelle membrane changes instigated by PDT trigger intracellular signaling pathways that activate the aforementioned transcription factors, leading to the production of various pro-inflammatory cytokines [Kick *et al*, 1995; Ryter and Gomer, 1993]. Heightened expression of stress proteins and early response genes, activation of genes regulating the process of apoptotic cell death, and up-regulation of some cytokine genes has been documented [Gomer *et al*, 1996; Agarwal *et al*, 1993]. Increasing evidence collected in the Korbelik lab strongly suggests that PDT-induced expression of the stress protein HSP70 may participate in the development of the PDT-induced inflammatory/immune responses manifested by this therapy (unpublished), in particular deposition of complement proteins on PDT-treated cells/tissue.

Plasma membrane alterations prompt a rapid activation of membranous phospholipases with the release of products of phospholipid degradation such as arachidonic acid (AA) metabolites. In addition, the endothelial wall contracts with rearrangement of cytoskeletal structure and a loss in tight junctions between cells

[Wieman *et al*, 1991; Nelson *et al*, 1987]. Cell rounding and exposure of the basement membrane with an increase in the expression of adhesion molecules, promotes neutrophil and platelet attachment. This leads to progressive impairment of vascular function and a massive release of various inflammatory mediators from all of these activated and damaged cells [Dellian *et al*, 1995; Fingar, 1996]. Conditions favoring platelet aggregation appear with the release of clotting factors such as von Willebrand factor [Fingar, 1996]. Activated platelets can in turn release the eicosanoid thromboxane to promote aggregation that leads to vessel plugging through accelerated thrombus formation [Fingar, 1996]. Activated mast cells infiltrating a PDT-treated tumor provide a source of histamine and serotonin [Dellian *et al*, 1995]. Changes in the tumor microenvironment induced by PDT such as vessel damage, infiltration of inflammatory cells and plasma proteins, lead to the production and release of multiple sources of pro-inflammatory mediators that create a feedback loop amplifying the immune response. A main focus of our lab has been to characterize the role of neutrophils in the response of solid tumors to PDT and this is discussed in the following section.

1.1.2 PDT-induced neutrophilia and the significance of neutrophils in the outcome of PDT

Release of inflammatory signaling outlined above during and following PDT ensures the recruitment and sequestration of neutrophils in PDT-treated solid tumors [Krosl *et al*, 1995; Gollnick *et al*, 1997; Cecic *et al*, 2001, Sun *et al*, 2002]. Neutrophils are recruited from bone marrow stores and, speculatively, through de-marginalization of

lung, liver and general vasculature storage pools [Cecic *et al*, 2001; Appendix]. The influx of immune cells into PDT-treated tumors is led by neutrophils (followed by mast cells and monocytes/macrophages) and paralleled by a rise in the number of neutrophils in systemic circulation, namely neutrophilia. In response to PDT applied in the treatment of experimental murine tumor models, we documented that a neutrophilia is maintained for at least 10 hours, values corrected for the non-specific response that would occur in the absence of photosensitizer [Cecic *et al*, 2001]. Neutrophils play a pivotal role in mediating tumor cures by PDT, demonstrated in studies where neutrophil depletion or inhibition of their activity was shown to have a negative impact on the outcome of this therapy [Cecic *et al*, 2001; Korbelik and Cecic, 1999; de Vree *et al*, 1997, 1996].

The significance of neutrophil accumulation and their contribution to PDT-mediated tumor cure rates has been described as indispensable for the curative effect of treatment. Neutrophil activation in PDT-treated tumors may partly be compared to ischemia-reperfusion (I/R) injury reported for renal or myocardial I/R injury [Hernandez *et al*, 1987]. Up-regulated levels of adhesion molecules expressed on the vessels of these tissues promote neutrophil aggregation contributing to blood flow stasis, releasing mediators that promote platelet aggregation and subsequently starving the tissue of oxygen and nutrients [de Vree *et al*, 1996a]. Activated neutrophils release a combination of toxic oxygen radicals, pro-inflammatory factors, and proteolytic enzymes, inflicting damage that prolongs and amplifies tissue-localized inflammation [Malech and Gallin, 1988; Weiss, 1989]. The release of pro-inflammatory mediators from PDT-treated tumors into the circulation leads to elevated circulating neutrophil numbers. This chapter describes the mediators involved in promoting PDT-specific neutrophilia and begins to

unravel the importance of the complement system in this phenomenon. Details of the complement system are described in detail in Chapter Two of this thesis.

1.2 MATERIALS AND METHODS

All plastics and glassware were obtained from VWR Canlab, Missisauga, Canada, unless otherwise specified. All chemicals and media obtained from Sigma Chemical Co., St. Louis, USA, unless otherwise specified.

1.2.1 Tumor models

Murine EMT6 mammary sarcoma [Rockwell *et al*, 1972] and FsaR fibrosarcoma [Volpe *et al*, 1985] tumor cell lines were grown in culture conditions as follows: alpha-MEM media supplemented with 10% fetal calf serum (HyClone Laboratories Inc., Logan, USA) and streptomycin/penicillin, adhering to the bottom of T80cm^2 tissue culture flasks, then incubated at 37°C, 5% CO_2, and 95% humidity. Once confluent, 1X trypsin-EDTA (ethylenediaminetetraacetic acid) solution was added to a monolayer of cells to promote detachment. The cells were then suspended in complete medium (to neutralize the trypsin solution), washed once using 600-rpm centrifugation, and re-suspended in serum-free alpha-MEM prior to subcutaneous inoculation. The lower dorsal regions of female Balb/c, SCID, or C3H/HeN mice, including C3H/HeN mice whose adrenal glands were surgically removed (Adrex, Charles River), were prepared for tumor cell inoculation by first shaving with animal clippers then depilating using a depilatory cream. A concentration of one million EMT6 or FsaR cells in 30 μL alpha-MEM was prepared and inoculated subcutaneously onto the depilated backs (EMT6) or left leg (FsaR) of un-anesthetized mice restrained in a cone

holder. The tumors were allowed to form during a period of 7-8 days, or until they reached 7-8mm in largest diameter, at which time they were used in all experiments.

The Lewis lung carcinoma tumor model (LLC) [Sugiura and Stock, 1955] was grown on the depilated backs of C57BL/6 or the C3 knockout B6.129S6-*Cybb*^{tm1} mice (Jackson Laboratory, USA) of the C57BL/6 background strain. LLC was maintained *in vivo* by biweekly intramuscular brei inoculation. Mice were sacrificed by CO_2 inhalation and the tumors removed from both hind legs, and minced using two #22 scalpel blades. Subsequently, the tumor tissue was repeatedly passed through two 20-gauge needles, and diluted 5 times in phosphate buffered saline (PBS). 0.1 mL of tumor brei was inoculated into the thigh muscles of anesthetized mice. For experiments, the tumor was removed using aseptic technique, chopped using #22 scalpel blades, suspended in 5 mL of PBS and enzymatically digested with gentle rotation at 37°C for 20 minutes. The three enzyme cocktail used for disaggregation contained: DNase (type I) 0.6 mg/ml, collagenase (type IV) 0.24 mg/ml and dispase (Boerhinger, Mannheim, Germany) 0.18 mg/ml, diluted in 5 ml of cold PBS. The enzymes were added to the tumor just prior to incubation. The tumor cell suspension was then filtered through a 100 μm nylon mesh filter using a 6 cc syringe, and centrifuged at 600 rpm, then suspended in PBS. Cell concentration was determined by hemacytometer count. For experiments, 2 x 10^6 cells suspended in serum-free media was inoculated subcutaneously on the depilated backs of mice using a 26-gauge needle.

Mice used in our studies were either all male or all female and age-matched. At the start of all experiments, mice were at least 6 weeks of age at the time of subcutaneous tumor cell

inoculation. All animals were housed in the joint animal facility at the B.C. Cancer Research Centre where they were supplied with food and water *ad libitum.*

All animal protocols were approved by the Animal Ethics Committee of the University of British Columbia, Vancouver, Canada.

1.2.2 Photodynamic therapy

Photofrin® (porfimer sodium), supplied by Axcan Pharma Inc. (Mont-Saint-Hilaire, Quebec, Canada), was reconstituted in D_5W (5% dextrose in ddH_2O) and used at a concentration of 10 mg/kg. A volume of 0.2 ml/20 gram mouse was administered intravenously (i.v.) 24 hours prior to light treatment. Tetra(*m*-hydroxyphenyl)chlorin (mTHPC), known as Foscan®, supplied by Scotia pharmaceuticals Ltd. (Sterling, UK), was dissolved in a solvent mixture containing ethanol-polyethylene glycol 400-distilled water at 2:3:5 (vol/vol/vol) and used at a concentration of 0.1 mg/kg. A volume of 0.1 ml/20 gram mouse was administered (i.v.) 24 hours prior to light treatment.

Photofrin® and mTHPC were activated with 630 nm or 650 nm wavelength of light, respectively, delivered superficially to the tumors through an 8mm diameter liquid light guide, model 77638 (Oriel Instruments, Stratford, CT). The light guide was attached to a high throughput fiber illuminator (Sciencetech Inc., London Ontario, Canada) equipped with a 150W QTH lamp with integrated ellipsoidal reflector and a 630 ± 10 nm or 650 ± 10 nm

interference filter. During light treatment individual animals were restrained un-anesthetized in lead holders designed to expose only the sacral region of their backs to light. The light spot encompassed the tumor plus ~1mm of surrounding skin.

EMT6 tumor was treated with a dose of 60 J/cm^2, the FsaR tumor was treated with a dose of 200 J/cm^2 and the LLC tumor was treated with either 150 J/cm^2 or 200 J/cm^2. Time duration of the light treatment was dependent on three parameters: (1) largest diameter of the tumor, (2) power output of the light source, and (3) light dose to be delivered. On average the fluence rate was 100 mW/cm^2, and the treatment times did not exceed 20 minutes.

Initial PDT response was defined as de-bulking, leaving no visible sign of tumor mass by 24 hours following PDT light delivery. The mice were subsequently inspected three times per week, and they were designated "tumor-free" unless there were visible/palpable signs of tumor recurrence. Those mice that remained free of tumor by 90 days post treatment were considered cured.

1.2.3 Complement inhibition and tumor cures

Two groups of eight subcutaneous EMT6 tumors were treated with PDT, one of the two groups were also administered two intra-peritoneal injections of 50 mg/kg each of N-acetyl-L-aspartyl glutamic acid (NAAGA) at 24 and 0.5 hours prior to PDT light delivery. NAAGA is an inhibitor of C3 cleavage by both classical and alternative pathway C3 convertases [Etievant *et al*, 1988; Feuillard *et al*, 1991]. Tumors treated with either PDT

alone or PDT combined with NAAGA were fully de-bulked by 24 hours following treatment then monitored for tumor re-appearance.

1.2.4 Circulating blood neutrophil levels

Six to eight animals per time-point were used to obtain a white blood cell count. Only one blood sample was taken per animal to avoid all non-specific fluctuations in the level(s) of circulating white blood cells. To induce ease of blood flow from lateral tail veins, vasodilatation was induced by holding the tail of the mouse in a warm water bath for about 30 seconds. Subsequently, using a sterile scalpel blade a small nick was made in the tail and allowed to bleed freely. The first drop of blood (approximately 10 μL) was discarded to avoid collecting a non-specific surge of cells. The sequential drop 10 μL of blood was collected using a pipet tip and dropped immediately into 90 μL of erythrocyte NH_4Cl lysing solution and left on ice. Erythrocytes were lysed for up to 20 minutes at which time 900 μL of lysing solution was added to obtain a 100X dilution of white blood cells. A 10 μL aliquot was placed on a hematocytometer to determine total leukocyte count per ml of blood.

Simultaneously, a second sample of blood was collected from the tail vein into a heparinized micropipet, smeared onto a clean glass slide, and left to air-dry. Sampling was undertaken in most cases at 2 or 8 hours post PDT treatment (with other time points included in some experiments). Two slides for each mouse were prepared. The air-dried specimens were stained using the Wright's stain (filtered using No. 1 Whatman paper prior to use) according

to the manufacturer's instructions. Identifying distinguishing morphological features, a differential white blood cell count was obtained using a 20X objective lens on a Zeiss microscope. Cells were grouped as neutrophils, lymphocytes, monocytes, band neutrophils, and other, and counted until a total of at least 200 cells were obtained from an unlimited number of fields on each slide. From that total, percent of each cell type was calculated. Absolute number of neutrophils in circulation at the time of sampling was then determined as follows:

$$\frac{\%\ \text{neutrophils} \times \text{total number of white blood cells per mL}}{100}$$

1.2.5 Clamping of tumors

Blood vessel occlusion within the tumor to avoid release of inflammatory mediators from the PDT-treated tumor into circulation was achieved by tumor clamping. A metal D-clamp was mounted around a tumor immediately after the termination of photodynamic light treatment. The clamp was removed from the tumor no later than 6 hours. Blood samples were collected at 1, 3 and 6 hours following initial clamping of the tumors then circulating neutrophil levels were determined as indicated above.

1.2.6 Mediators of PDT-induced neutrophilia

To determine the factors mediating PDT-specific neutrophilia, blocking agents of likely pro-inflammatory candidates known to be produced and released in response to PDT, were

administered intraperitoneally at 30 minutes before the onset of PDT light treatment. Blood samples were collected from PDT-treated tumor-bearing mice at either 2 or 8 hours following treatment to investigate change(s) in circulating neutrophil levels. Tables 1.1 and 1.2 summarize the blocking antibodies and chemical inhibitors used, the dose administered, and the commercial or academic source from which the agents were obtained. The isotype match for the anti-mouse C5 was a mouse IgG1 derived from the hybridoma 1B7.11 (ATCC TIB-191) recognizing trinitrophenyl.

1.2.7 Statistical analysis

Data are presented as mean ± standard error of the mean (SEM). Analysis of variance using one-way ANOVA and a post-hoc comparison using the LSD test was used to test for significant differences between control and treated samples. The significance in differences in tumor growth delay was tested by the log-rank test. P-values less than 0.05 were considered statistically significant. The software program used for statistical analyses is the Statistica 6.1 (StatSoft Inc).

Table 1.1 List of antibody blockers of pro-inflammatory cytokines, ICAM-1 and C5

Mediator	**Dose per mouse**	**Commercial/academic source**
Antibody blocker of:		
IL-6 (clone 20F3)	50 μg	Endogen, Woburn, MA
IL-1β (clone1400.24.17)	50 μg	Endogen, Woburn, MA
IL-10	50 μg	PeproTech, Inc., Rocky Hull, NJ
TNF-α	50 μg	PeproTech, Inc., Rocky Hull, NJ
G-CSF	50 μg	PeproTech, Inc., Rocky Hull, NJ
KC	5 0 μg	PeproTech, Inc., Rocky Hull, NJ
ICAM-1 (clone 3E2)	50 μg	BD Pharmingen, San Diego, CA
Complement C5 protein	750 μg	BB5.1 hybridoma from the lab of Dr. B. Stockinger

Table 1.2 Chemical inhibitors of pro-inflammatory agents

Chemical:	Acts to block:	Dose:	Commercial source:
Trans-BTP Dioxalane	Platelet activating factor (PAF) receptor antagonist	10 mg/kg	Cayman Chemical, Ann Arbor, MI
SQ 29548	Thromboxane receptor antagonist Inhibits platelet aggregation	10 mg/kg	Cayman Chemical, Ann Arbor, MI
SC-19220	Competitive antagonist of prostaglandin E2	10 mg/kg	Cayman Chemical, Ann Arbor, MI
REV 5901	Competitive antagonist of leukotrienes	10 mg/kg	Cayman Chemical, Ann Arbor, MI
Oxypurinol	Inhibits xanthine oxidase	17 mg/kg	Sigma, St. Louis, MO
3-aminobenzamide	Poly ADP-ribose polymerase	20 mg/kg	Sigma, St. Louis, MO
Warfarin (Sodium salt) 3-(α-acetonylbenzyl-4-hydroxy-coumarin)	Antagonist of vitamin K-dependent synthesis of coagulation system factors II, VII, IX and X	10 mg/kg	Sigma, St. Louis, MO
Pyrilamine Mepyramine; N-[4-Methoxyphenyl] methyl-N'N'-dimethyl-N-[2pyridinyl]-1,2-ethanediamine	Histamine by acting as a H_1 histamine receptor antagonist	0.5 mg/kg	Sigma, St. Louis, MO

N-acetyl-L-aspartyl glutamic acid (NAAGA)	Inhibitor of C3 cleavage by the C3 convertase	50 mg/kg	Sigma, St. Louis, MO

1.3 RESULTS AND DISCUSSION

1.3.1 The effect of complement inhibition on tumor response to PDT

The first hint that activation of complement, a key mediator of inflammation, plays a role in secondary effects to PDT-induced damage came from comparing the effect of PDT alone compared to a combined treatment of complement inhibition and PDT. Two groups of subcutaneous EMT6 tumors on the dorsal side of Balb/c mice were treated with Photofrin-PDT. One of the two groups was administered the C3 cleavage inhibitor NAAGA at 24 and 0.5 hours prior to PDT light treatment. NAAGA is a non-toxic synthetic peptide very similar to a natural peptide present in mammalian brains [Auditore, 1966]. NAAGA can intercept the cleavage of C3 and C5 into their respective anaphylatoxins C3a and C5a. It has been suggested that NAAGA is an analogue of either a part of the substrate site on C3 for the enzymatic effect of C3 convertase or a part of the binding site(s) for non-enzymatic interactions with factor B or properdin [Etievant *et al*, 1988]. Additionally, NAAGA is a mast cell stabilizer and is used in the treatment of allergic conjunctivitis [Denis *et al*, 1998]. NAAGA attenuates the release of preformed and newly synthesized histamine and leukotrienes at sites of inflammation and may therefore inhibit recruitment and activation of leukocytes in inflamed tissues [Miadonna *et al*, 1998; Miadonna *et al*, 1994; Goldschmidt *et al*, 1990]. In both groups of tumors, PDT was initially successful in de-bulking the tumor mass. Shown in Figure 1.1 however, over time, a greater number of tumors were without palpable sign of tumor in the PDT only group compared to those treated with the NAAGA-PDT combined

treatment. This result suggests a role for the complement system in PDT-mediated tumor control. It is understood that a key role of complement activity is mediating the intricate release of pro-inflammatory mediators from a site of tissue injury, events that act on several types of leukocytes. The effector functions of activated neutrophils are important for the outcome of PDT and therefore, it was hypothesized that complement may have a key role in mediating the chemotaxis and activation of neutrophils in response to PDT-inflicted tumor injury. The mechanism of neutrophil trafficking in response to PDT in oncologic applications is a key interest of our lab and discussed further in subsequent sections of this Chapter 1.

1.3.2 Inflammatory mediators are released from PDT-treated tumors

It is apparent that the task to observe and document the mediators involved in neutrophil chemotaxis induced by PDT would be a tremendous contribution in the continuing study to describe the role of the host immune system in the success of Photofrin-based PDT. In response to Photofrin-based PDT, neutrophil sequestration is not restricted to the treated site. To maintain homeostasis, neutrophils are recruited from their storage/marginated pools, an event paralleled with accelerated maturation of their progenitors in the bone marrow [Cecic and Korbelik, 2002]. The systemic host response to PDT, applied as a localized treatment of solid tumors, results in the manifestation of neutrophilia. PDT mediated by either Photofrin or mTHPC results in a significant rise in circulating neutrophil numbers following the end of PDT light delivery, and resolves

back to baseline levels by 24 hours post treatment (Figures 1.2, 1.3; Table 1.3). This event reflects the multifarious release of signals into circulation from the site of treatment and subsequent sequestration of neutrophils into the treated lesion where they play out their inflammatory effector function [Cecic *et al*, 2001; Korbelik *et al*, 2001]. Drug injection via tail vein did cause a significant rise in circulating neutrophil in tumor-bearing mice. However, these levels subsided back to pre-injection levels at 24 hours following injection, the time at which light was delivered to the tumors. The level of circulating leukocytes other than neutrophils was also investigated. Although lymphocyte levels fall significantly 1 hour post PDT and monocyte numbers rise significantly at 3 hours post PDT, it is exclusively neutrophils that remain at significantly high numbers compared to untreated controls even at 24 hours post PDT although the levels already beginning to fall toward baseline (Table 1.3). Interestingly, band (immature) neutrophil numbers increase significantly at 3 hours post treatment both post PDT and in the absence of photosensitizer, light treatment only. This is indicative of neutrophil release from bone marrow in animals undergoing a stress response and is not necessarily PDT-specific.

To reflect the data presented, elevated post-PDT serum levels of various agents acting on neutrophil chemotaxis such as complement, histamine, eicosanoids, IL-1β, KC and other chemokines have been determined by various investigators [Fingar *et al*, 1993; de Vree *et al*, 1997; Cecic *et al*, 2001; Henderson and Gollnick, 2002]. Interestingly, decreased PDT-mediated cure rates have been reported after blocking complement, IL-1β, IL-6, KC, histamine, thromboxane, and other eicosanoids, xanthine oxidase and PARP [Fingar *et al*, 1993; Korbelik *et al*, 2001; Henderson and Gollnick, 2002; Korbelik

and Cecic, 2002]. Evidently these systemic effects of tumor-localized PDT are instigated by signals emanating from the PDT-treated lesion. To confirm that signals released from the treated lesion directly affect circulating neutrophil numbers, tumors were clamped and circulating neutrophil levels quantitated (Figure 1.4). PDT-specific neutrophilia is inhibited in mice bearing PDT-treated tumors that were clamped immediately following light treatment. Notably, no visible signs of damage or edema were detected in these mice during and after PDT. In contrast, the non-clamped tumors showed signs of strong edema within 2 hours post treatment and became completely ablated 10-12 hours later. The examination of blood samples following PDT reveals that the level of neutrophils in circulation rises dramatically and remains significantly elevated at 24 hours post treatment, although already begin to fall toward baseline levels. Light alone (no photosensitizer administered) controls lead to a significant rise by 3 hours following light treatment but levels return to baseline by 6 hours. When the tumors are clamped immediately following PDT light treatment circulating neutrophil levels did not reach levels significantly higher than baseline. This was direct evidence that signals mediating PDT-specific neutrophilia are released from the treated lesion. For control groups in these experiments we used mice with either clamped or non-clamped tumors treated with light only (no photosensitizer), revealing the extent of the rise in circulating neutrophil levels induced by non-specific stress effects.

1.3.3 Mediators of PDT-induced neutrophilia

A comprehensive study was designed to describe the inflammatory mediators involved in mediating PDT-specific neutrophilia. With the knowledge that a barrage of

inflammatory mediators is released from PDT-treated tumors, various antibodies or chemical antagonists were administered to tumor-bearing mice 30 minutes prior to PDT light treatment and their blood neutrophil levels quantitated at ~2 (early phase) and ~8 hours (late phase) following treatment. These 2 time points were chosen on the basis of past published data that within the first 24 hours following PDT there is a bi-phasic rise in circulating neutrophil levels in PDT-treated tumor-bearing mice [Cecic *et al*, 2001]. The early phase includes a non-specific response characteristic of any acute insult or injury, whereas the sustained elevation of neutrophil levels of the late phase was designated as "PDT-specific neutrophilia" [Cecic *et al*, 2001].

To rule out non-specific effects of the blocking agents utilized in this investigation on blood neutrophil levels, control EMT6 tumor-bearing mice without PDT treatment were administered the blocking agent with subsequent blood collection at the same time intervals as though they were treated with PDT. As shown in Figure 1.5 no significant effect of the blocking agent itself affected circulating neutrophil numbers, with the exception of the leukotriene antagonist REV 5901. The leukotriene inhibitor induced an increase in the absolute number of neutrophils in EMT6 tumor-bearing mice in the absence of PDT (second column from the left in Figure 1.5). This particular inhibitor of leukotriene function may not completely inhibit leukotriene function when administered in conjunction with PDT.

1.3.3a Cytokines and mediators of oxidative stress

Figure 1.6 defines the many cytokines involved in mediating inflammation during PDT. Interleukin (IL)-1β and tumor necrosis factor (TNF)-α mediated the early response

as seen by the ability of neutralizing antibodies to inhibit the rise in circulating levels following treatment at 2 hours but not at 8 hours post treatment. Anti-IL-6 had the greatest effect on inhibiting the early phase neutrophilia and also a significant inhibitory action at late-phase neutrophilia. The role of IL-6 indicates the engagement of the acute phase response to PDT in addition to an inflammation-like response. Blocking either granulocyte colony-stimulating factor (G-CSF) or IL-10 produced a significant inhibition of late-phase neutrophilia, but did not have an effect upon the early phase neutrophil response. This result is intriguing since IL-10 dampens the effect of pro-inflammatory mediators such as the chemokine KC that act on neutrophils. Perhaps when IL-10 is blocked the host responds in an attempt to return to homeostasis by producing higher levels of IL-10 to compensate for the temporary loss. In this way, the immunosuppressive action of IL-10 is maintained. Blocking the potent neutrophil-specific chemokine KC (murine analogue of human interleukin-8) reveals its role in late-phase neutrophilia.

Other factors besides cytokines may act to influence neutrophil trafficking. It is clear from the data presented that histamine is a highly potent mediator at both the early and late-phase response. The coagulation and/or other plasma cascade systems also participate in the induction of the advanced-phase neutrophilia with no apparent involvement in the early phase. Factors blocked by the coagulation inhibitor warfarin include the Vitamin K-dependent prothrombin, and factors VII, IX, and X; warfarin is a commonly used agent in the prevention of venous thromboembolism following surgery [Shapiro, 2003; Francis *et al*, 2003]. Arachidonic acid metabolites are well-known participants in tumor response to PDT [Fingar *et al*, 1993; Henderson and Donovan,

1989]. In a rat chondrosarcoma study, pre-treatment with either aspirin or indomethacin (non-specific cyclooxygenase inhibitors) markedly reduced the effect of PDT [Fingar *et al*, 1993a]. Treatment with a thromboxane receptor antagonist markedly diminished the extent of the advanced-phase whereas it exhibited no significant influence on the early-phase of PDT-induced neutrophilia. Pronounced reductions of both early- and advanced-phase neutrophilia occurred with the receptor antagonists for prostaglandin E_2 and leukotrienes.

Poly ADP-ribose polymerase (PARP) inhibitor indicated that neutrophil chemotaxis may be mediated in part by an indirect effect of PARP on other molecules affecting neutrophil trafficking, with an inhibition of late-phase neutrophilia following PDT. Evidence has accumulated that an important mechanism of tissue injury during oxidative stress was the activation of PARP. PARP is an enzyme abundantly present in the eukaryotic cell nucleus [Liaudet, 2000]. *In vivo*, PARP activation has been shown to act as a common effector of oxidant-dependent damage in various pathophysiological conditions including ischemia-reperfusion injury, localized inflammation, and endotoxic shock [Liaudet, 2000], and was recently shown to be induced by PDT in tumors [Korbelik *et al*, 2003b]. Administering oxypurinol to inhibit xanthine oxidase (XO), a key mediator of oxidative stress by ischemia/reperfusion, demonstrated no effect on early phase neutrophilia but a small yet significant decrease on late-phase neutrophilia. The effects of PARP and XO could act together to promote oxidative stress in a PDT-treated tumor and thereby sustain signals released into circulation leading to late-phase neutrophilia that would not otherwise occur in the absence of the photodynamic process. Inhibiting the activity of platelet activating factor (PAF) did not have an effect on

circulating neutrophil levels and therefore it was not deemed a significant player toward PDT-specific neutrophilia. Lastly, adhesion molecule expression can also affect neutrophil trafficking, however, blocking ICAM-1 diminished the intensity of early-phase but not the more PDT-specific late-phase neutrophilia.

Blocking any of the above listed inflammatory mediators one at a time to study its effect on PDT-specific neutrophilia has revealed that during an inflammatory response to PDT there exists a network of redundant pathways that overcome the temporary loss of function of a single agent.

1.3.3b Complement and adrenal hormones

In addition to the many inflammatory mediators discussed thus far, complement participates in the induction of neutrophilia following PDT. In Figure 1.6 the top pair of columns show the effect on circulating neutrophil levels obtained with antibodies blocking the activity of the fifth component of murine complement (C5), which prevents the generation of C5a anaphylatoxin and the C5b-9 membrane attack complex [Frei *et al*, 1987; Kilgore *et al*, 1998]. Figure 1.7 indicates changes in neutrophilia induced by the C3 convertase inhibitor N-acetyl-L-aspartyl glutamic acid (NAAGA) [Etievant *et al*, 1988; Feuillard *et al*, 1991]. C5a is a potent neutrophil-specific chemoattractant, and non-lytic quantities of C5b-9 can also influence neutrophil chemotaxis. While blocking C5 had no significant effect on the development of the early-phase, it reduced by close to 30% the extent of late-phase post PDT neutrophilia. Blocking C5 in theory still left the possibility for breakdown of C3 by C3 convertase with subsequent production of C3a

anaphylatoxin that in turn triggers the release of histamine, prostaglandins and leukotrienes [Goldstein, 1992]. Findings arranged in Figure 1.7 demonstrate a more abrupt and complete inhibition of PDT-induced neutrophilia by the complement inhibitor NAAGA, suggesting the important role that the complement system plays downstream of the C3 convertase and C5 convertase activity toward mediating the many networks involved in inflammation. NAAGA on its own had no effect on neutrophilia compared to untreated, tumor-bearing mice. Interestingly, treating tumors with PDT in C3 knockout mice elevated the absolute numbers of neutrophils in the circulation of these mice compared to PDT applied in normal C57BL/6 mice (Figure 1.8, A). However, the relative rise in circulating neutrophil numbers following PDT compared to untreated levels is significantly greater in the C57BL/6 mice (Figure 1.8, B), since the absolute number of neutrophils are higher in the C3 knockout prior to treatment compared to normal mice. In the C3 knockout model there was a significant rise in circulating neutrophil levels at 4, 10, and 24 hours post PDT light delivery, but the degree of neutrophilia was not as high as that observed in the C57BL/6 background mouse strain with a fully functional complement system. This observation emphasizes the complications that may be involved in using knockout mouse models, in particular when characterizing events as intricate as inflammation. In the absence of the pivotal complement protein C3, the knockout mice seem to compensate for this loss of function, elevating neutrophil levels in circulation prior to treatment, for example. In addition, the inflammatory response to PDT-inflicted tumor damage may still continue in the C3 knockout, mediated by other pro-inflammatory agents such as adrenal hormones, IL-6 and histamine. Although the C3 knockout mice do not produce C3 (assessed in C3

ELISA assay of sera isolated from tumor-free C3 knockout mice, n=4, not shown), components of the LLC tumors transplanted from complement-proficient C57BL/6 mice may produce endogenous levels of C3 in response to PDT. Presumably, C3 knockout mice produce all other components of the complement cascade, therefore, the PDT-treated lesion may become a source of C3 and a starting point for complement activation leading to classical events in acute inflammation, namely neutrophilia. It would be of interest to compare serum and tumor C3 levels following PDT in the C3 knockout and C57BL/6 complement-producing mice.

Adrenal gland hormones, such as corticosterone, are released as part of the normal stress response to injuries [Barazzone-Argiroffo, 2003]. For this reason the effect of PDT on circulating neutrophil levels in adrenalectomized mice (Adrex) was investigated. FsaR tumors were grown and treated on the left flank of both adrenalectomized and normal C3H/HeN mice, to avoid any complications at the site of surgery on the dorsal side of the animals whose adrenal glands were removed prior to tumor inoculation (Adrex). Figure 1.9 shows how neutrophilia, a significant rise above normal levels, in the normal C3H/HeN mice is bi-phasic, with a rise at two hours followed by a fall and then another rise at eight hours post treatment. In comparison, the Adrex mice did have a rise in mice bearing PDT-treated tumors, however this rise in circulating neutrophil levels was not as high as in normal mice. A stress response in mice will occur in mice due to simple handling during PDT treatment, characterized partly by the rise in circulating neutrophil levels 1-2 hours post handling [Cecic *et al*, 2001]. The early rise in C3H/HeN mice at one hour post light delivery is reduced in the Adrex mice indicating a role of adrenal hormones such as gluco-corticoids on the non-specific, stress response to PDT. It

is apparent that adrenal hormones are also included among mediators of PDT-specific neutrophilia. Adrenal hormones are classified as classical acute phase reactants, therefore, the inhibition of early- and late-phase neutrophilia following PDT in Adrex mice demonstrates the role of these hormones in the induction of systemic acute phase response by tumor-localized PDT treatment. These results indicate that adrenal hormones contribute but are not the only mediators of neutrophil chemotaxis during and following PDT. Together these observations imply that the network of pathways that builds up an inflammatory response becomes redundant and therefore makes it difficult to single-out any one mediator whole sole action is to mediate PDT-induced neutrophil chemotaxis. Nevertheless, blocking complement activation upstream of effector proteins in the cascade, does seem to have the most significant role in mediating the host response to tumor injury inflicted by PDT.

1.3.4 Summary and conclusions

The data presented in this chapter reiterate that localized inflammation is a very complex process that involves the integrated and synergistic actions of multiple effector systems [Franks and Fries, 1991]. Neutrophilia elicited in mice bearing PDT-treated tumors results from the integrated action of multiple mediators that are released into circulation from the targeted lesion. Some of these mediators participate in both the early and late-phase neutrophilia (IL-6, prostaglandins, leukotrienes, and histamine), while others contribute selectively to either the early-phase (IL-1β, and TNF-α) or late-phase (G-CSF, IL-10, thromboxane and coagulation cascade components). Moreover, there are

indirect mediators (exemplified by the activity of xanthine oxidase, PARP, and ICAM-1) that appear to exert their influence in early- or late-phase neutrophilia. The effect on neutrophil chemotaxis can be augmented by a synergistic interaction of various mediators [Struyf *et al*, 2001]. Rather than acting independently, these mediators appear integrated in a network that renders the neutrophil trafficking regulated within the inflammatory framework aimed at resolving the lost homeostasis of the inflamed, PDT-treated tumor, and thereby contributes to the destruction and clearance of the lesion. Understanding the role of mediators involved in neutrophil trafficking during and following Photofrin-based PDT enhances our knowledge of the inflammatory response to this form of cancer treatment. A key event responsible for this phenomenon appears to be PDT-induced complement activation. While some components of the complement cascade act directly as neutrophilia mediators, a number of secondary mediators, most of which can be generated as a consequence of complement activity, are also involved; some are produced rapidly during the PDT treatment and others at later time periods. It is known from the literature that complement is a potent mediator of inflammation. Hints gained from this chapter include that complement activity drives the action of most other pro-inflammatory mediators released from a PDT-treated tumor, since the complement inhibitor NAAGA had the greatest effect on blocking PDT-specific neutrophilia. In addition to inhibiting anaphylatoxin release, NAAGA can inhibit histamine release by mast cells, leukotriene synthesis, and also hamper adhesion of leukocytes to activated endothelial cells [Bouhlal et al, 2002]. Gaining a broader understanding of the mechanism of action against solid tumors by the complement system creates excellent potential for further development of this modality.

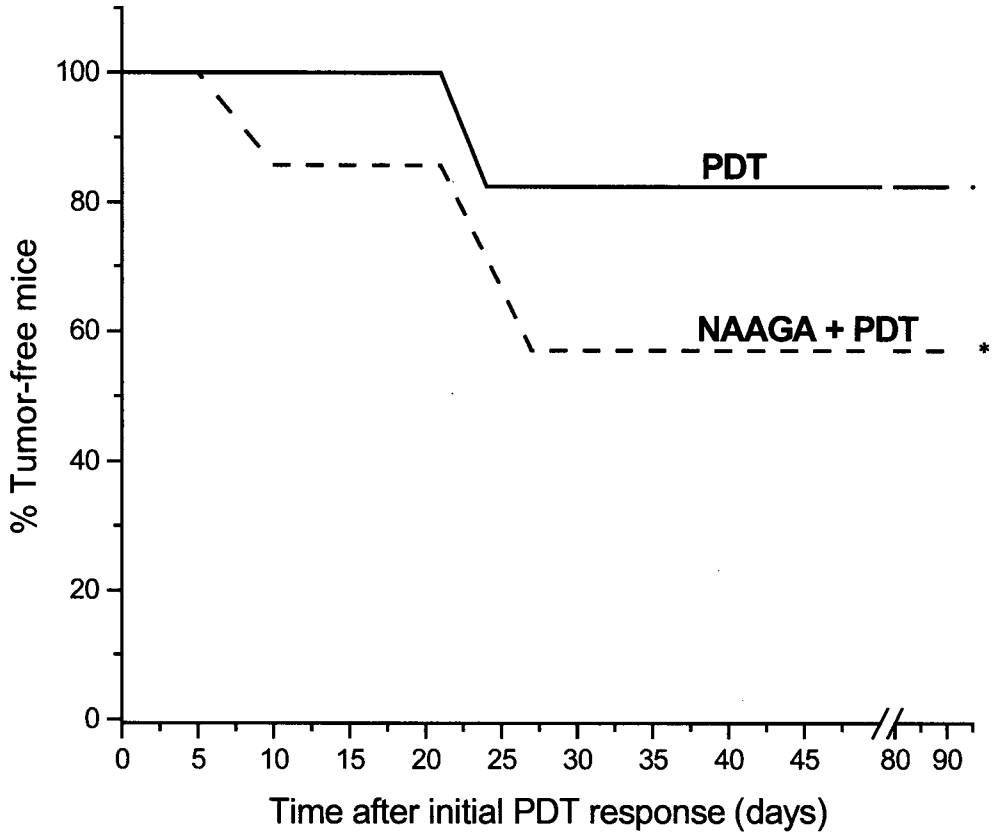

Figure 1.1 PDT-mediated tumor cure rate decreases by chemical inhibition of complement activation. Two groups (n=8 per group) of subcutaneous EMT6 tumors in Balb/c mice were treated with PDT: Photofrin 5 mg/kg and 50 J/cm^2. One of the two groups was also administered 2 doses of NAAGA (50 mg/kg), an inhibitor of the C3 convertase, 24 and 0.5 hours prior to PDT light delivery. PDT response corresponds to de-bulking of tumors 24 hours following PDT light delivery. No sign of palpable growth at 90 days following treatment was considered cured. The difference between the two groups is significant, statistical test applied was the log rank test.

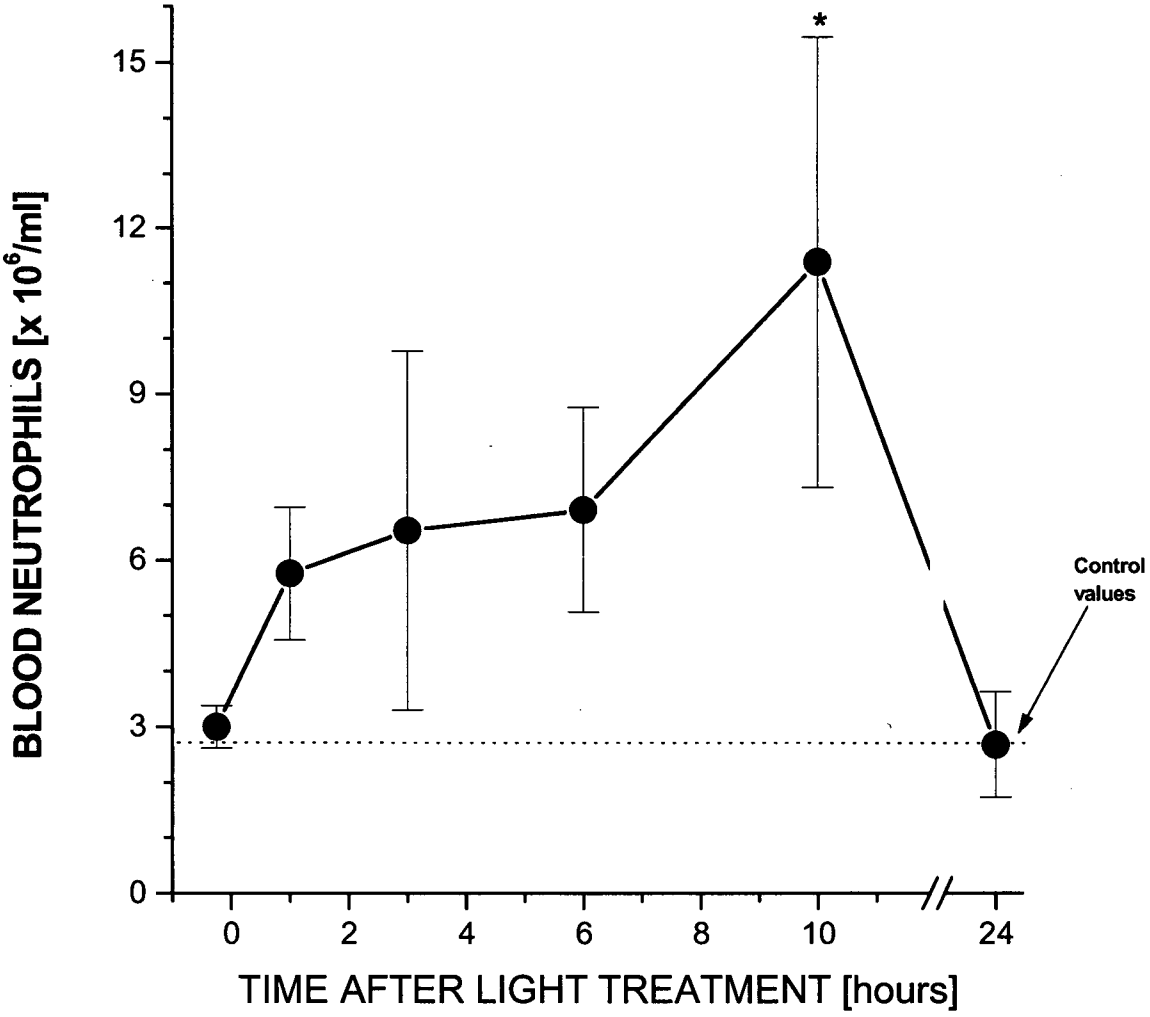

Figure 1.2 Photofrin-mediated PDT induces neutrophilia in systemic circulation. EMT6 tumors growing on the lower dorsal side of Balb/c mice were treated with PDT: Photofrin 10 mg/kg and 60 J/cm^2, and blood samples collected from the tail vein of these mice were analyzed for total neutrophil content up to and including 24 hours following treatment. * $p < 0.05$ considered significantly different from untreated control values. All values are a mean ± s.e of a group of 4-6 mice per time point, corrected for the effect of light alone in the absence of Photofrin. Statistical analysis was conducted by the ANOVA analysis of variance, with post-hoc comparison by the LSD test.

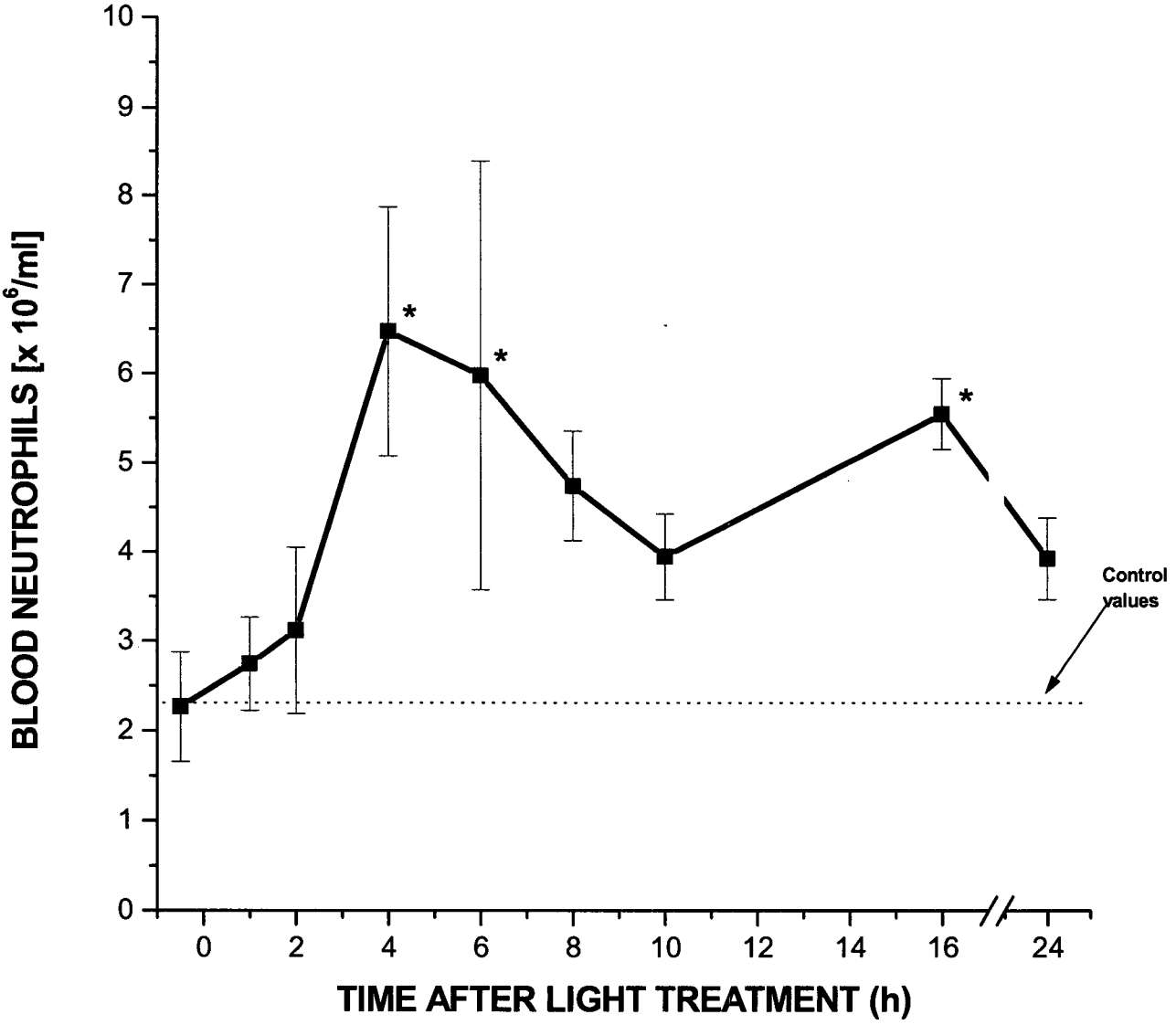

Figure 1.3 mTHPC-mediated PDT induces neutrophilia in systemic circulation. EMT6 tumors growing on the lower dorsal side of Balb/c mice were treated with PDT: mTHPC 0.1 mg/kg and 10 J/cm^2, and blood samples collected from the tail vein of these mice were analyzed for total neutrophil content up to and including 24 hours following treatment.
* $p < 0.05$ were considered significantly different from untreated control values.
All values are a mean ± s.e. of a group of 4-6 mice per time point. Statistical analysis was conducted by the ANOVA analysis of variance, with post-hoc comparison by LSD test.

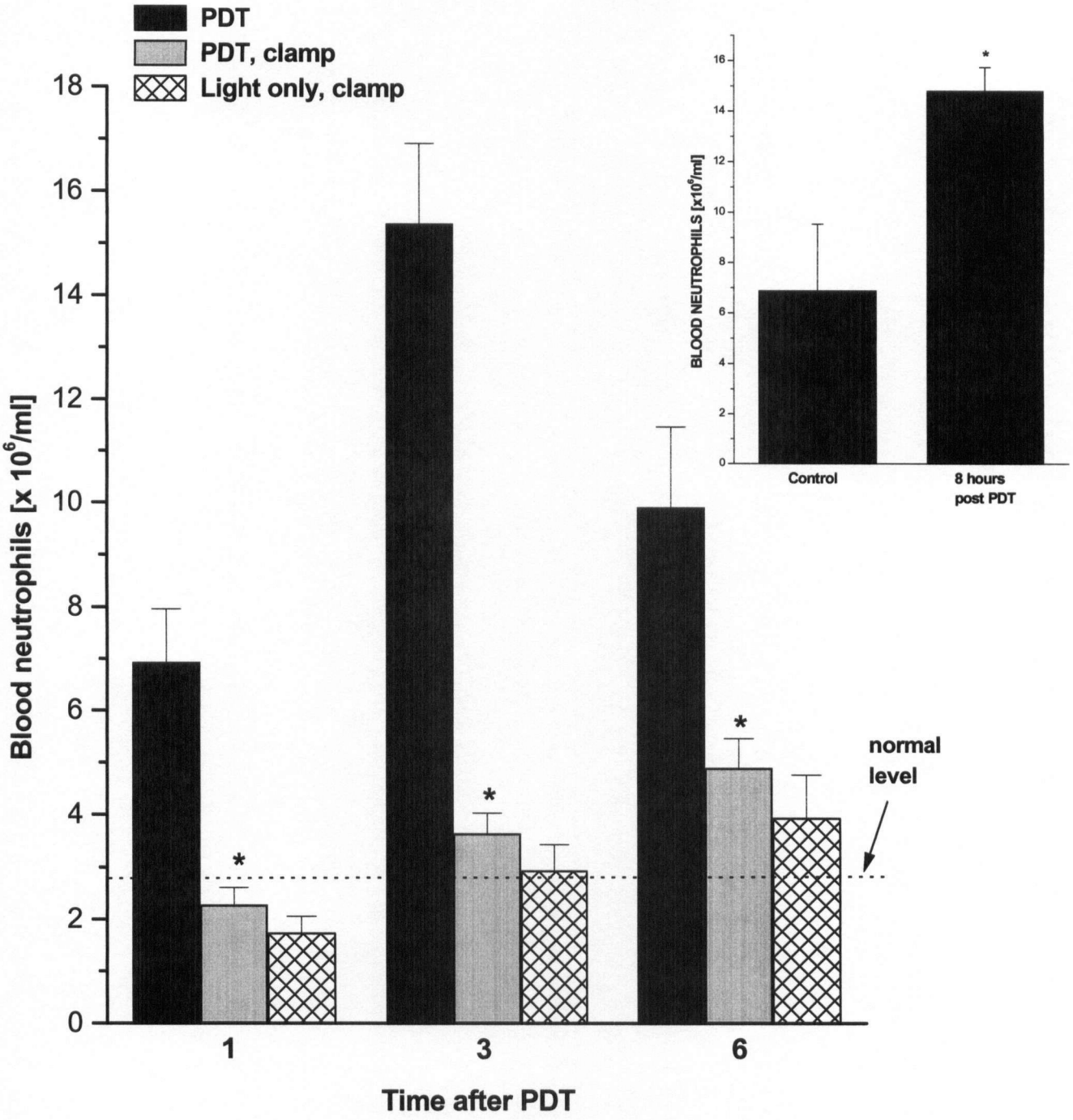

Figure 1.4 PDT-induced neutrophilia in Balb/c and scid mice, and the effect of tumor clamping. Dorsal EMT6 tumors growing in either Balb/c or scid mice were treated with PDT: Photofrin 10 mg/kg and 60 J/cm^2, then blood samples were collected at different times therefter and circulating neutrophil levels determined. Tumors in some of the mice were clamped immediately after PDT light treatment and the clamps were not removed until after blood collection. Light-only were treated in the absence of photosensitizer. The data obtained from scid mice are shown separately (inset). Bars are SEM, n=4 per column. *p<0.05 for statisticaly significant inhibition of a rise in circulating neutrophil levels following PDT (blue columns).

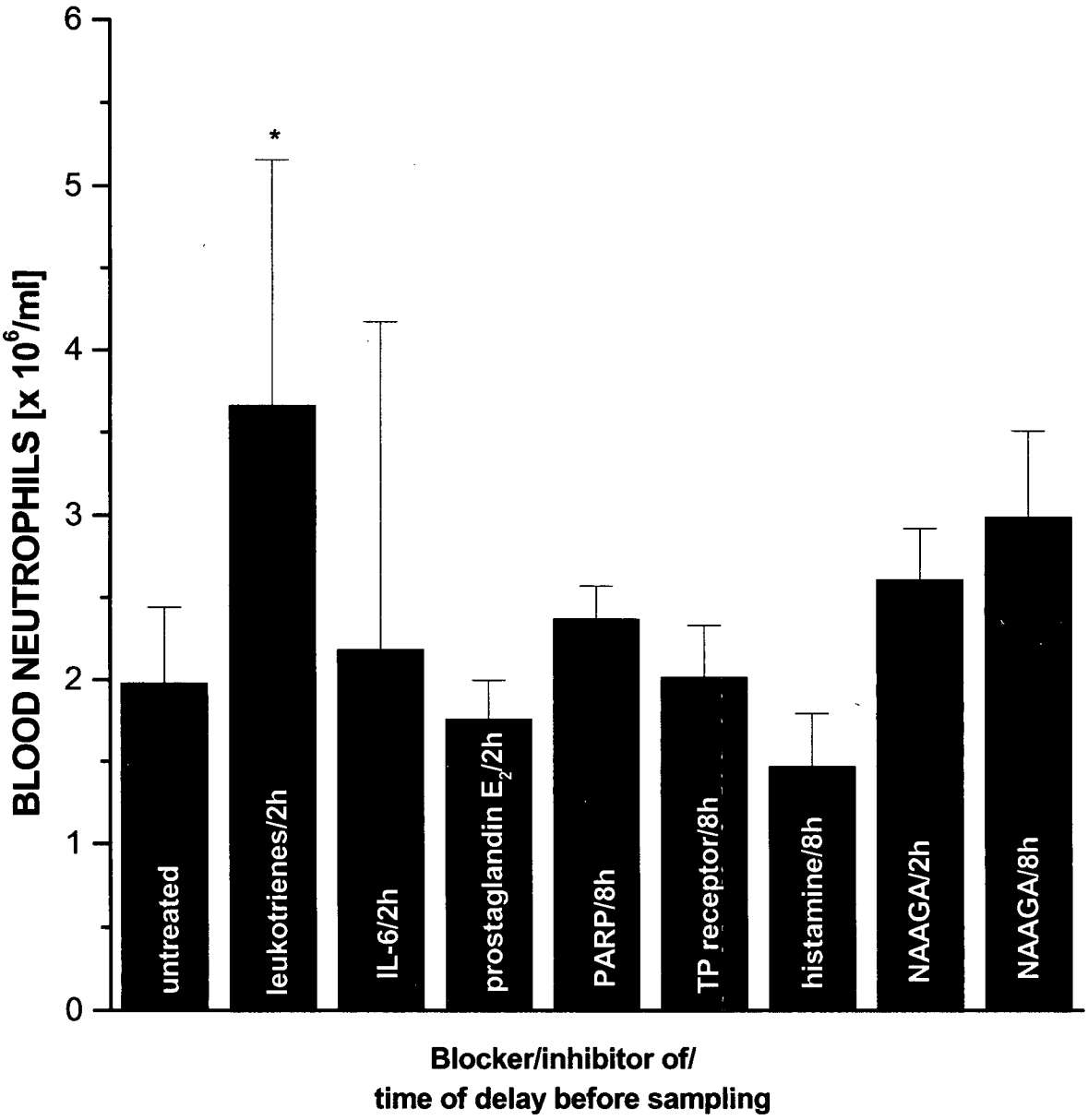

Figure 1.5 Effect of blockers of inflammatory mediators in the absence of PDT on circulating neutrophil levels. Inhibitors of a select, key group of inflammatory mediators were administered to EMT6-tumor bearing mice that were not treated with PDT. Blood was collected either 2 or 8 hours following administration of the blocking agent used. Columns represent mean ± SEM, n=4. * $p<0.048$ were considered statistically different from levels of neutrophils in mice prior to administration of an inhibitor.

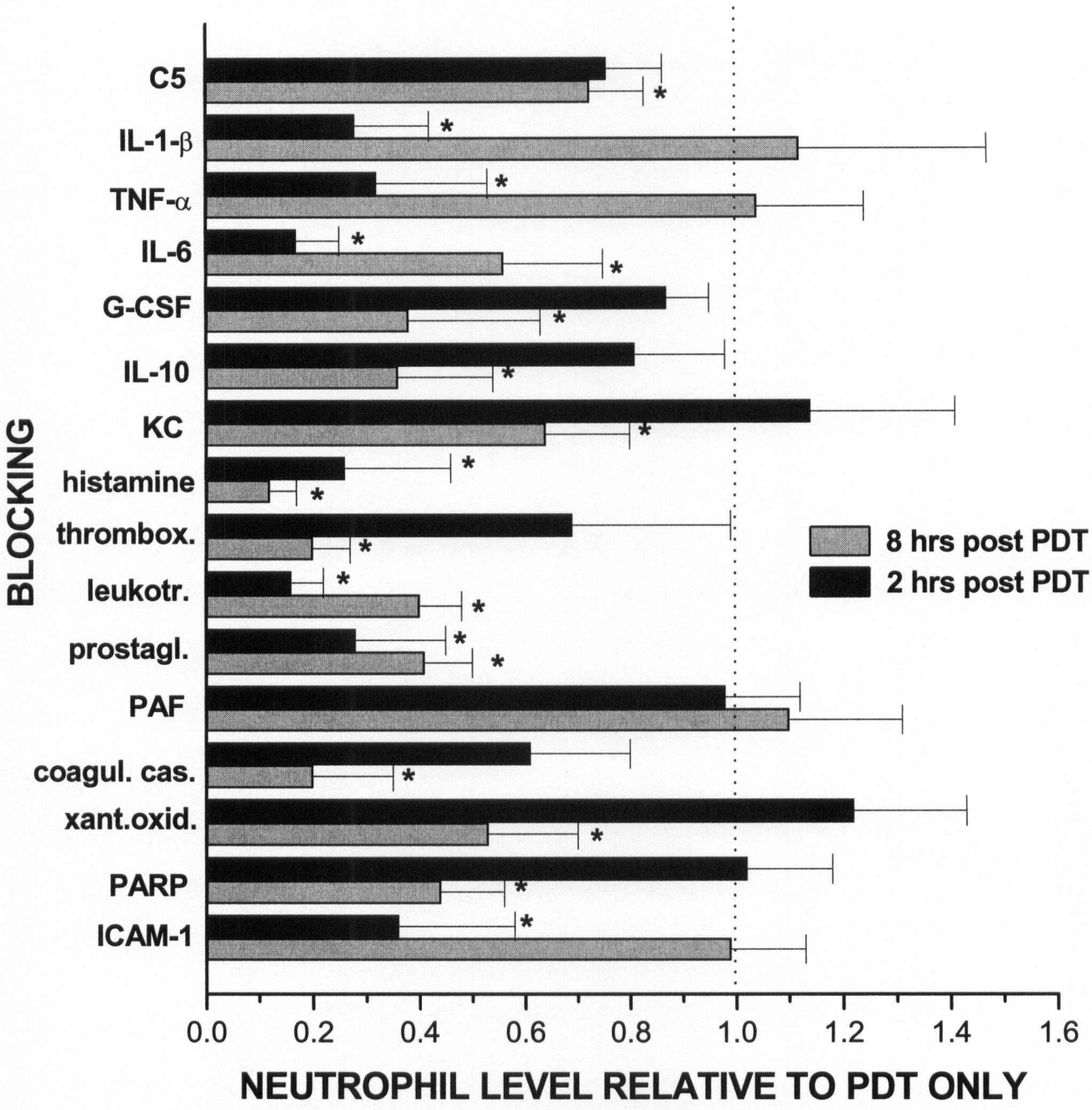

Figure 1.6 Mediators of PDT-induced neutrophilia. Dorsal EMT6 tumors growing in BALB/c mice were treated by PDT and blood collected for determination of neutrophil content at either 2 or 8 hours post PDT. The results are presented as the ratio of PDT-specific increase in absolute blood neutrophil counts obtained with and without the blocking agent. The agents used were the antibodies against C5, IL-1β, TNF-α, IL-6, IL-10, G-CSF, KC, and ICAM-1, receptor antagonists of thromboxane (SQ 29,548), prostaglandin E2 (SC-19220), leukotrienes (REV 5901), histamine (pyrilamine) and PAF (trans-BTP Dioxolane), anticoagulant warfarin, and inhibitors of xanthine oxidase (oxypurinol) and PARP (3-aminobenzamide). The doses used for all these agents are specified in Table 1.1 and 1.2. One-way ANOVA with a post-hoc comparison by the LSD test was applied. Neutrophil numbers in mice whose blood was collected at 2 or 8 hours post treatment (mediator blocker and PDT) were compared to their respective standard defined as either 2 or 8 hours post PDT only. Bars are SD, n = 4. *$p<0.05$ for statistical difference from PDT-only.

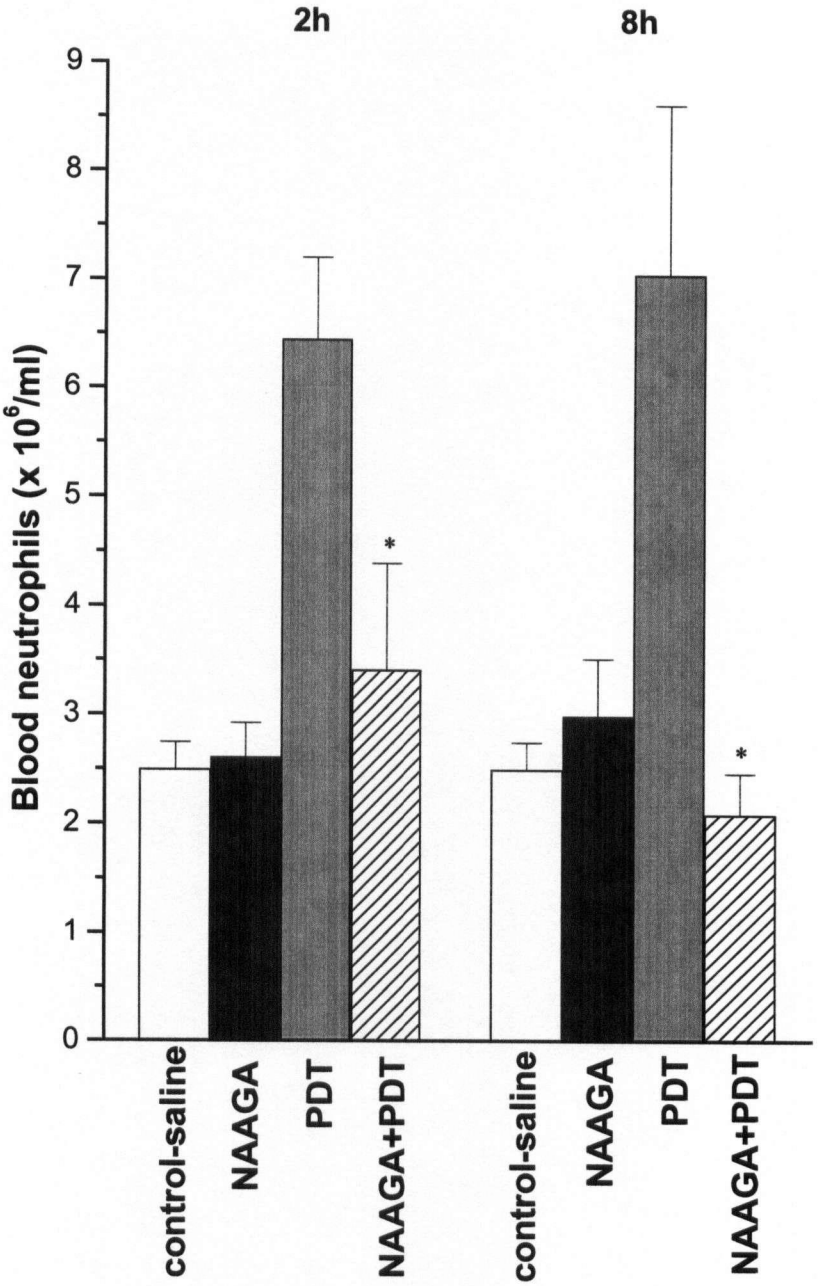

Figure 1.7 Complement mediates PDT-induced neutrophilia. Complement activation was inhibited in mice bearing EMT6 back tumors prior to PDT and subsequent blood collection either 2 or 8 hours following treatment for the assessment of blood neutrophil levels. Blocker of C3 convertase NAAGA (50mg/kg) was administered i.p. 24 hours and 0.5 hours prior to PDT light delivery (n=5). PDT: Photofrin 10 mg/kg and 60 J/cm^2. * $p<0.05$ compared to PDT alone.

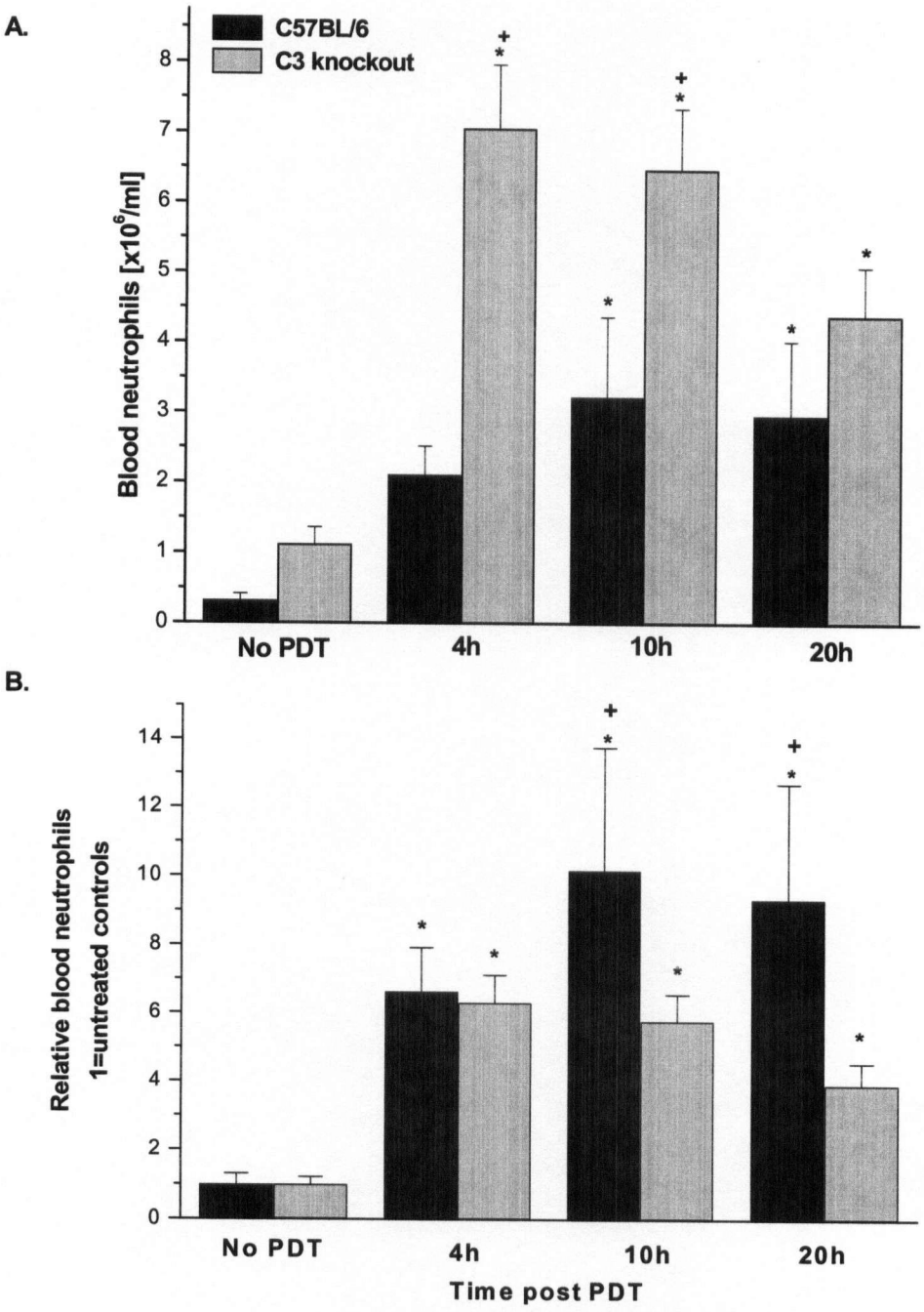

Figure 1.8 Blood neutrophil levels in C57BL/6 mice compared to C3 knockout mice following PDT of the Lewis lung carcinoma. The Lewis lung carcinoma tumor was treated by PDT: Photofrin 10 mg/kg and 150 J/cm^2, in both the C57BL/6 and C3 knockout mice. Neutrophil levels were assessed from blood smears collected 4, 10, and 24 hours post PDT. Each column represents the mean +/- SEM (n=6). Absolute numbers are plotted in panel A and the results in panel B are depicted as relative values compared to untreated controls in panel B. * $p<0.05$ considered statistically different from untreated control levels and + $p<0.05$ considered statistically different between the 2 mouse strains in the same time point.

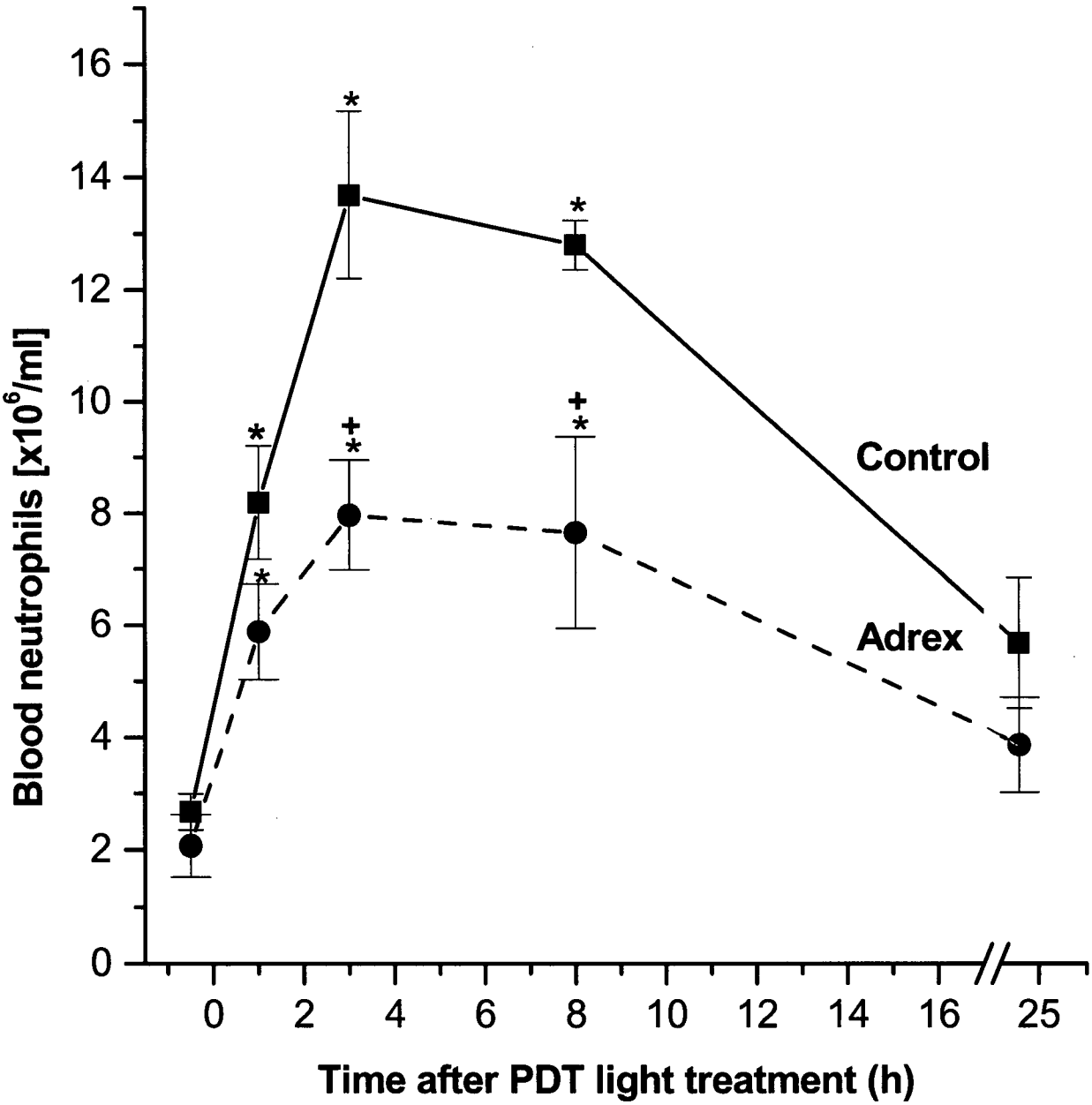

Figure 1.9 Adrenal hormones mediate PDT-induced neutrophilia. Subcutaneous FsaR fibrosarcoma tumors were grown in two groups of C3H/HeN mice (n=8 per group), the adrenal glands of one of the two groups of mice were removed surgically. PDT: Photofrin 10 mg/kg and 200 J/cm^2 was applied to all tumors and blood samples collected at 1,3,8,and 24 hours following light delivery. Data are presented as mean ± S.E., and * $p<0.01$ were considered statistically significant compared to baseline within each strain of mice; + $p<0.005$ significant difference between the two strains of mice at time points 3h and 8h post PDT.

Table 1.3 : Differential leukocyte counts in peripheral blood of mice bearing PDT-treated EMT6 back tumors

Time after treatment	Totals	Neutrophils	Lymphocytes	Monocytes	Band cells
			(x 10^6/mL of blood)		
non-treated	13.8 ± 1.11	3.00 ± 0.38	11.00 ± 0.73	0.42 ± 0.09	0.06 ± 0.02
Light only					
1 hour	8.78 ± 1.51	4.17 ± 0.61	3.80 ± 0.40*	0.14 ± 0.05	0.02 ± 0.01
3 hours	36.5 ± 4.12*	11.83 ± 2.85*	23.57 ± 2.18*	0.81 ± 0.30	0.17 ± 0.03*
6 hours	16.4 ± 3.72	2.89 ± 1.00	12.94 ± 2.82	0.44 ± 0.23	0.04 ± 0.03
10 hours	14.2 ± 1.94	4.13 ± 0.71	9.26 ± 1.20	0.54 ± 0.15	0.10 ± 0.05
24 hours	15.7 ± 2.93	2.54 ± 0.51	12.68 ± 2.36	0.34 ± 0.10	0.02 ± 0.02
PDT					
1 hour	10.49 ± 2.25	6.93 ± 1.03*	4.87 ± 0.93*	0.19 ± 0.04	0.07 ± 0.02
3 hours	26.02 ± 6.81*	15.37 ± 1.54*	13.24 ± 4.41	0.95 ± 0.26*	0.11 ± 0.05*
6 hours	15.74 ± 2.86	9.91 ± 1.56*	7.21 ± 0.55	0.67 ± 0.21	0.07 ± 0.02
10 hours	24.45 ± 8.53*	12.52 ± 4.01*	9.06 ± 4.13	0.43 ± 0.23	0.04 ± 0.03
24 hours	15.56 ± 1.90	5.68 ± 0.80*	8.05 ± 0.52	0.26 ± 0.04	0.09 ± 0.02

Blood samples for each time point were collected using individual sampling, n=6 per time point. PDT: Photofrin 10 mg/kg, 60 J/cm^2. Mean values, based on hemacytometer counts and Wright stain analysis of blood smears, are presented ± SE. * $p < 0.05$ for statistical difference compared to non-treated controls by the ANOVA analysis of variance and the post-hoc comparison by the LSD test.

Chapter 2

PDT applied in the treatment of solid tumors results in both local and systemic engagement of the complement system

2.1 INTRODUCTION

2.1.1 The complement system

The immune system consists of two main arms of defense: innate and adaptive immunity. Until very recently the two systems were generally thought to work independent of each other; however, it is becoming increasingly clear how these two systems are bridged by the complement system. Complement was first identified as a heat-labile substance in serum that "complemented" antibodies in the killing of bacteria, and its nomenclature simply followed the historical order of discovery of each protein. Since its discovery, the complement system has been defined as a group of more than thirty interacting proteins making up a cascade of unidirectional enzymatic reactions involved in the control of inflammation, disposing immune complexes, the activation of phagocytes and the lytic attack on cell membranes [Roitt, 2001].

Complement evolved as a first line of defense against invading pathogens. It has since been discovered that not only is complement a manner in which the body rids itself of foreign invaders, it can also impose severe damage to normal, healthy tissue, hence its role in transplant rejection, glomerular and myocardial ischemia-reperfusion injury, and burn injury. Other pathologies mentioned in the literature as complement-mediated tissue injury include: allergic neuritis, type II collagen-induced vasculitis, myasthenia gravis, hemolytic anemia, glomerulonephritis, immune complex-induced vasculitis and multiple sclerosis [Kalli, 1994].

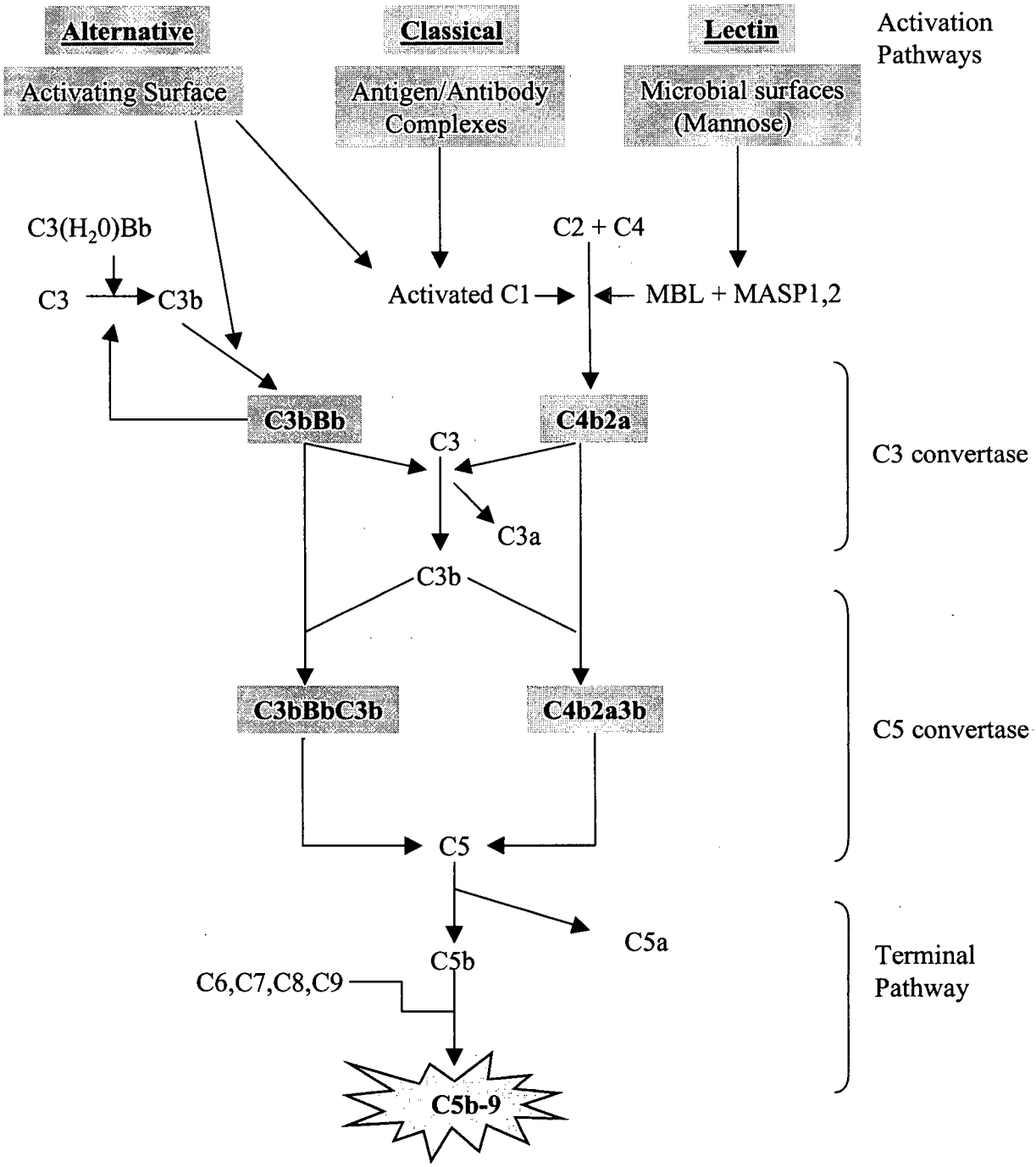

Schematic 1: The complement cascade describing the activation by all three pathways: Alternative, Classical and Lectin. Adapted from Cole and Morgan, 2003.

Although proteins of the complement system can be produced locally by epithelial, endothelial and various immune cells such as monocytes/macrophages and neutrophils, they are primarily produced by hepatocytes and constitutively released into circulation [Morgan and Gasque, 1997]. The plasma component of complement makes up about three grams per liter of total protein and about fifteen percent of the globulin fraction [Walport, 2001]. More than 30 plasma and membrane-bound proteins are involved in the unidirectional series of enzymatic reactions making up the complement system that can be split up into 3 main arms of activation: classical, alternative, and mannose-binding lectin pathways. These activation processes are described in Schematic 1 [page 55]. Classical pathway of complement mediates specific antibody responses and is activated when an antibody molecule (IgM or IgG) binds to a foreign particle or altered/wounded cell. Binding of the antibody molecule to the complement protein C1q initiates the assembly of the C3 convertase, the catalyst for promotion of the pathway to proceed. The alternative pathway is key in host defense mechanism against bacterial infection, but also now known to be involved in promulgating tissue damage, as for example in ischemia-reperfusion injury. The alternative pathway triggers the complement cascade without the need for participating antibody molecules to produce activation. Bacterial products such as endotoxin, and wounded tissue, can activate the alternative pathway, which results in the pro-inflammatory and membrane-injuring mediators also produced by the classical pathway. Activation of the lectin pathway of complement is mediated by mannose-binding lectin, which is a pattern-recognition receptor specific for microbial carbohydrates [Medzhitiv and Janeway, 2000]. The lectin pathway is also antibody-independent. In all activation pathways, the cleavage of C5

leads to eventual assembly of the membrane attack complex (MAC). This is the terminal step in the complement cascade made up of proteins C5b through C9, a complex of about 20 proteins in total inserted into a targeted cell membrane creating a lytic pore, releasing intracellular contents into the immediate surroundings. These signals enhance the inflammatory response and can subsequently lead to wound healing [Cole and Morgan, 2003].

Among all the known complement proteins, C3 interacts in the cascade as the pivotal factor. C3 is a highly versatile and multi-functional molecule. It is the most abundant complement protein in serum (1-2mg/mL) whose cleavage products C3b and C3a, once bound to their cell-surface receptors, serve as mediators of complement-dependent leukocyte functions. The three activation pathways converge to generate C3 convertase, the pivotal enzyme in this intricate network of reactions that cleaves C3. C3 is therefore at the heart of the complement system. Its cleavage into C3b and C3a activates its internal thioester bond and allows the stable covalent binding of C3b to hydroxyl groups on carbohydrates and proteins in the immediate surroundings. C3b that does not bind to a targeted cell surface is inactivated when its thioester interacts with a water molecule. Bound C3 on invading microorganisms for example, becomes a focus for further complement activation on and around a microbe or altered host cell, a process that results in the production of anaphylatoxins and the assembly of the membrane-attack-complex in the outer membrane of targeted cells.

Biological activities of complement do not only involve the formation of the C5b-9 membrane attack complex to direct cell lysis. Products of the enzymatic cleavage of C3 and C5 include the anaphylatoxins C3a and C5a mediating the acute effects of drug

(i.e. penicillin) or insect venom hypersensitivity, termed anaphylatoxic shock. Increased vascular permeability and mast cell degranulation (histamine release) occurs by the action of anaphylatoxins C4a, C3a, and C5a, in addition to C5a inducing neutrophil attraction and aggregation, chemotaxis, and cytotoxic activity by the release of reactive oxygen metabolites and proteases [Hugli, 1981; Chenoweth, 1987; Entman, 1991; Dreyer, 1991]. C5a is also involved in up-regulation of vascular P-selectin after systemic activation of complement [Chakroborti *et al*, 2000]. Smooth muscle contraction can be induced by C3a and C5a in the absence of histamine release [Hugli, 1981]. Anaphylatoxins play a key role in chemotaxis of eosinophils and monocytes and C3a is thought to mobilize neutrophils directly from the bone marrow [Goldstein, 1992]. The several biological activities of the anaphylatoxins C3a and C5a are exerted through binding to G-protein-coupled receptors C3aR and C5aR, respectively [Monsijohn *et al*, 2003]. C3aR and in particular the C5aR are expressed by monocytes/macrophages and neutrophils, as well as non-myeloid cells in several tissues such as lung, liver and brain. C5aR is also expressed by endothelial and epithelial cells [Gasque *et al*, 1995; Gasque *et al*, 1997; Fayyazi *et al*, 2000; Drouin *et al*, 2001]. Understanding of the signal transduction pathways triggered by interaction between anaphylatoxins and their receptors is still in its infancy, however, the MAP kinase pathway seems to be of key importance [Monsijohn *et al*, 2003]

C3b, the second by-product of direct C3 cleavage, attaches covalently to immune complexes for example, labeling them for clearance, an event that is followed by C5 binding and its enzymatic cleavage by C5 convertase to C5a and C5b [Bao *et al*, 2002]. Phagocytosis of immune complexes or other particles by neutrophils, mononuclear

phagocytes, and B-lymphocytes is initiated through the interaction of the opsonin C3b and its receptors on the surface of these cells. In addition, C3b is required for the generation of B-memory cells and T cell-dependent antibody responses [Bottger and Bitter-Suermann, 1987; Fearon and Carter, 1995; Carroll and Fischer, 1997].

C3b can further be cleaved into the opsonin iC3b. iC3b has been documented to deposit on human endothelial cells subjected to hypoxia and subsequent reoxygenation. Activated endothelium releases several factors such as IL-8, monocyte chemotactic protein 1 (MCP-1), LTB4, and platelet activating factor (PAF) that act either as chemotactic or activating factors for neutrophils, or may contribute to increased vascular permeability and cellular edema [Monsinjon, 2001]. Upon reperfusion after ischemia, complement may be activated through the classical and alternative pathway, but also the lectin pathway. MAC assembly in reperfusion injury may not cause lysis of nucleated cells, but in non-lethal amounts C5b-9 can add to endothelial activation, and also further promote an inflammatory response with activation of neutrophils, in addition to free radical and cytokine release [Cole and Morgan, 2003].

2.1.2 Complement activation by PDT

Inflammation induced by PDT has led to the study of the effects of various inflammatory mediators on the development of the anti-tumor effects of PDT. Pro-inflammatory cytokines interleukin 1beta (IL-1β), tumor necrosis factor-alpha (TNF-α), IL-6, breakdown products of arachidonic acid metabolism, histamine, and also complement have been shown to hold pivotal roles in the progression of an immune response against a PDT-treated tumor. In the early 1980s, work published by Kamide *et al* [1984] described

the involvement of the complement system and mast cell degranulation in the full development of the immediate phase of normal skin phototoxicity induced by PDT. Complement activation was shown in the sera of patients with erythropoietic protoporphyria and porphyria cutanea tarda. This was associated with the appearance of cleavage products of C3, and the generation of C5-derived chemotactic factor for human polymorphonuclear cells [Gigli, 1980; Lim, 1981]. In guinea pigs depleted of functional complement activity by intravenous delivery of cobra venom factor (CVF), the increase in vascular permeability induced by hematoporphyrin-PDT was significantly suppressed [Kamide *et al*, 1984]. These studies were, however, conducted studying cutaneous non-cancerous lesions. PDT in oncologic applications results in the participation of mast cells and the complement system in the immediate phase of porphyrin-based PDT phototoxicity. This process leads to the release of chemotactic factors by mast cells, or generated by complement activation, leading to neutrophilic infiltrate in the delayed phase of phototoxicity. Using the technique of immunohistochemistry, Cecic and Korbelik [2002] showed direct *in vivo* evidence of complement protein deposition. Elevated C5b-9 membrane attack complex in the murine EMT6 excised 30 minutes following the end of Photofrin-based PDT light treatment has been shown [Cecic and Korbelik, 2002]. To the best of my knowledge, this is to date the first published report of PDT-mediated engagement of the complement system against solid tumors.

2.1.3 Complement regulation

The effector branch of the complement system is constantly in a level of low activation and has therefore evolved alongside an intricate regulatory mechanism

avoiding homologous complement attack. These aforementioned protective molecules are expressed both on the surface of cells, and also in the fluid/plasma phase, inhibiting unprovoked activation and promulgation of the complement cascade to maintain homeostasis [Mollnes *et al*, 2002; Gelderman *et al*, 2002]. Complement components are very labile when activated and will undergo spontaneous inactivation unless bound to a subsequent complement protein required for the cascade of reactions to proceed.

Virtually every cell in the body expresses membrane-bound complement regulatory proteins (mCRPs), including tumor cells which often express higher levels than their normal tissue counterparts [Bjorge *et al*, 1997; Hakulinen and Meri, 1994; Hoffman *et al*, 1994; Jarvis *et al*, 1997; Koretz *et al*, 1993; Yamakawa *et al*, 1994]. This may be a mechanism by which tumors evade the cytolytic effects of an activated complement system, and also facilitates the survival of metastatic tumor cells as they enter circulation [Gorter and Meri, 1999]. The mCRPs of interest include CD46, CD55, Crry, and CD59. CD46 (membrane cofactor protein; MCP), a 60 kDa integral membrane protein, inhibits complement activation by acting as a cofactor for factor I-mediated cleavage of C3b and C4b [Cooper, 1999]. CD55 (decay accelerating factor; DAF) is a 70 kDa glycosyl phosphatidylinositol (GPI)-linked or trans-membrane protein that accelerates the dissociation of C3bBb and C4b2a complexes [Cooper, 1999]. The 65 kDa Crry is found only in rodents and displays functional overlaps to human CD46 and CD55 and seems to play a key role as a complement regulator in mice, although its full function has yet to be characterized [Xu *et al*, 2000]. CD59 (protectin) is a membrane inhibitor of reactive lysis and provides constitutive protection against complement-mediated lysis. CD59 is a 18 kDa protein expressed on most nucleated cells which binds to C8 or C9,

preventing polymerization of C9 and membrane pore formation by the membrane attack complex [Cooper, 1999].

2.1.4 Complement and cancer

One focus of complement-mediated cancer treatment is oriented toward blocking the inhibitory molecules found to be upregulated on the surface of tumor cells [Caragine, 2002; Caragine, 2002; Maenpaa, 1996; Li, 2001; Liszewski, 1996; Koretz, 1992]. C3b and C5b-9 binding has been documented on tumor and surrounding cells *in vivo*; however, this has been correlated and counteracted with upregulated expression of complement inhibitory molecules. Immunotherapy targeted at using complement activation has mainly been based on using monoclonal antibody inhibition of mCRPs and then following (perhaps) with antibody conjugates. For example, exposing cervical cells to either anti-CD59 or bispecific monoclonal antibody designed to inhibit both tumor antigen Ep-CAM and CD59 results in 80% cell lysis. Anti-CD55 therapy, however, had little response [Gelderman, 2002].

The host immune system's cancer cell surveillance mechanism is generally accepted to be cell-mediated cytotoxicity. The host immune response is equipped with cancer-fighting effectors such as NK cells. However, this is complicated by changes in surface molecule expression on tumor cells leading to escape from immune recognition and subsequent accelerated uncontrolled tumor growth [Campoli *et al*, 2002]. In addition, loss of major histocompatibility complex (MHC) Class I expression on primary and metastatic lesions decreases surveillance of cancerous lesions by cytotoxic T cells (CTLs) with the depression of tumor antigen peptide-MHC class I complex formation

[Marincoloa *et al*; 2003]. The authors describe how tumor-host interactions remain uncharacterized despite significant progress in the identification of tumor antigens recognized by autologous T cells.

Despite these complications indicated, immunotherapy remains a hot topic in the fight against cancer today [Korbelik, 1996], and the idea of non-specifically stimulating the immune system to reject tumors has begun to make a comeback since the pioneering applications some one hundred years ago [Roitt *et al*, 2001]. Non-specific stimulation of immune response against cancerous tissue using intralesional Bacillus Culmette-Geurin (BCG) can cause regression of melanoma [Vilella *et al*, 2003] and non-specific local immunization with BCG is effective against bladder cancer [Okamura *et al*, 2003; Chabalgoity *et al*, 2002]. Immunotherapy with cytokine can cause tumor regression and although successes have not been consistent, IFN-α, IL-2, IFN-γ and TNF-α have all seen some use in treating a few types of cancers [Roitt *et al*, 2001]. The *in vitro* expansion of T-cells and re-introduction into patients and/or *in vivo* expansion of CD4+ T cells in patients suffering advanced melanoma and metastases saw some success in reducing tumor burden [Curti *et al*, 1998; Li *et al*, 1999]. T-cell immunotherapy is perhaps the best known approach that at first gained great interest, after patients treated with this modality responded very well. However, in almost all cases, recurrent tumors and metastases were diagnosed. It seems as though the recurrent tumors have down-regulated levels of HLA-I antigens which render them unable to participate in HLA I-peptide complex formation on CTLs. The loss of MHC antigens is a particularly important escape mechanism of tumors that leads to the inability to present tumor antigen peptides [Chabalgoity *et al*, 2002]. Other forms of immunotherapy include use of anti-

cancer antibodies. Antibodies have been approved by the FDA for use in the treatment of non-Hodgkin's lymphoma and breast cancer [Saleh, 2003; White *et al*, 2001]. Cell death by antibody therapy may be driven by complement-mediated cytotoxicity via the classical pathway.

Treating cancer using the host complement system has been gaining increasing attention. Tumor cells have both C3 deposits and regulatory protein expression on their surface, rendering complement-mediated cell lysis ineffective in killing tumor cells. Tumor cells labeled with iC3b can, however, be recognized and destroyed by leukocytes bearing primed complement receptor 3 (CR3) [Xia and Ross, 2000]. The challenge is to prime CR3-expressing leukocytes against C3-opsonized tumor cells. Beta (β)-glucan polysaccharide therapy has been shown to be effective against tumors opsonized with C3, and even greater success can be achieved when the tumor is treated using a tumor-specific monoclonal antibody and polysaccharide combined therapy [Xia and Ross, 2000]. It is interesting to note that cytotoxic T-lymphocyte-mediated tumoricidal activity fails when tumors and metastases fail to or no longer express MHC I molecules [Seliger, 1997; Hicklin, 1998]. Beta-glucan therapy can however enable tumor antigen-specific cell mediated cytotoxicity of MHC Class I-deficient tumors [Xia and Ross, 2000]. Major tumor escape mechanisms of immune surveillance include loss of MHC Class I expression or by counter-veiling C3b deposition with increased expression of complement membrane-bound regulatory proteins. By priming leukocytes expressing CR3 and administering polysaccharide therapy or inducing local tumor damage for example by PDT to engage the complement system against a solid tumor seems quite justifiable.

The soluble fungal β-glucan schizophyllan (SPG) isolated from the culture filtrate of *Schizophyllum communae* has been employed in the treatment of cancer patients. In an experimental solid murine tumor model, SPG administered prior to PDT light treatment resulted in a significant increase in cell kill and overall tumor cure rate [Krosl *et al*, 1994a]. It was suggested that enhanced success of PDT in the presence of SPG was due to an increase in Mac-1 positive host cells (monocyte/macrophages), a cell population that retains high levels of Photofrin photosensitizer, infiltrating the tumor. The authors did not speculate that SPG polysaccharide treatment had primed CR3-bearing neutrophils, monocytes, macrophages, and/or NK cells to kill tumor cells at the PDT-treated site. The increased success of combined β-glucan therapy and PDT compared to PDT alone against the metastatic Lewis lung carcinoma may lie in the ability to overcome the inhibition of NK cell effector function against MHC Class I deficient metastatic lesions by increasing CR3-leukocyte mediated tumor cell kill.

The aim of the following studies was to demonstrate how the complement system responds to PDT applied to solid tumors in a murine experimental model. The effect on serum complement protein C3 levels, the actual changes in complement protein deposition on cell surfaces, expression of surface mCRPs, and the activity of complement in the tumors following treatment is outlined.

2.2 MATERIALS AND METHODS:

All flow cytometry was undertaken using the Coulter Epics Elite ESP apparatus from Coulter Electronics.

2.2.1 Cell culture and animal models

Squamous cell carcinoma SCCVII cells [Suit *et al*, 1985] were plated on 30 mm petri plates and allowed to divide in alpha-MEM + 10% FBS until 50% confluent. HUVEC cells (gratefully obtained from the laboratory of Dr. Dorovini-Zis, Vancouver General Hospital) from primary culture and used no later than four passages, were grown on 0.8 mg/mL fibronectin coated 30 mm petri plates in alpha-MEM containing horse serum. At 50% confluence 20 μg/mL Photofrin was added to the media and the cells further incubated at 37°C. Twenty-four hours following, the Photofrin-containing complete media was aspirated, the cells rinsed with cold PBS, then placed on ice and exposed to 630 nm red light for a total of 1 J/cm^2.

Two million SCCVII cells in a 30 μL volume were inoculated subcutaneously on the depilated lower dorsum of C3H/HeN female mice. The tumors were allowed to grow until they reached a largest diameter of 8 mm, at which point they were treated with PDT. PDT was applied as follows: 10 mg/kg Photofrin i.v., a volume of 0.2 mL/20 grams, and 24 hours later followed by 630 nm light illumination. For further details of the mode of

light delivery and instrument used please refer to Materials and Methods of Chapter 1, Section 1.2.

2.2.2 Serum collection for *in vitro* studies

The source of C3 for the *in vitro* studies described was freshly isolated mouse (C3H/HeN mice) or human (healthy volunteer lab member) serum included in the growth medium of SCCVII or HUVEC cells, respectively. C3H/HeN mice were exsanguinated by cardiac puncture and blood was placed directly into1.5 mL Eppendorf microcentrifuge tubes. The blood was left to clot at room temperature for 30 minutes, centrifuged, and the serum collected while discarding the remaining clotted leukocytes and other blood components. The serum was collected on the day of the experiment and kept on ice until added to cell cultures. For human HUVEC cell studies, a healthy volunteer donated his blood the morning of the experiment. The serum collected was kept on ice until utilized.

Mice in all experiments were either male or female and age-matched.

2.2.3 Flow cytometry

C3, HSP70, apoptosis

In vitro samples: During PDT light delivery of 1 J/cm^2, at a fluence rate of 15 mW/cm^2 and following treatment, the cell cultures were diligently kept on ice. Light delivery lasted on average 40 seconds per sample. Following light treatment, the PBS in which

the cells were treated was aspirated and replaced with alpha-MEM containing 20% freshly isolated serum. The cells were incubated at 37°C for 1 hour at which time they were harvested using 3 mg/mL dispase dissolved in Mg^{2+}/Ca^{2+}-free Hanks' buffer. All the cells were collected and washed twice with PBS and kept on ice. The SCCVII cell pellets were dislodged and 1μg of goat anti-mouse C3 conjugated to fluorescein isothiocyanate (FITC) (ICN pharmaceuticals, Canada) was placed in each. Following 30 minutes of incubation on ice, the unbound antibody was washed away and the cells analysed by flow cytometry. Controls incorporated into the experiment were Photofrin-no light, light-no Photofrin, and IgG control (Goat IgG-FITC from Jackson Immunoresearch, USA). The HUVEC cell pellets were dislodged and 1:100 dilution of goat anti-sera to human C3 (Quidel/Cedarlane Labs. Inc) was added to each sample for about 1 hour on ice. Incubation with donkey anti-goat-Alexa 488 (Jackson ImmunoResearch, USA) on ice was followed for 20 minutes. Another set of HUVEC cells was stained with mouse anti-human C3b (Research Diagnostics Inc, USA) followed by anti-mouse-Alexa488. Once surface staining of C3 binding was complete, a group of HUVEC cells was also labeled for apoptosis using the phycoerythrin (PE)-conjugated active caspase-3 monoclonal antibody apoptosis kit 1 (BD Pharmingen, CA) according to the manufacturer's instructions.

Heat shock protein HSP70 expression and the link between HSP70 expression and C3 binding onto PDT-treated SCCVII cells were analysed as follows. Following PDT treatment and incubation with naïve mouse serum, cells were separated into two groups: one group was analysed for surface HSP70 labeling and the other for intracellular HSP70.

Surface staining was assessed using an anti-HSP70 antibody (chicken IgY, Santa Cruz biotechnology, Santa Cruz, CA) followed by biotin-labeled donkey anti-chicken IgY (Jackson Immunoresearch, USA) and streptavidin-FITC. Prior to intracellular staining, cells were incubated in a permeabilizing buffer Cytofix/Cytoperm^{TM} (BD Pharmingen, CA). IgY isotype control was included using a ChromPure Chicken IgY whole molecule followed by biotin-labeled donkey anti-chicken IgY and streptavidin-FITC.

The link between HSP70 expression and C3 surface-labeling was evaluated by incubating a triplicate group of $1x10^6$ SCCVII cells per petri dish at 37°C with 1μg anti-HSP70 antibody (Santa Cruz Biotechnology), which was added to the complete media of alpha-MEM and 20% mouse serum following PDT treatment, then stained for C3 surface binding. Negative controls incorporated in this experiment included substituting freshly isolated serum with heat-inactivated (h.i) mouse serum or fetal bovine serum, and also adding EDTA into the reaction mix with 20% serum. EDTA acts as an inhibitor of complement activity.

C5b-9 assembly and C3b deposition on SCCVII cells following PDT was determined by incubating cells that had been harvested following PDT and exposed to freshly isolated mouse serum with either mouse monoclonal anti-human (cross-reactive with mouse) SC5b-9 (Quidel, CA) or rat anti-mouse C3b hybridoma supernatant (clone 3/26, courtesy of Dr. Anna Erdei, Hungary). Each sample of cells was exposed to a 1:100 dilution of antibody in Hanks buffered saline solution (HBSS)/1 mg/mL Bovine serum albumin (BSA)/0.02% sodium azide (NaN_3) for 1 hour on ice. Goat anti-mouse Alexa 488 or biotinylated anti-rat and streptavidin-phycoerythrin (PE) was added to the cells for 0.5

hours on ice to detect any bound SC5b-9 or C3b antibody, respectively. The cells were then analysed by flow cytometry.

To study the role of apoptosis in the complement protein binding to PDT-treated cells, 50 μM of the apoptosis inhibitor, caspase-3 substrate, Z-Asp(OME)-Glu(OME)-Val-Asp(OME) (Z-DEVD) (Enzyme Systems Products, Livermore, CA), was incubated with SCCVII cells in the hour-long incubation with freshly isolated mouse serum following PDT light delivery. The cells were then harvested and stained for C3 surface binding and analysed by flow cytometry.

The gating strategy of these experiments was as follows: Cell surface expression of C3, C3b, HSP70, and C5b-9 was assessed by separating cell populations that were either positive or negative for the fluorescent labeled detection antibody. After gating out cell debris defined as events at extreme low and high forward/side scatter, and doublets based on time of flight parameters, the cells were gated according to fluorescence label intensity, where negative was defined by the IgG isotype controls. Cells positive for surface staining were gated above the cutoff for the negative controls. The mean fluorescence per cell displayed as arbitrary units (a.u.) was plotted in a histogram then averaged among triplicate samples per treatment group. Apoptotic cells were separated along the same criteria then plotted against the fluorescence of the antibody labeling the surface protein in question. Cell surface labeling of C3 or HSP70 was quantified either as mean fluorescence per cell, or a percentage of the total number of cells/events positive for the C3 or HSP70 detection antibodies.

2.2.4 Immunohistochemistry for C5b9

EMT6 tumors were fixed in 10% phosphate-buffered formalin with a minimum 24-hour incubation time prior to embedding in paraffin. EMT6 tumors were used in these studies as a continuation of results outlined in Chapter 1. Untreated and PDT-treated tumors were sectioned (5 μm) onto glass slides and re-hydrated, then placed in antigen-retrieval citrate buffer (Biogenex, San Ramon, CA). The slides were heated in a microwave set at 40% of total power. Once the sections were cooled, they were incubated in a 3% hydrogen peroxide (H_2O_2) solution (30% H_2O_2 diluted in methanol) to block for endogenous peroxidase activity. Subsequently, sections were incubated overnight at 4°C in diluent alone in the absence of antibody (negative control), or a 1:100 dilution of either monoclonal mouse anti-human SC5b-9 (cross-reactive with murine SC5b-9) (Quidel, CA), or isotype-matched control immunoglobulin (mouse IgG2aκ, Sigma, St. Louis, MO). The immunohistochemistry protocol was based on a standard ABC procedure using a mouse-on-mouse Vectastain kit (Vector Laboratories, Burlington, Ontario, Canada) according to the manufacturer's instructions. The biotinylated anti-mouse IgG (H+L) secondary antibody was provided with the kit. Color was developed using a diaminobenzidine substrate (DAB). Images were collected using the NIKON coolpix 995 digital camera attached to a NIKON Eclipse E400 microscope and Nikonview software.

2.2.5 Membrane-bound complement regulatory proteins, antibody-labeling and flow cytometry

SCCVII tumors were excised either untreated or at 0.5 hour and at 3 hours following PDT, then minced between two #22 scalpel blades, and suspended in PBS. Dispase (3 mg/mL), collagenase (4 mg/mL), and DNase (10 mg/mL) were added to the minced tumor and the suspension placed to incubate, rotating, at 37°C for 30 minutes. The suspension was then filtered through a 100 μm nylon mesh filter and centrifuged. The cell pellet was dislodged and the cell concentration determined by hemacytometer. Approximately one million cells were used per sample. Fc-gamma receptors were blocked with Fc gamma receptor antibody concentrated hybridoma supernatant then stained for CD45 pan-leukocyte marker and either hamster anti-mouse CD55 (hybridoma clone RIKO-2, Dr. N. Okada, Japan), rabbit anti-mouse CD59-biotin (Santa Cruz Biotechnology, Santa Cruz, CA, USA), or rat-anti-mouse Crry-biotin (BD Pharmingen, San Diego, CA, USA). The detection antibodies used were either anti-hamster IgG-cychrome conjugate (Sigma), or streptavidin-cychrome conjugate (BD Pharmingen). Isotype controls were incorporated in flow cytometry preparations.

2.2.6 Mouse C3 isolation and purification

The protein mouse C3, a β-glycoprotein of m.w. 210,000 consisting of two non-identical, disulfide-linked polypeptide chains [Gyöngyössy and Assimeh, 1977], was isolated and purified from the plasma of male DAB/2J (C5-deficient) mice (The Jackson Laboratory, Bar Harbor, ME, USA) with the assistance of Dr. Katherine Serrano (Canadian Blood

Services, Department of Pathology and laboratory Medicine, UBC, Vancouver, Canada). Blood was collected by cardiac puncture into syringes containing 0.1 mL of 0.1M Na_4EDTA, pH 7.6. A total of 17 mL of EDTA-plasma was collected by centrifugation and stored at –80°C for one week prior to C3 isolation and purification according to the protocol by Gyöngyössy and Assimeh (1977). A protein yield of 1.46 mg active mouse C3 was obtained. The purity of mouse C3 collected in elution fractions was verified by resolving SDS-page gel electrophoresis, shown in Figure 2.10. Purified mouse C3 was used as the protein standard in an enzyme-linked immunosorbent assay (ELISA) to quantify C3 levels in the sera of mice bearing PDT-treated tumors.

2.2.7 Serum collection

At multiple time points following PDT treatment of their dorsal, subcutaneous tumors, mice were sacrificed by CO_2 inhalation then exsanguinated, the blood allowed to clot at room temperature for 30 minutes, centrifuged and the serum then collected, separated into aliquots, and placed immediately at -80°C where it was stored until tested. All sera were thawed only once and stored at 4°C thereafter for no longer than one week prior to analysis. All time points (0, 1, 3, 6, 12, 24, 72 hour, 1 week) were compared to sera obtained at the same bleeding from tumor-bearing mice that were not treated with PDT.

2.2.8 Tumor homogenates

For the following studies we had to employ the Lewis lung carcinoma (LLC) since it is a tumor cell line that is syngeneic to the C57BL/6 mouse strain, and therefore able to form tumors in the C3 knockout mouse strain of the same background. The C3 knockout was employed in the studies outlined in Chapter 3. LLC tumors were treated with PDT (Photofrin 10 mg/kg and 150 J/cm^2) then excised at various time points following light delivery. Immediately following excision, the tumors were placed in 1 mL of PBS containing 10 μL of a protease inhibitor cocktail (Sigma). Each tumor was homogenized for 10 seconds with a Polytron PT 3100 homogenizer (Kinematica AG, Switzerland), placed on ice, and centrifuged at 20,000g in a Micromax bench-top ultracentrifuge (International Equipment Company, Needham Heights, MA, USA) to obtain supernatant. The supernatant was stored at –80°C until analysed.

2.2.9 Mouse C3 ELISA

Complement protein C3 ELISA was performed according to a slightly modified version of that described by Taktak and Stenning [1992]. A volume of 100 μL containing 1:1000 dilution of goat anti-mouse C3 F(ab')2 fragments (Cappel Laboratories, Durham, NC, USA) in PBS was added to coat each well of a NUNC Maxisorp 96-well plate followed by incubation overnight in a 4°C cold room. Following 3 washes in PBS/0.05% Tween20, 100 μL of 5% heat-inactivated fetal bovine serum in PBS, 0.05% Tween20 and 0.001% Dextran sulfate solution was added to each well to block non-specific binding

sites. After 1.5 hours of incubation at 37°C the blocking solution was decanted and the plate blotted on a stack of dry paper towels. The plate was not washed prior to the addition of C3 standard or the test sera samples. Standard and test samples (sera or tumor homogenate supernatants) were diluted in blocking solution and added to designated wells in 100 μL volumes. The serial dilution of protein C3 standard increased from blank (buffer only) to 0.4 μg/mL. All test sera were diluted 2.5-5 x 10^4 times prior to being added to their designated wells in the test plate. Following a 1 hour incubation at 37°C, the wells were washed three times and 100 μL peroxidase-conjugated goat anti-mouse C3 (1:5000; Cappel) in PBS/0.05% Tween20/1% normal goat serum was added to all wells but negative controls and the plate incubated covered with Parafilm at 37°C for 1 hour. The plate was washed and 100 μL of 0.4 mg/mL OPD in phosphate-citrate buffer pH 5.0 was added to each well for 20 minutes at 37°C. The reaction was stopped by the addition of 150 μL 1M H_2SO_4 per well and absorbance determined at 490nm in a Dynex MRX micro-plate reader (Dynex Technologies Inc, Chantilly, VA, USA). The standard curve acted as a reference for protein concentration at a particular absorbance allowing quantification of C3 levels in the sera and tumors of mice harvested following PDT.

2.2.10 Semi-quantitative mouse C3b ELISA

The presence of C3b in tumor homogenates is indicative of the breakdown of C3 by the activation of the alternative pathway. C3b ELISA was slightly modified from the C3 ELISA described above. Undiluted tumor homogenate supernatants were placed in the wells of a 96-well NUNC Maxisorp plate in 100 μL aliquots. The plates were incubated

for 1.5 hours at 37°C. The plates were then washed three times with PBS/0.05% Tween20 and 100 µL of blocking solution (5% FBS/PBS/0.05% Tween20/ 0.001% dextran sulphate solution) was added to each well with an additional 1.5 hour incubation at 37°C. The plates were washed three times and a concentration of 0.8 µg/mL of rat anti-mouse C3b hybridoma supernatant (courtesy of Dr. Anna Erdei, Hungary) was added to each well, with the exception of negative controls which were filled with buffer only. Upon a one hour incubation at 37°C the wells were washed three times and a 1:100 dilution of goat anti-rat IgG conjugated to horseradish peroxidase was added to each well for 30 minutes at 37°C. Following three more washes, OPD solution was added to each well for 20 minutes at 37°C and the reaction stopped with the addition of 150 µL of 1M H_2SO_4 per well. Absorbance was read at 490nm on a Dynex MRX micro-plate reader (Dynex Technologies Inc). The results were expressed as relative values compared to the level in untreated tumors.

2.2.11 Alternative pathway activation

Zymosan A particles, derived from the yeast cell wall of *Saccharomyces cerevisiae* (Sigma) at a concentration of $1x10^9$/mL in endotoxin-free Dulbecco's PBS (DPBS) were activated by boiling for 60 minutes in a double boiler system, then washed twice in DPBS before being added to reaction tubes. The reaction tubes contained: 10 µL of zymosan particle solution, 10 µL EGTA and $MgCl_2$ to their respective final concentrations 10 mM and 5 mM, 10 µl of serum and 70 µL of DPBS to make a total of 100 µL volume per tube. The reaction tubes were incubated at 37°C for 30 minutes to allow C3 to bind to

the zymosan particles, indicative of alternative pathway activation. The reactions were stopped with the addition of 200 μL of 20 mM EDTA and the tubes set immediately on ice. The particles were centrifuged and washed in DPBS/1% FBS, then incubated on ice for 30 minutes with goat anti-mouse C3 (Cappel). The particles were washed and re-suspended in 0.5 mL DPBS/1% FBS prior to analysis by flow cytometry. Whole molecule goat IgG conjugated to FITC was used as an isotype control. Experimental design was adapted from Dr. Damian Kraus (University of Colorado Health Sciences Center, Denver, Colorado) [Foley *et al*, 1993; Quigg *et al*, 1998]. Due to the small size of the zymosan particles the parameters of detection in flow cytometry were changed compared to analysis of tumor and/or endothelial cells. The volts were set to 190 compared to 370 and the forward scatter gain was increased 25 times from 2.0 to 50.0 for the eukaryotic cells and zymosan particles, respectively.

2.2.12 Classical pathway activation

Experimental design was loosely based on a protocol described in Molina *et al* (1992) and Quigg *et al* (1998). SCCVII tumor cells were grown in culture and harvested using 3 mg/mL dispase in Hanks' Mg^{2+}/Ca^{2+}-free buffer and suspended in alpha-MEM containing 2 mM $MgCl_2$ and 0.15 mM $CaCl_2$ (alpha-MEM/Mg/Ca) at a concentration of $2x10^5$ per 100 μL. To each 100 μL vial of cells was added 5 μg of anti-cytokeratin 5 and 8 monoclonal antibody (Chemicon International, Temecula, CA, USA) diluted in 80 μL of alpha-MEM/Mg/Ca and 20 μL of serum to be tested. The reaction was allowed to proceed at 37°C for 60 minutes. The reaction was stopped by the addition of 100 μL of

100 mM EDTA to all samples and the reaction tubes set on ice immediately. All samples were washed in DPBS/1% FBS and stained for the presence of mouse C3 using FITC-conjugated goat anti-mouse C3 antibody and analyzed by flow cytometry.

2.2.13 Statistical analysis

Data are presented as mean ± standard error of the mean (SEM). Analysis of variance using one-way ANOVA and a post-hoc comparison using the LSD test were used to test for significant differences between control and treated samples. $p<0.05$ was considered a statistically significant difference. Statistical analyses were performed using the software program Statistica 6.1 (StatSoft, Inc.).

2.3 RESULTS AND DISCUSSION

The hypothesis underlying the work described in this chapter is that damage inflicted by PDT to cells/tissue results in the engagement of the complement system against a solid tumor. Results compiled and summarized in Figures 2.1 through 2.5 show the deposition of complement proteins on PDT-treated cells/tissue both *in vitro* and *in vivo*. Results of experiments described in Figures 2.6 through 2.8 describe one mechanism by which cell surface deposits of complement proteins are enhanced by conjunctive HSP70 expression, the latter a response to PDT. Thirdly, the state of membrane-bound regulatory protein expression was investigated and described in Figure 2.9. Ultimately it was sought out to define that complement protein deposits on cell surfaces in response to PDT-inflicted damage, and initiates the activation of the complement cascade that leads to leukocyte stimulation and direct cell lysis. Complement activation by the alternative pathway was confirmed to occur both systemically in serum and locally in the tumor following PDT treatment. These results are defined in Figures 2.11 through 2.18.

2.3.1 Complement protein deposition on tumor cells *in vitro* and *in vivo*

Damage inflicted by PDT can induce complement deposition on cells/tissue. SCCVII cells were treated by Photofrin-based PDT and exposed to freshly isolated C3H/HeN mouse serum as a source of complement protein C3. C3 is a pivotal protein in the complement system and therefore its presence on the surface of cells is an indicator of complement activation. Our initial test was to determine the time point following PDT at

which the greatest levels of C3 deposition are detected by flow cytometry on cells. PDT-treated cells were harvested following 30 minutes, 1 hour, and 2 hours of incubation at 37°C in the presence of mouse serum. As Figure 2.1 indicates, the most enhanced C3 deposition compared to untreated controls was detected 1 hour following treatment. This time point was thereafter designated as the time of cell harvest in all subsequent *in vitro* PDT treatment experiments. No significant increase in C3 deposition was detected in the absence of light (Photofrin only), absence of photosensitizer (light only), or PDT in the absence of mouse serum (heat-inactivated fetal bovine serum only). Blocking apoptosis with the addition of an active caspase-3 inhibitor Z-DEVD into the medium of PDT-treated cells significantly inhibited C3 surface deposition induced by PDT (Figure 2.1).

The majority of complement proteins are constitutively produced by hepatocytes and released into circulation to monitor their host for pathogens. Complement proteins have the intrinsic ability to distinguish self from non-self, their prime purpose was to evolve as a natural defense against foreign invaders [Embers, 1997]. In coming in contact with their target, complement proteins act as opsonins, labeling a pathogen for phagocyte recognition and clearance with C3 and its subsequent breakdown products C3b and iC3b. Alternatively, complement proteins can induce lysis of a cell directly with the formation of the membrane attack complex (MAC). When the complement system is activated with uninterrupted continuance of the cascade of enzymatic reactions, the process ends with the formation of the MAC comprised of the complement proteins C5b through C9. The C5b-9 complex is formed once the C5 convertase enzyme splits C5 into its breakdown products C5a and C5b. C5a the anaphylatoxin acts as a potent neutrophil chemoattractant and activator. C5b however binds to its membrane receptor promoting

the subsequent docking of C6, C7, and C8. The C5b678 complex initiates the binding and penetration of the lipid bilayer by C9, an event that leads to the production and assembly of a membrane pore by sequential additions of C9 proteins until a physical pore is created releasing intracellular contents into its immediate surroundings with promulgation of inflammation and cell death, or in non-lethal quantities, can promote neutrophil chemotaxis [Kilgore *et al*, 1998]. C5b-9 has multiple pro-inflammatory functions. The effect on leukocytes includes chemoattraction, enhanced expression of CD11b, enhanced toxic oxygen metabolite production and also increased expression and release of pro-inflammatory substances such as leukotrienes and chemokines MIP-1 alpha and MIP-2. In addition, C5b-9 can augment the expression of the adhesion molecules P-, E-selectin, and ICAM-1. MAC can increase vascular permeability, vasoconstriction and induce endothelial cell lysis. This protein complex can also bind to normal host cells when activated, as in reperfusion injury [Kilgore *et al*, 1999; Zhou *et al*, 2000]. In this case, activated complement is implicated to be the main mediator of ischemia/reperfusion injury. In similar circumstances, following Photofrin-based PDT, C5b-9 assembly was shown to occur both *in vitro* and *in vivo*. Using flow cytometry C5b-9 assembly on PDT-treated SCCVII cells was detected to be significantly higher than untreated cells. Control groups of cells following incubation in the absence of light treatment (Photofrin only), absence of photosensitizer (light only), or IgG isotype control, had no significant effect on C5b-9 assembly (Figure 2.2). The ability of PDT to induce changes on the membrane of SCCVII cultured tumor cells that instigate complement deposition was then verified *in vivo*. Using the technique of immunohistochemistry, C5b-9 assembly was demonstrated in SCCVII and EMT6 tumor sections excised within 1

hour of PDT (Figures 2.3 and 2.4, respectively). Compared to untreated control tumors, C5b-9 assembly stained in significantly higher levels following PDT. The staining was shown to be extra-nuclear, concentrated on the cell surface and cytoplasm, throughout the tumor parenchyma and also on endothelial cells (see endothelial cells on a small vessel indicated by black arrows). Complement protein deposition and lytic complex assembly on PDT-treated tumors and cultured cells has not been studied to date. The finding that complement activity on tumor cells can be initiated by PDT may lead to many answers to further characterize the mechanism of action of the secondary, immune-mediated, effects of PDT.

The presence of C5b-9 on PDT-treated cells may play a dual role by inducing direct cell lysis to otherwise PDT-damaged cells and/or in non-lytic concentrations, the C5b-9 terminal complement protein complex can act as a neutrophil chemoattractant and activator. Therefore, the C5b-9 complex may be inducing secondary damage to PDT-treated tissue and also promote the inflammatory response through the amplification of neutrophil chemotaxis and enhanced stimulation. Generation of superoxide anion is enhanced in neutrophils by complement protein interactions with their complement receptor CR3, CD11b/CD18 (Mac-1) [Vaporciyan, 1993].

In addition to tumor cells, we investigated C3 levels on normal, endothelial cells, more specifically, human umbilical-vein endothelial cells (HUVEC). The vascular bed is highly vulnerable to homologous complement attack since it is in constant interaction with complement proteins in circulation. These cells were treated with the same dose of Photofrin-based PDT as were the SCCVII tumor cell cultures, and were than exposed to human serum as a source of native complement C3. The serum was collected on the

morning of experiment from a healthy volunteer. Using flow cytometry, C3 deposition was detected following PDT and compared to multiple control groups including PDT-treated cells exposed to heat-inactivated fetal bovine serum, heat-inactivated human serum, and untreated cells exposed to human serum (Figure 2.5). All control groups had low but insignificant levels of C3 staining above naïve, untreated cells, yet C3 deposition is significantly enhanced on PDT-treated HUVECs compared to untreated controls. Protein C3 will deposit as an opsonin on cells undergoing apoptosis, the mechanism by which apoptotic cells are recognized by complement receptors on phagocytic macrophages and neutrophils, and is an important event in wound healing. Low levels of sialic acid and/or other changes defining the overall change in carbohydrate pattern on the surface of apoptotic cells such as increased levels of galactose and N-acetylglucosamine characterize apoptotic cell-associate molecular patterns and are proposed to be recognition sites for complement proteins [Elward and Gasque, 2003]. Figure 2.5 demonstrates that following PDT, non-lethal damage to cells designated as viable cells, do have a significantly elevated level of C3-labeling, however, cells undergoing apoptosis in response to PDT have the most significant increase in surface C3-labeling following treatment of all cell groups tested in the presence or absence of PDT. It follows that blocking apoptosis inhibits PDT-induced C3 surface deposition on SCCVII cells (far right column in Figure 2.1).

HUVEC cells following PDT treatment were also stained and evaluated by flow cytometry for surface deposits of C3b. C3b is a breakdown product of C3 and is therefore indicative of complement activation, with a major role as opsonin of cells undergoing cell death by apoptosis. As the inset graph of Figure 2.5 shows, there is a

significant rise in C3b on HUVEC cells following PDT compared to untreated controls with an increase of 20% more cells positive for C3b deposition following PDT treatment. Phagocytosis of complement–opsonized targets is a primary function of neutrophils at sites of inflammation, and the clearance of neutrophils that have phagocytosed wounded cells is important in the resolution of inflammation and wound healing [Zhang *et al*, 2003]. C3b labels apoptotic cells for clearance from a site of injury by macrophages and subsequently carried over to draining lymph nodes [Cole and Morgan, 2003]. It is through this mechanism that there may be a bridging link between complement activation and the formation of immune cell memory instigated by PDT of solid tumors. The recognition and phagocytosis of apoptotic bodies from PDT-treated lesions by macrophages and transport to draining lymph nodes, may lead to the presentation of tumor cell antigens on MHC molecules and subsequent presentation of these tumor-specific antigens to T cells. Complement plays a strong and pivotal role in the development and directing of an adaptive immune response, as well as maintenance of immunological memory [Song *et al*, 2000].

With its role in acquired immunity, the complement system has become a primary focus of investigators to define the underlying mechanism(s) by which PDT-generated vaccines function. Complement binding to tumor antigens strongly promotes immune recognition, T-cell recruitment, and co-stimulatory action on T cell signaling with enhanced proliferation of antigen-specific T cells [Arvieux *et al*, 1988; Dempsey *et al*, 1996; Kerekes *et al*, 1998; Song *et al*, 2000; Tsuji *et al*, 2000]. The link between tumor antigen presentation and complement activity was elegantly demonstrated in an experiment in which a PDT-generated Lewis lung carcinoma (LLC) vaccine did not

retard the growth of LLC tumors in mice with impaired complement activation (C3 knockouts) as it did in C57BL/6 mice with normal complement function [Korbelik, 2002]. It was speculated that normally PDT-treated cancer vaccine cells in a C57BL/6 mouse are opsonized with C3 proteins [Korbelik and Sun, 2003]. This opsonization may lead to recognition by macrophages and dendritic cells for example, and processed onto the surface of these cells on MHC molecules then carried to draining lymph nodes, where tumor antigens may be presented to T-cells with subsequent formation of immune cell memory specific for that tumor. In experiments delivering PDT-treated tumor cell lysates as a vaccine, Gollnick *et al* realized that PDT-generated lysates are more effective tumor vaccines than are ultraviolet, freeze-thaw, or gamma-irradiated vaccines, due to increased dendritic cell maturation, measured by the expression of MHCII or CD86 flow cytometry [Gollnick *et al*, 2002].

C3b opsonization of PDT-generated vaccines or PDT-treated cells in general is mediated, at least in part, by the expression of the stress protein heat shock protein 70 (HSP70) [Korbelik and Sun, 2003]. Heat shock proteins play a complex role in the function of the immune system, activating both humoral and cellular immune responses, as well as the complement system [Kocsis *et al*, 2002]. The action of HSP70 induces potent pro-inflammatory responses in human monocytes, acts as a messenger of stress and activator of the complement system [Prohaszka *et al*, 2002]. A common receptor for many of the heat shock proteins including HSP70 is CD91 [Basu *et al*, 2001]. Interactions between HSPs and CD91 seem to mediate phagocytosis of apoptotic cells by macrophages [Ogden *et al*, 2001; Vandivier *et al*, 2002]. For these reasons, HSP70 expression on *in vitro* PDT-treated cells was investigated using HSP70 flow cytometry on

HUVECs. Approximately ten percent of untreated, naïve cells do express surface HSP70 however, 1 hour incubation at 37°C in the presence of human serum post PDT increases the percentage of cells in the population expressing HSP70 to twenty-five. Exposing PDT-treated HUVEC cells to media containing heat-inactivated human serum did not raise the level of HSP70 expression (Figure 2.6). SCCVII tumor cells also express increased levels of HSP70 on their surface paralleled with a decrease in the expression of intracellular HSP70 expression shown in Figure 2.7 following PDT. PDT evidently induces a quick response in cells to express HSP70 on their surface by the transfer of intracellular stores of HSP70 to the outer membrane. Isotype controls replacing the anti-mouse HSP70 antibody with the isotype control Chicken IgY for flow cytometry confirmed no significant unspecific background antibody staining in the procedure.

Attempting to understand the effect of HSP70 expression on C3 deposition, SCCVII tumor cells were treated with PDT then incubated with either freshly-isolated mouse serum or serum in the presence of an anti-HSP70 antibody. Blocking HSP70 following PDT significantly dropped the level of C3 surface labeling compared to incubating with mouse serum, or heat-inactivated fetal bovine serum (h.i. FBS). Untreated, naïve cells exposed to either mouse serum or h.i. FBS had little C3 deposited on their outer membranes. This experiment verifies that HSP70 expression promotes C3 surface deposition on PDT-treated cells. Furthermore, in Figure 2.8 an inset graph also indicates significantly higher levels of C3b-labeling on SCCVII cells following PDT. The presence of C3b is indicative of complement activation by the alternative pathway. Evidently, C3b-labeling is elevated on both tumor cells and endothelial cells (Figure 2.5) when the alternative pathway of complement is activated by changes inflicted on the

surface of cells by PDT *in vitro*. Alternative pathway activation can be verified by detecting a product of C3 cleavage via this complement pathway, namely C3b. The latter is indicative of alternative pathway activation as also described for elevated C3b deposition on HUVEC cells in Figure 2.5.

2.3.2 Expression of membrane-bound complement regulatory proteins

In addition to the pro-inflammatory effects of complement proteins outlined in the beginning of this chapter, anaphylatoxin C5a is also a potent stimulator of neutrophil superoxide production and adherence to endothelium, initiating tissue damage mediated by neutrophils. In a model of myocardial ischemia/reperfusion injury, elevated expression of adhesion molecules CD18 on neutrophils and P-selectin on endothelial cells in part by the action of complement activation, led to enhanced adherence by neutrophils to coronary artery endothelium [Chakraborti *et al*, 2000]. The complement cascade, particularly the alternative pathway is activated during myocardial ischemia/reperfusion, effects of which parallel those that occur during and in response to Photofrin-mediated PDT of solid tumors. During ischemia/reperfusion injury, complement fragments such as anaphylatoxins C3a and C5a are produced both locally and systemically, and the membrane attack complex is deposited on cell membranes at the site of injury. Subsequent release of mediators such as histamine and platelet activating factor (PAF) ensues, causing an increase in vascular permeability associated with cellular edema [Chakraborti *et al*, 2000]. These events seem to parallel the host

inflammatory response to Photofrin-mediated PDT in solid tumors and allows one to speculate the role that complement activation may have in PDT-treated tumors.

The complement cascade may be separated into two main parts that evolved in tandem. One is the effector system enhancing immune cell activation and inflicting direct cell death through cell lysis, and the other, internal regulation. The complement system is in a constant state of low activation and therefore normal cells are protected from autologous complement attack by expressing membrane-bound regulatory complement proteins (mCRPs). These regulatory proteins inactivate complement enzymes and proteins on cell surfaces [Liszewski, 1996; Atkinson, 1991; Devine, 1991]. In a disease or pathological state, cells tend to shed mCRPs allowing complement proteins to bind to receptors and promote tissue damage [Gorter and Meri, 1999]. MCRP expression if often elevated on tumor cells, a mechanism by which tumors may escape immune surveillance [Gorter and Meri, 1999]. Recently it has been hypothesized that elevated mCRP expression may be a reason why some patients suffering B-cell malignancies do not respond as well to Rituximab therapy as others [Cerny *et al*, 2002]. Loss of mCRPs may contribute to direct damage of cells in PDT-treated tumors by no longer protecting against MAC assembly and C3(b) deposition. This could in theory be advantageous to the host by further engaging complement attack in response to PDT. This rationale led to the investigation of mCRP expression in tumors. Evaluating the levels of CD55, CD59 and Crry (the latter exclusive to rodents) in SCCVII tumors excised without treatment, or 1 and 3 hours post PDT, Figure 2.9 reveals a significant drop in the expression of these molecules following treatment.

2.3.3 The status of complement activity in mice bearing PDT-treated tumors

In addition to demonstrating that the balance between complement protein deposition and mCRP expression is skewed in response to PDT, it is pertinent to demonstrate the status of local and systemic complement activation following treatment. The significance of complement activation is multifarious. Activation of the cascade along the alternative pathway promotes continuation of the unidirectional series of enzymatic reactions leading to both the promulgation of white blood cell chemotaxis in particular neutrophils, and also platelets to migrate toward the PDT-inducted injury. The result can be a sequestration and aggregation of these cells to promote cell plug formation leading to blood flow stasis. Moreover, these cells when activated can further promote the inflammatory response leading to the formation of oxygen metabolites in addition to singlet oxygen production via the photodynamic process. Cumulatively, these events in part lead to the classical signs of inflammation: increased vascular permeability, edema, heat, and discomfort. Activated complement reactions can induce precarious damage to target cells.

The complement system is activated by a variety of disease-associated stimuli including via the classical pathway by antibodies or immune (antibody-protein) complexes, or the alternative pathway by injured or ischemic tissue, altered cell surfaces or infections. An indication that the potential for activation of the complement cascade is elevated levels of C3 protein in circulation. In a time-course experiment, the sera of mice were collected from separate groups following Photofrin-PDT of the Lewis lung carcinoma tumor model. Using the technique of enzyme-linked immunosorbent assay, C3 concentration was quantified. Figure 2.10 shows the purity of isolated mouse C3 on a

resolving SDS-page gel that was used as the protein standard in the C3 ELISA protocol. In Figure 2.11 the kinetics of C3 levels in circulation following PDT is shown. Prior to PDT, the level of circulating C3 is elevated above baseline in mice bearing untreated subcutaneous tumors. Baseline was measured from tumor-free mice. Following PDT, C3 levels fall significantly compared to untreated tumor-bearing mice 1 hour post treatment. This implies a prompt catabolism and consumption of existing complement proteins following PDT above the rate at which this protein is produced and released into circulation by hepatocytes. Levels of C3 in circulation increase back to untreated levels 6 and 12 hours following treatment suggesting an increased rate of production and significant rise at 24 hours that begins to fall back to untreated levels at 72 hours following treatment, but remains significantly higher than in untreated tumor-bearing mice. Quantity of C3 in the sera of mice falls back to untreated levels by one week following treatment. A similar pattern was also observed in mice bearing PDT-treated FsaR tumors (Figure 2.14).

Activation of the complement cascade via the classical pathway in the sera of mice bearing PDT-treated tumors was assessed. Using the Lewis lung carcinoma tumor model, serum was collected in either untreated tumor-bearing mice or in separate groups of mice at the following time points following the end of PDT light treatment: 0, 1, 6, and 24 hours. Detection of classical pathway activation depends on coating of cells with the anti-cytokeratin 5/8 antibody, specific for carcinoma cells, prior to analysis. The results summarized in Figure 2.12 demonstrate that applying sera collected from PDT-treated mice to SCCVII cells upon coating of these cells with antibody, leads to little, insignificant variation in the level of classical pathway activation following treatment.

Since Photofrin-based PDT applied in the treatment of solid tumors results in events that parallel ischemia/reperfusion injury, it seemed logical to test for activation of the complement cascade via the alternative pathway. Figure 2.13 indicates that, indeed, alternative pathway activation can be induced by the sera of mice bearing PDT-treated LLC tumors collected at various time points following treatment and exposed to heat-activated baker's yeast wall zymosan particles. Serum that was collected immediately (0 min), 1, 3, 6, and 12 hours post treatment showed insignificant changes in the level of complement activation evaluated by C3 flow cytometry compared to untreated controls;, however, 24 and 72 hours following treatment, these sera samples demonstrated a highly significant rise in complement activity via the alternative pathway. Complement activation fell to baseline pre-treatment levels at one week following PDT. Alternative pathway activation of the complement cascade in the sera of mice bearing PDT-treated FsaR tumors parallels a fall of circulating C3 at 6 hours and a significant rise at 24 and 72 hours following treatment (Figure 2.15). Complement activity via the alternative pathway in mouse serum was unaffected by the administration of either Photofrin or BPD (a photosensitizer applied in studies outlined in Chapter 3). Inflammation is normally cleared in three days, therefore it was interesting to observe that complement activation in serum remains elevated at 72 hours following tumor-PDT treatment. This is indicative of a highly potent response by the complement cascade with emphasis of its potential to sustain pro-inflammatory activity against a PDT-treated tumor.

The level of protein C3 in the sera of mice bearing PDT-treated tumors was compared to the C3 content locally at the site of PDT treatment, the tumor. LLC tumors were excised at various time points following PDT light delivery and C3 content

determined as for serum samples by ELISA. Figure 2.16 indicates that the level of C3 increases significantly at 3, 6, and 12 hours whereas it decreases at 24 hours post treatment. It is important to note that at 24 hours, the tumors are nearly completely ablated with little tumor mass remaining to be collected and analysed. This may have an impact on the relative amounts of protein detected following PDT compared to untreated tumors. Nevertheless, this data importantly indicates that C3 protein quantities rise locally in the site of treatment in response to Photofrin-PDT. It will be of interest to demonstrate whether or not C3 is solely delivered from circulation in a PDT-treated tumor, or whether it is produced locally in tissue by immune cells such as macrophages (a proven source of extra-hepatic C3 production [Laufer *et al*, 1995; Hogasen *et al*, 1995]) in response to therapy.

In addition to C3 content in PDT-treated tumors over time, the status of complement activation in the LLC tumor following PDT was determined since systemic alternative pathway activation in serum does not directly reflect the status of complement activation locally at the site of PDT delivery. Two different methods were applied to determine complement activation via the alternative pathway in supernatants separated from crude tumor homogenates: C3b ELISA indicative of C3 breakdown by the alternative pathway C3 convertase enzyme, and by C3 flow cytometry on heat-activated zymosan particles. In Figure 2.17 C3b content is assessed as absorbance. Unfortunately, a source of purified mouse C3b was unavailable for this analysis therefore we were unable to quantitate absolute C3b content in tumors against a standard protein curve. Nevertheless, absorbance of antibodies covalently bound to C3b in tumor homogenate supernatants was plotted against time. The analysis demonstrates that C3b content is

elevated significantly at 3, 6 and 12 hours following treatment. Figure 2.18 defines that the activity via the alternative pathway of the complement cascade assessed by the latter method, is significantly elevated 3, 6, and 12 hours following PDT light delivery to the LLC tumor model compared to the level of activation in untreated tumors. Importantly, the level of activation falls toward untreated levels at 24 hours post treatment even though the level of activation in the serum remains significantly increased. At 24 hours following treatment the tumors were nearly completely ablated with little material to collect.

A peak in C3 content is documented later in serum (24 hours) compared to tumors (3, 6, 12 hours), while already within 1 hour following treatment C5b-9 levels are significantly elevated in tumors. This suggests two sources of complement: the liver and the tumor. PDT may initiate greater production of C3 in the liver but elevated levels are undetected as these stores are depleted and directed to the site of PDT damage. A significant drop in serum C3 levels at 1 hour was followed by a rise that remained at untreated levels until significantly increased 24 hours later. Peak C3 levels in tumors nonetheless was observed at 3, 6, and 12 hours following treatment. C3 already present in the tumor at the time of treatment may be engaged in the progression toward the early production and assembly of the C5b-9 complex. The source of C3 at later time points in PDT-treated tumors may be infiltrating cells such as neutrophils and macrophages that have been activated at the site of PDT injury or even resident tumor-associated macrophages. Preliminary results in our laboratory indicate that local complement gene expression and protein production does occur in tumors following PDT treatment (Brandon Stott, unpublished results).

2.3.4 Summary and conclusions

PDT induces an inflammatory response when applied to cells *in vitro* and also *in vivo* to solid tumors. Knowing that the complement system is a strong mediator of inflammation it was set out to define how complement reacts to PDT-induced tumor damage. The data compiled in this chapter characterize the deposition of complement proteins on treated cells and also indicate that the activation of the complement system in response to PDT occurs by the non antibody-mediated alternative pathway and not the classical pathway. In addition to promoting C3 (mediated by HSP70 expression and apoptosis) and C5b-9 deposition on the surface of cells, PDT also instigates a decrease in the level of protective, membrane-bound complement regulatory proteins. Thirdly, the complement system is activated in mice bearing PDT-treated tumors locally in the tumor and systemically in circulation. Together these data suggest that activation of the complement system by Photofrin-mediated PDT in a tumor model plays an integral role in an attempt by the host immune system to maintain homeostasis following acute tissue damage.

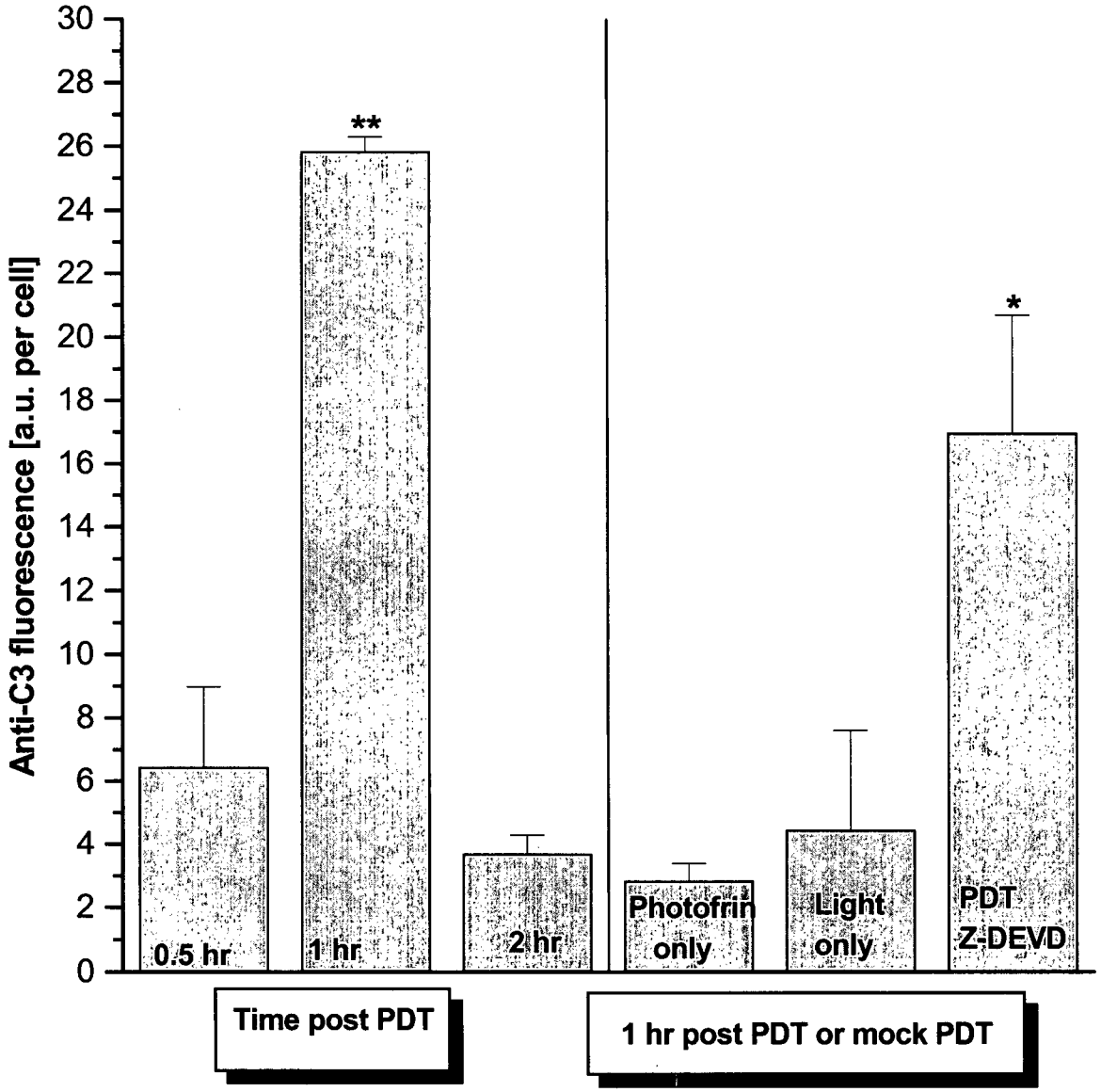

Figure 2.1 Mouse C3 deposits on the surface of PDT-treated tumor cells *in vitro*.

SCCVII tumor cells were treated with PDT: Photofrin 20 μg/mL and 1J/cm^2 and exposed to freshly isolated mouse serum, then harvested and analyzed by flow cytometry for surface C3 deposition. From left to right the columns represent cells harvested 0.5, 1, and 2 hours following PDT light delivery. Columns 4 and 5 represent control cell groups exposed to Photofrin alone, light alone, and column 6 depicts PDT followed by the addition of an apoptosis inhibitor, respectively. ** $p<0.05$ compared to untreated controls and * $p<0.05$ compared to PDT at 1 hour. Each column represents a triplicate group n=3; Mmean +/- SEM.

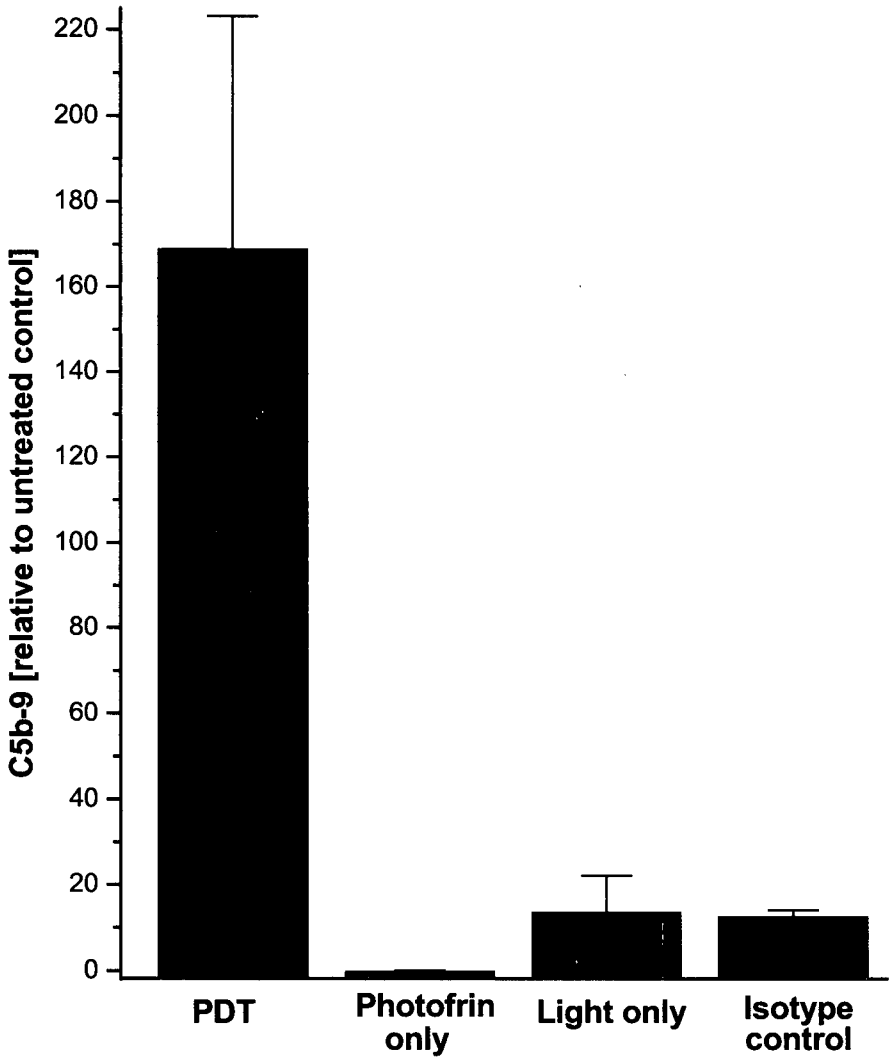

Figure 2.2 Mouse C5b-9 assembly on the surface of PDT-treated tumor cells *in vitro*.

Cells were treated with PDT: Photofrin 20μg/ml and 1J/cm^2 then exposed to freshly isolated mouse serum. Following 1 hour of incubation, cells were harvested and analyzed by C5b-9 flow cytometry. Control groups represent the effect of Photofrin only, light only, and isotype (mouse IgG) control. n=3 per column/treatment group; Mean +/- SEM.

A.

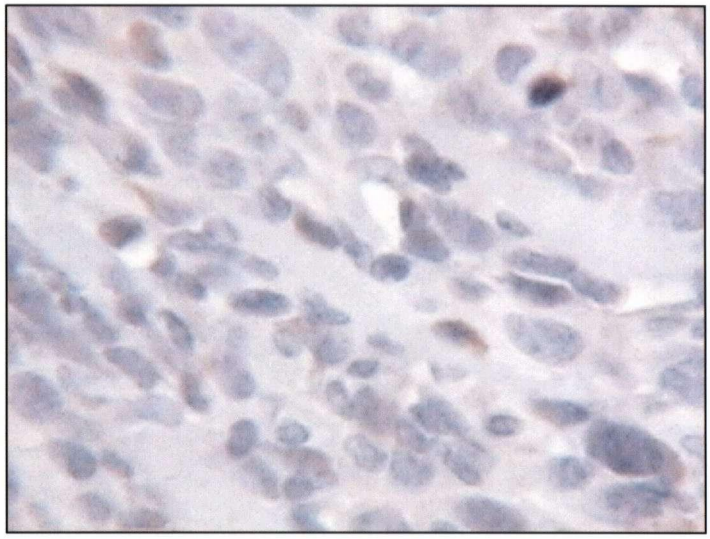

B.

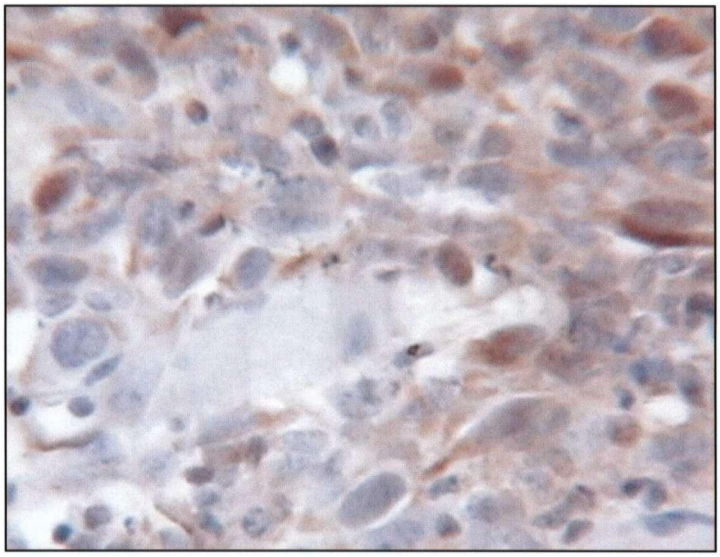

Figure 2.3 Photofrin-based PDT induces C5b-9 assembly in SCCVII tumor tumors. Paraffin-embedded SCCVII tumor sections were stained by the technique of immunohistochemistry for the detection of C5b-9 complex, indicated by the the prominent brown staining. Panel A represents untreated tumor, and panel B represents a section of a tumor excised one hour following PDT: Photofrin 10 mg/kg and 150 J/cm^2. Magnification: 400X.

A.

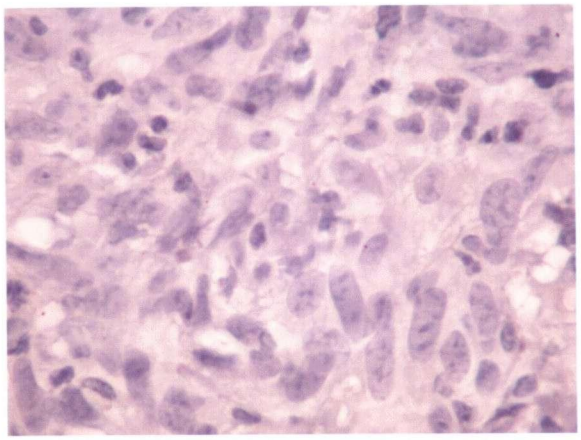

B.

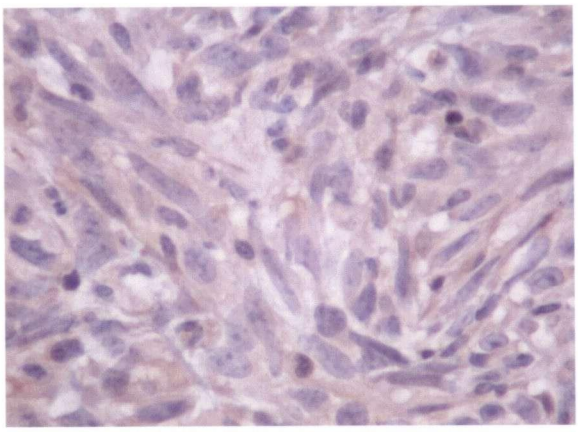

C.

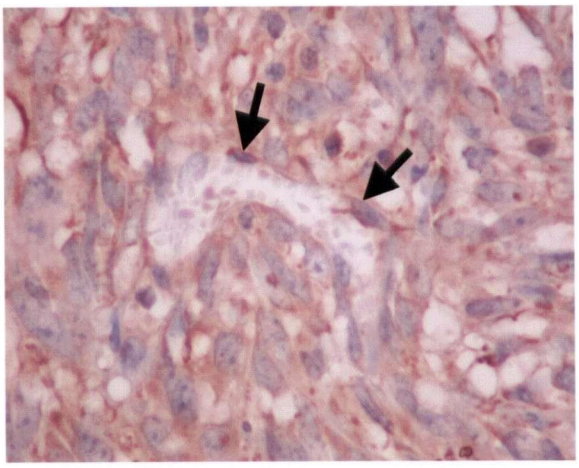

Figure 2.4 Photofrin-based PDT induces C5b-9 assembly in EMT6 tumors.
Subcutaneous EMT6 tumors were treated by PDT: Photofrin 10mg/kg and 60 J/cm^2 then excised 0.5 hours following treatment. Paraffin-embedded tumor sections were stained by the technique of immunohistochemistry for the detection of C5b-9 complex. Panels A, B, and C represent, untreated tumor, tumor sections stained in the absence of antibody (negative control), and sections of PDT-treated tumor, respectively. The arrows indicate endothelial cells lining a small vessel. Magnification: 400X.

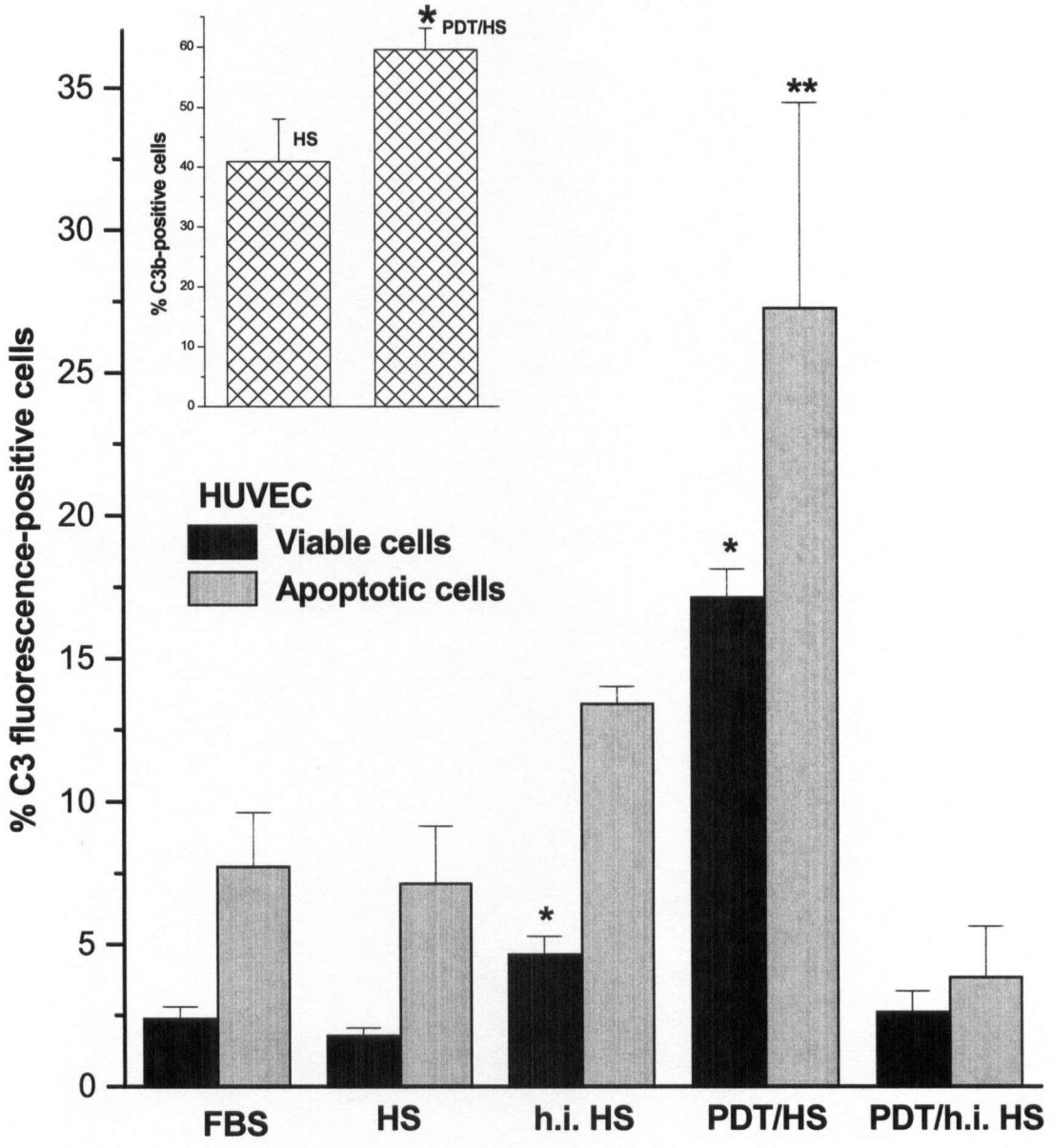

Figure 2.5 Mouse C3 deposits on PDT-treated HUVEC cells.

Triplicate petri dishes of HUVEC cells (n=3 per column) were separated into the following treatment groups: no PDT plus media containing either 10% heat-inactivated fetal bovine serum (FBS), 20% active human serum, or heat-inactivated human serum; PDT followed by 20% human serum (PDT/HS) or heat-inactivated human serum (PDT/h.i. HS). The cells were harvested one hour following treatment then analyzed by C3 flow cytometry, separating cell populations between viable and apoptotic cells. The inset graph indicates the level of surface C3b on PDT-treated HUVEC cells compared to untreated, naïve cells.

* p=0.01 compared to untreated cells (FBS) in the viable group, ** p<0.01 compared to untreated cells in apoptosis group. Each column represents Mean +/- SEM.

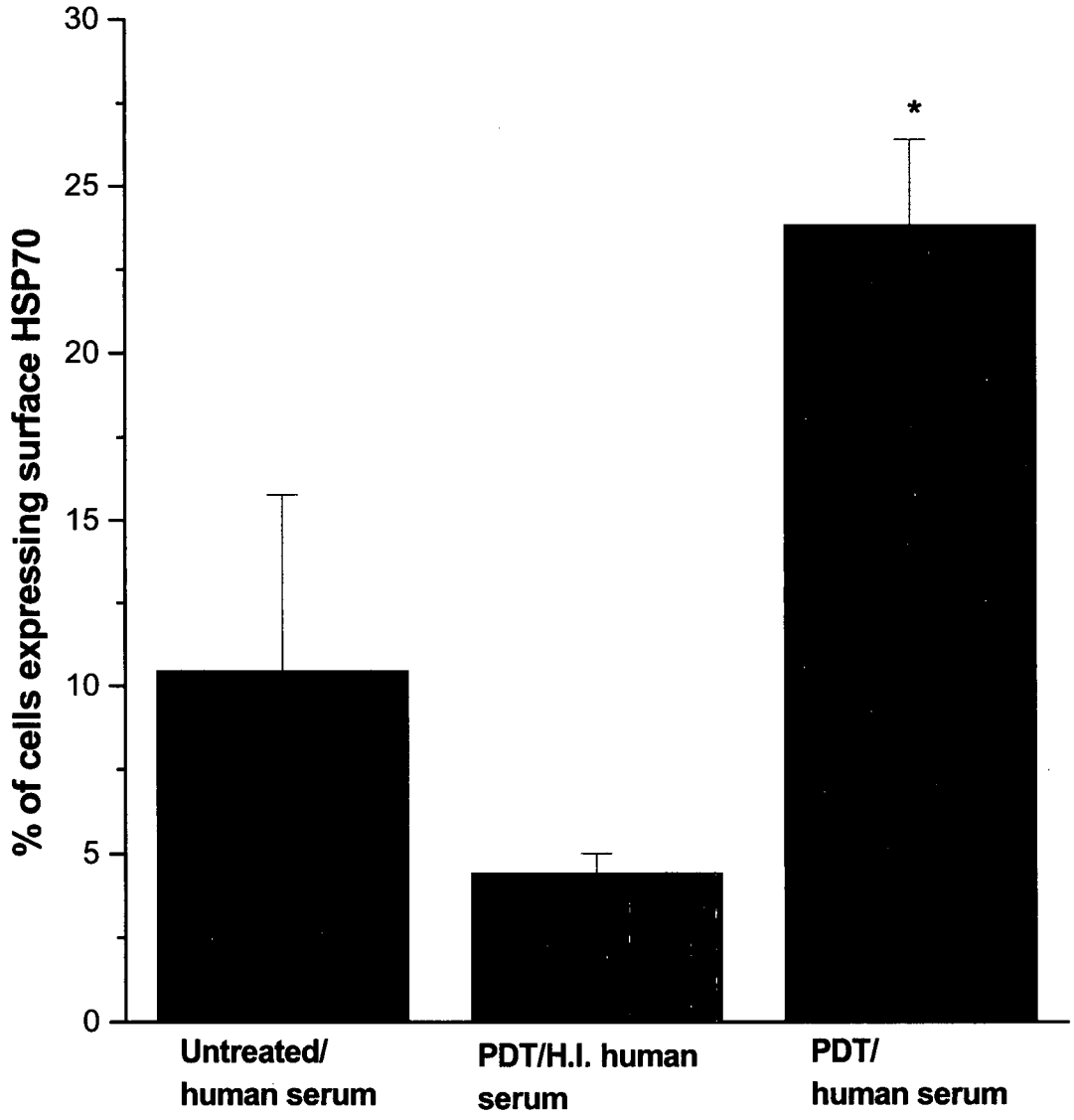

Figure 2.6 Surface expression of HSP70 on HUVEC cells increases following PDT and subsequent exposure to freshly isolated human serum. Each column represents the Mean ± S.E. of triplicate samples of monolayer HUVEC cell cultures. Cells were either untreated or treated with PDT: Photofrin 20μg/ml and 0.5 J/cm^2, then exposed to either heat-inactivated (H.I.) human serum or fully active human serum. The cells were analyzed by HSP70 flow cytometry. $P<0.05$ is considered statistically different compared to untreated controls.

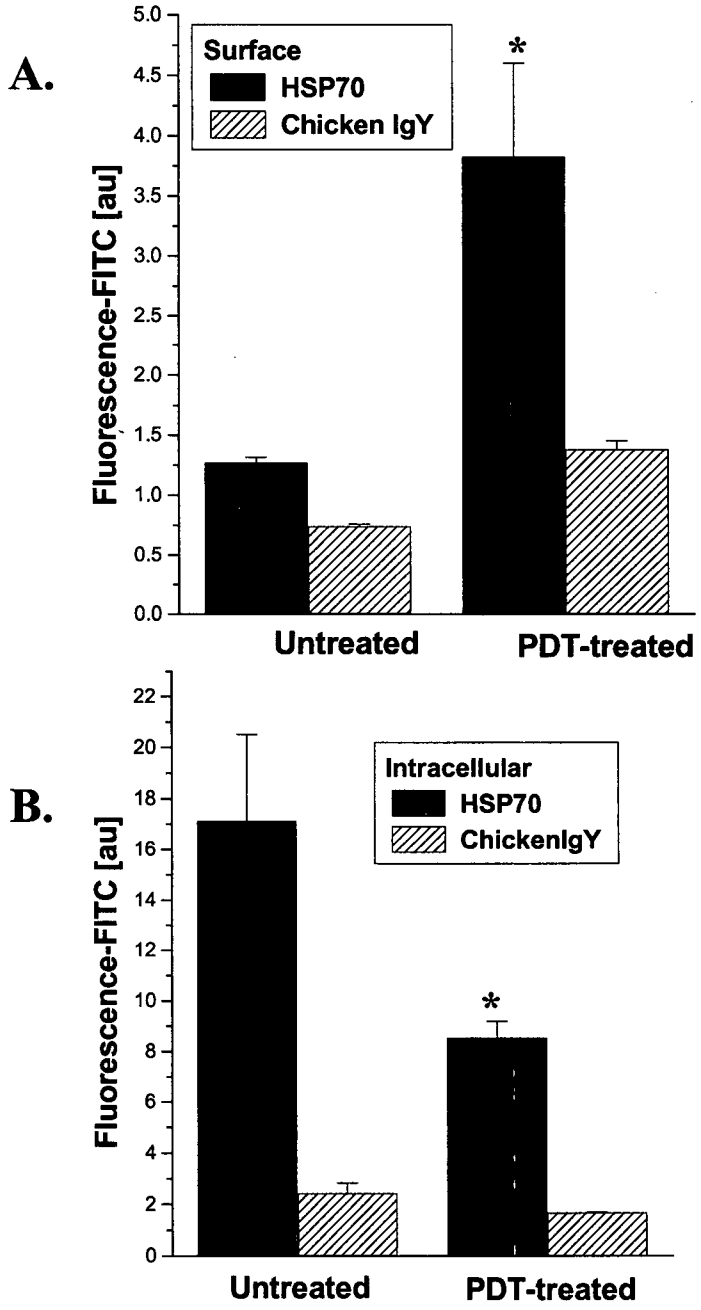

Figure 2.7 HSP70 surface (A.) staining rises on SCCVII cells as intracellular (B.) staining decreases in response to PDT. Each column represents the Mean ± S.E. of triplicate samples of monolayer SCCVII cell cultures. Cells were either untreated or treated with PDT: Photofrin 20μg/ml and 0.5 J/cm^2, then harvested following one hour of incubation in the presence of freshly-isolated mouse serum. All samples were analyzed by HSP70 flow cytometry and compared to isotype (Chicken IgY) controls.
* $p<0.05$ are statistically different compared to untreated controls.

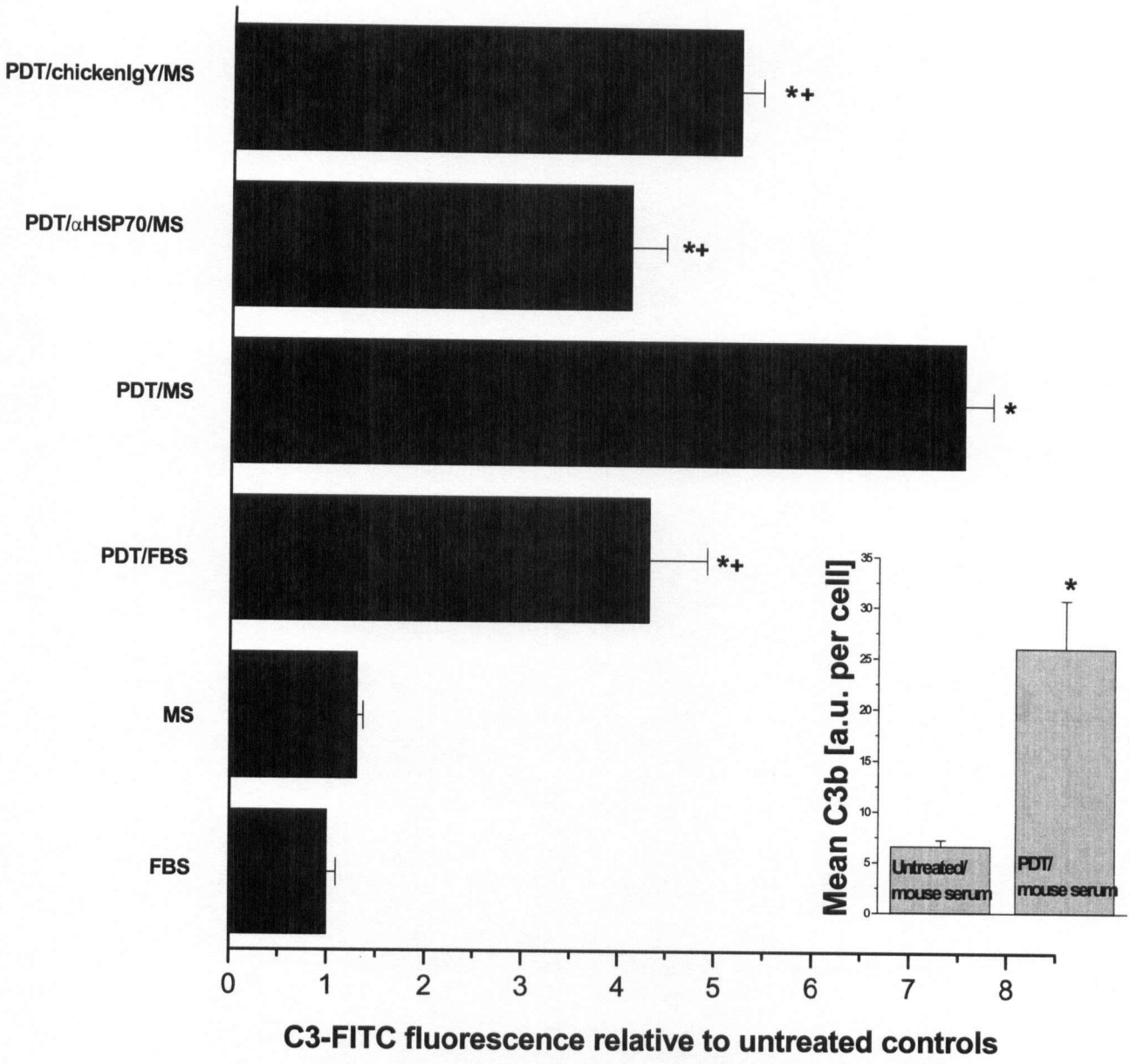

Figure 2.8 C3 surface deposition on PDT-treated SCCVII cells is inhibited by blocking HSP70. Four groups of PDT treated cells were exposed to either mouse serum and isotype control chicken IgY (PDT/chickenIgY/MS), mouse serum and HSP70 blocking peptide (PDT/αHSP70/MS), mouse serum alone (PDT/MS), or heat-inactivated fetal bovine serum (PDT/FBS). Two groups of untreated cells were exposed to mouse serum only (MS), or heat-inactivated fetal bovine serum (FBS). n=3 per column. All cells were harvested 1 hour following exposure to the serum combinations described above. The inset graph demonstrates the increased surface deposition of the breakdown product of C3, C3b indicating complement activation by the alternative pathway. PDT: Photofrin 20μg/ml and 0.5 J/cm^2. *$p<0.05$ indicates statistical difference compared to untreated controls (MS) and +$p<0.05$ indicates significant inihibition of C3 labeling compared to PDT/MS group. Each column = Mean +/- SEM.

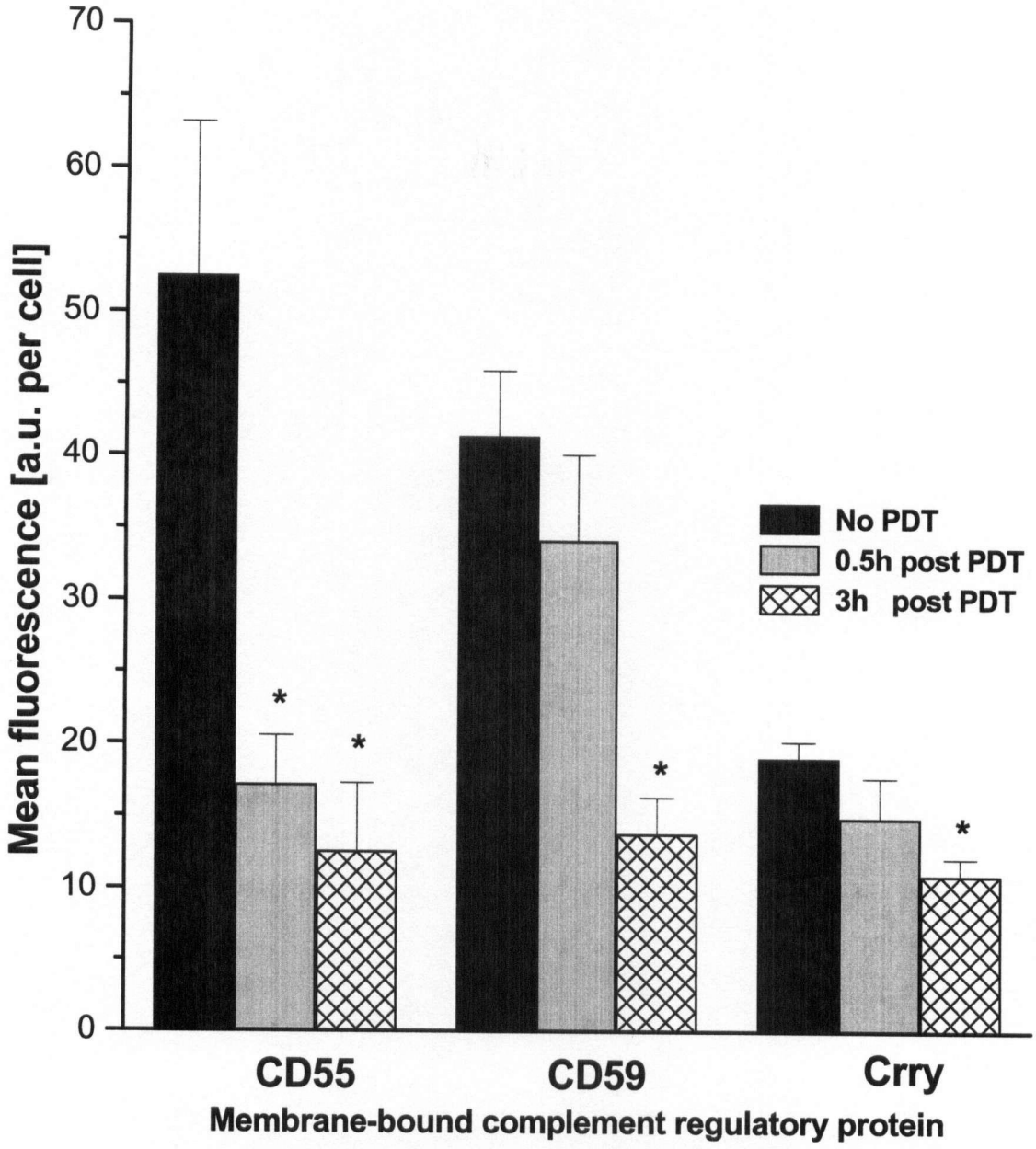

Figure 2.9 Membrane-bound complement regulatory protein (mCRP) expression decreases following PDT in SCCVII tumors. SCCVII tumors were excised untreated or 0.5 and 3 hours following PDT: Photofrin 10mg/kg and 150 J/cm^2, disaggregated into a single cell suspension and analyzed by CD55, CD59, and Crry flow cytometry. All bars shown represent CD45-negative cell population. All columns represent the mean fluorescence corresponding to each mCRP investigated. *$p<0.05$ compared to untreated controls.

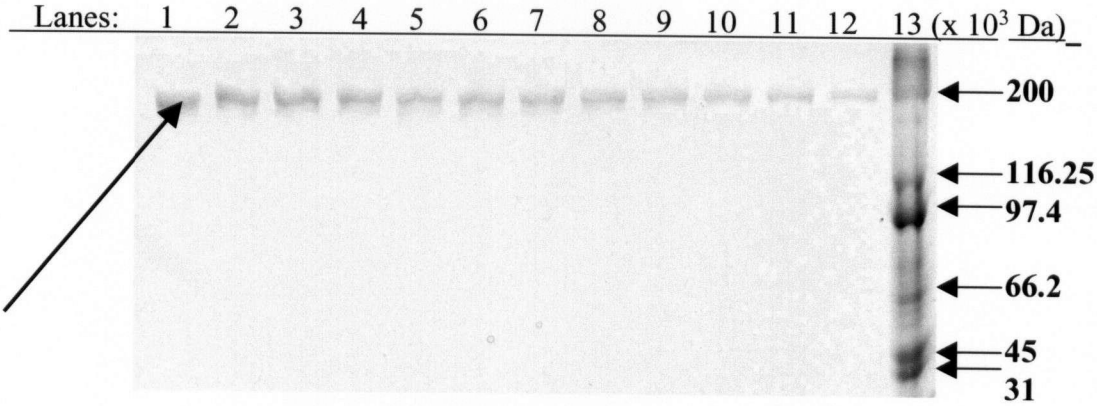

Figure 2.10 Resolving SDS-page gel of elution fractions containing mouse C3. Lanes 1-12 contain eluted samples that were positive for C3, assessed by an ouchterlony antibody test, and the molecular weight standards (BIORAD 80686, BIO-RAD technologies, CA) were loaded in lane 13. Purified mouse C3 at 210,000 MW is indicated by the arrow on the left.

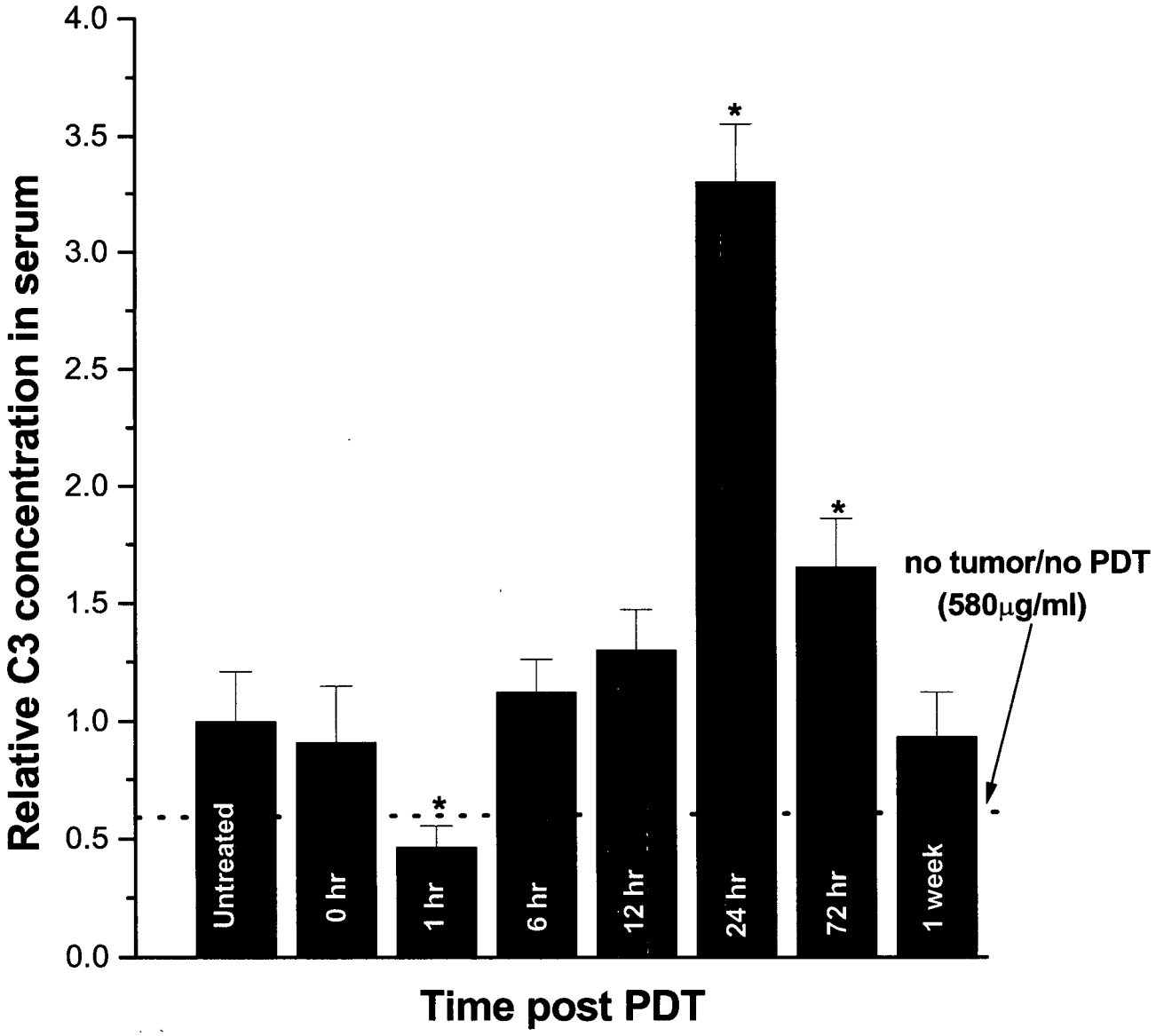

Figure 2.11 PDT applied in the treatment of the Lewis lung carcinoma tumor, influences serum C3 levels in mice. Lewis lung carcinoma tumors were treated by PDT: Photofrin 10 mg/kg and 150 J/cm^2 then the serum of these mice was collected at various time points following treatment: 0, 1, 6, 12, 24, 72 hours and 1 week following treatment (n=4 per time point). All sera was analyzed by a C3 ELISA. *$p<0.05$ compared to untreated, tumor-bearing, controls. Each column = Mean +/- SEM.

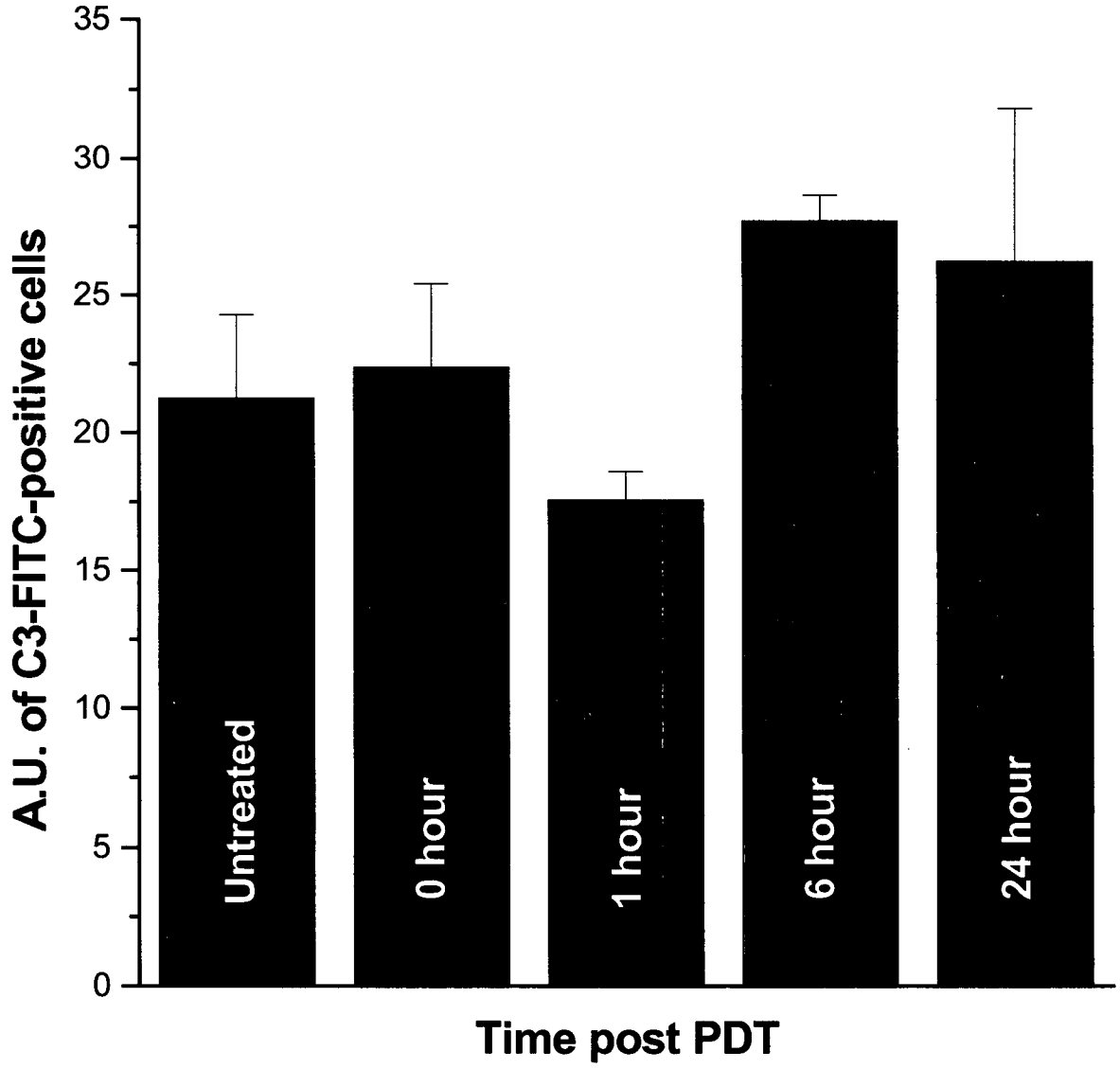

Figure 2.12 The classical pathway of the complement system is not activated by the serum collected from PDT-treated Lewis lung carcinoma tumor-bearing mice.
Serum samples collected at 0, 1, 6, and 24 hours (n=4 per time point) following PDT: Photofrin 10mg/kg and 150 J/cm^2, were exposed to untreated SCCVII cell cultures after these cells had been coated with antibody (anti-cytokeratin 5/8). Following 1 hour of incubation at 37 degrees celsius, cells were harvested and analyzed by C3 flow cytometry. Each column represents the Mean ± S.E. There was no statisticaly significant difference detected among the sera collected at the time points specified.

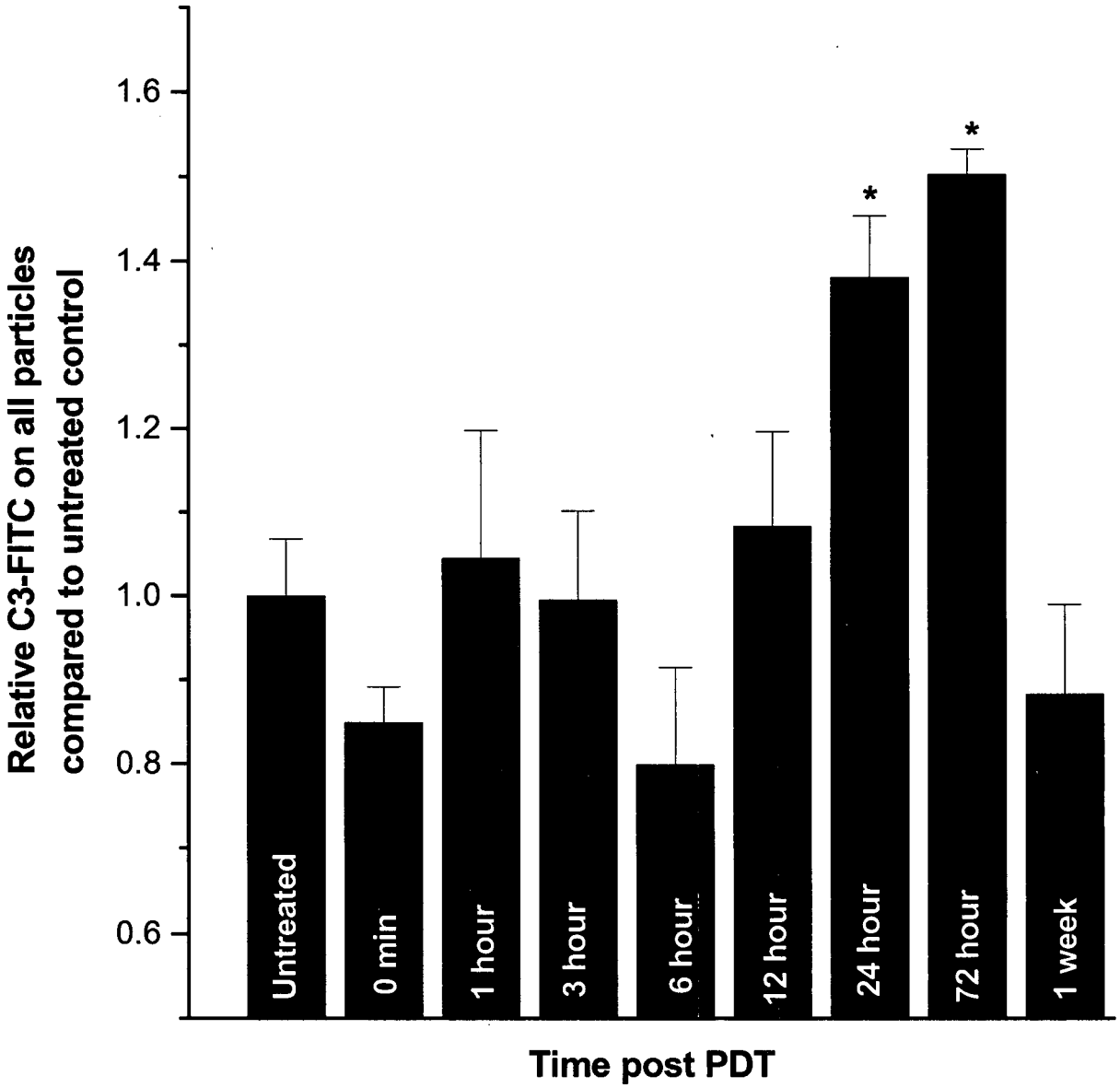

Figure 2.13 The alternative pathway of the complement system is activated by the serum collected from PDT-treated Lewis lung carcinoma tumor-bearing mice. Serum samples collected at 0, 1, 3, 6, 12, 24, 72 hours, and 1 week following PDT: Photofrin 10 mg/kg and 150 J/cm^2, were exposed to heat-activated zymosan particles. In the presence of $MgCl_2$-EGTA the samples were incubated at 37°C for 1 hour at which time they were analyzed by C3 flow cytometry. Columns represent mean +/- SEM; * $p<0.05$ compared to untreated controls.

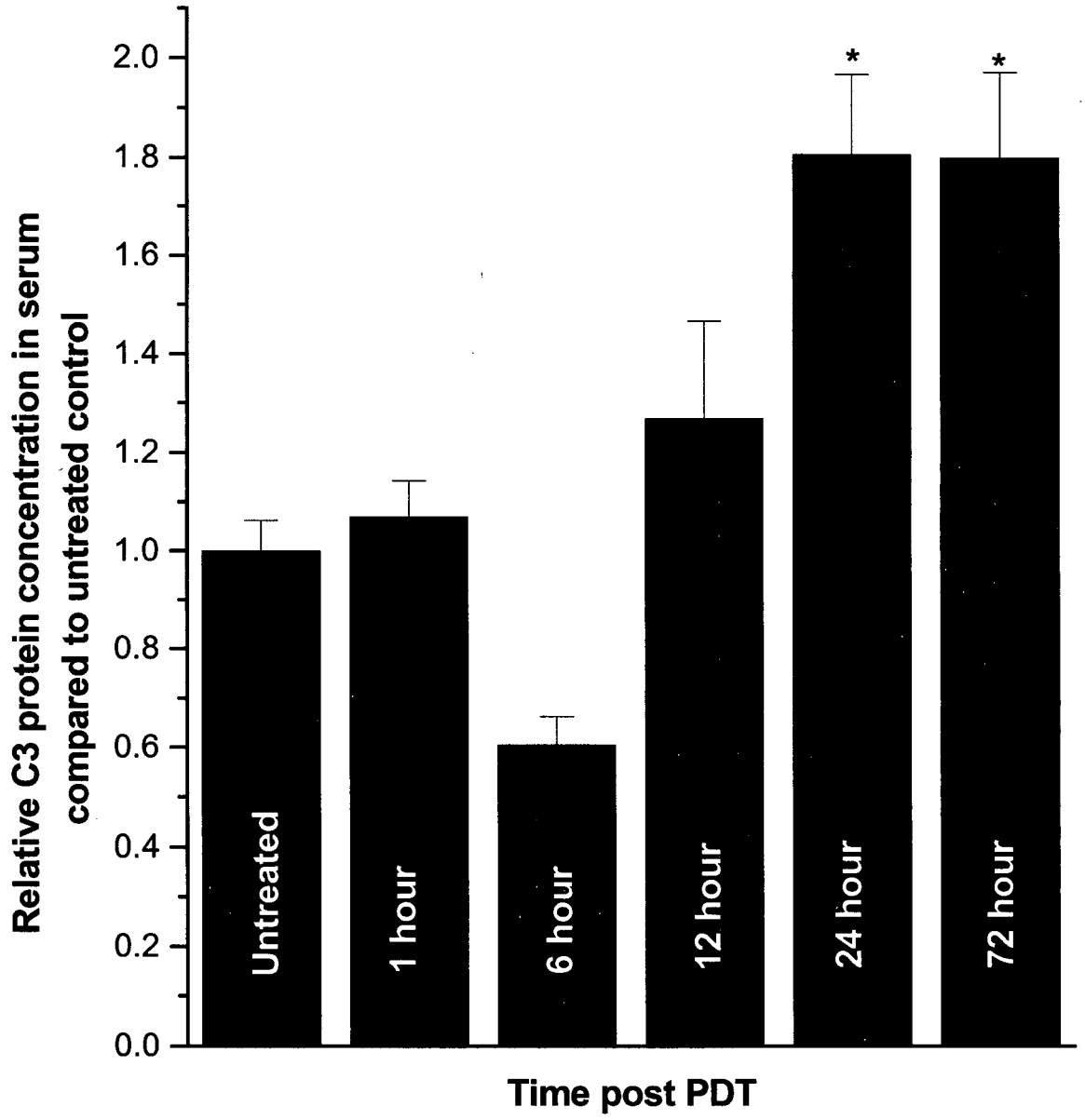

Figure 2.14 PDT applied in the treatment of the FsaR fibrosarcoma tumor, influences serum C3 levels in mice. FsaR fibrosarcoma tumors were treated by PDT: Photofrin 10 mg/kg and 150 J/cm^2 then the serum of these mice was collected at various time points following treatment: 0, 1, 6, 12, 24, and 72 hours following treatment (n=4 per time point). All sera was analyzed by a C3 ELISA. *$p<0.05$ compared to untreated controls. Each column = Mean +/- SEM.

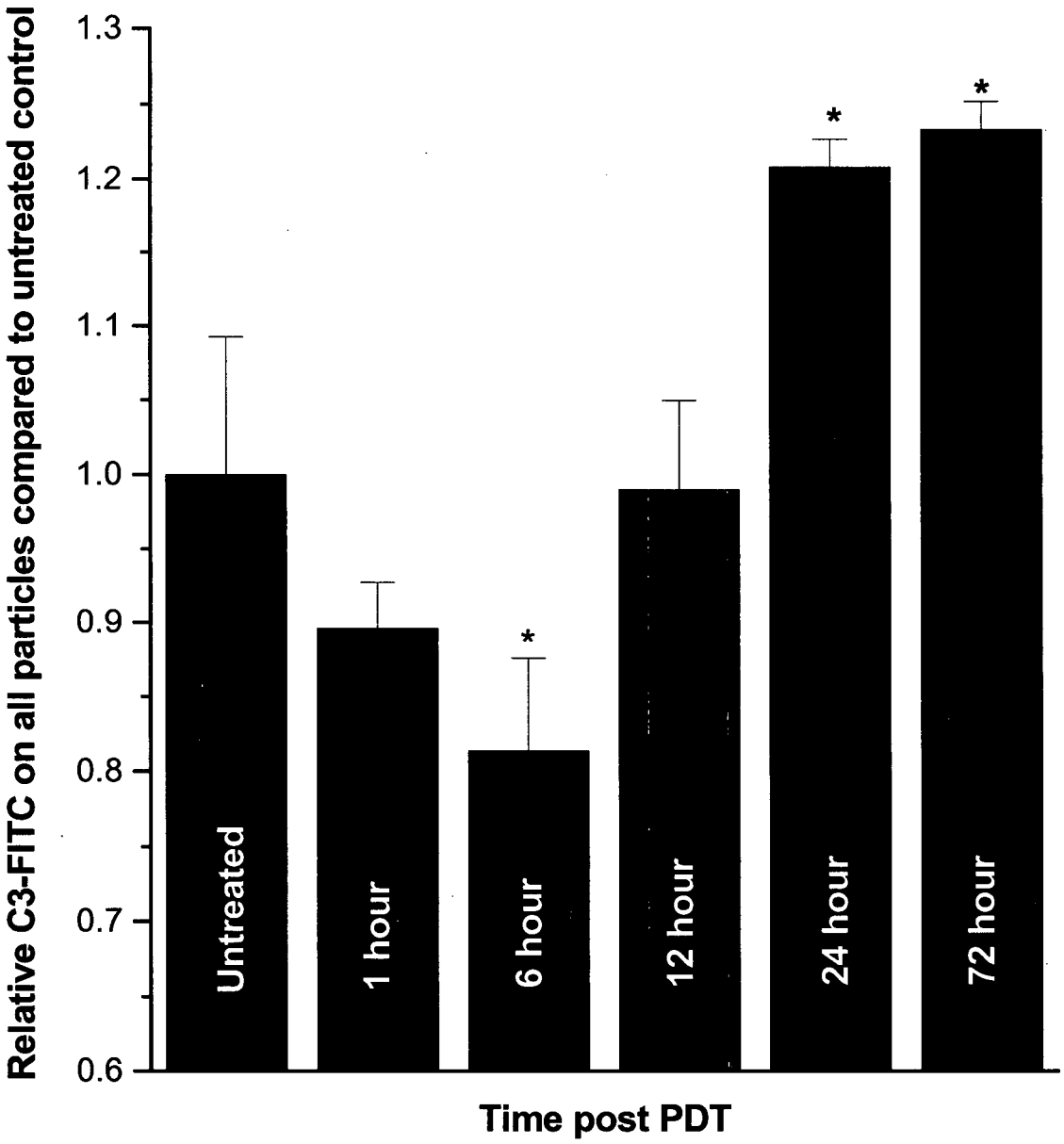

Figure 2.15 The alternative pathway of the complement system is activated by the serum collected from PDT-treated FsaR fibrosarcoma tumor-bearing mice. Serum samples collected at 0, 1, 3, 6, 12, 24, and 72 hours following PDT: Photofrin 10 mg/kg and 150 J/cm^2, were exposed to heat-activated zymosan particles. In the presence of $MgCl_2$-EGTA the samples were incubated at 37°C for 1 hour at which time they were analyzed by C3 flow cytometry. * $p<0.02$ compared to untreated controls.
Each column = Mean +/- SEM.

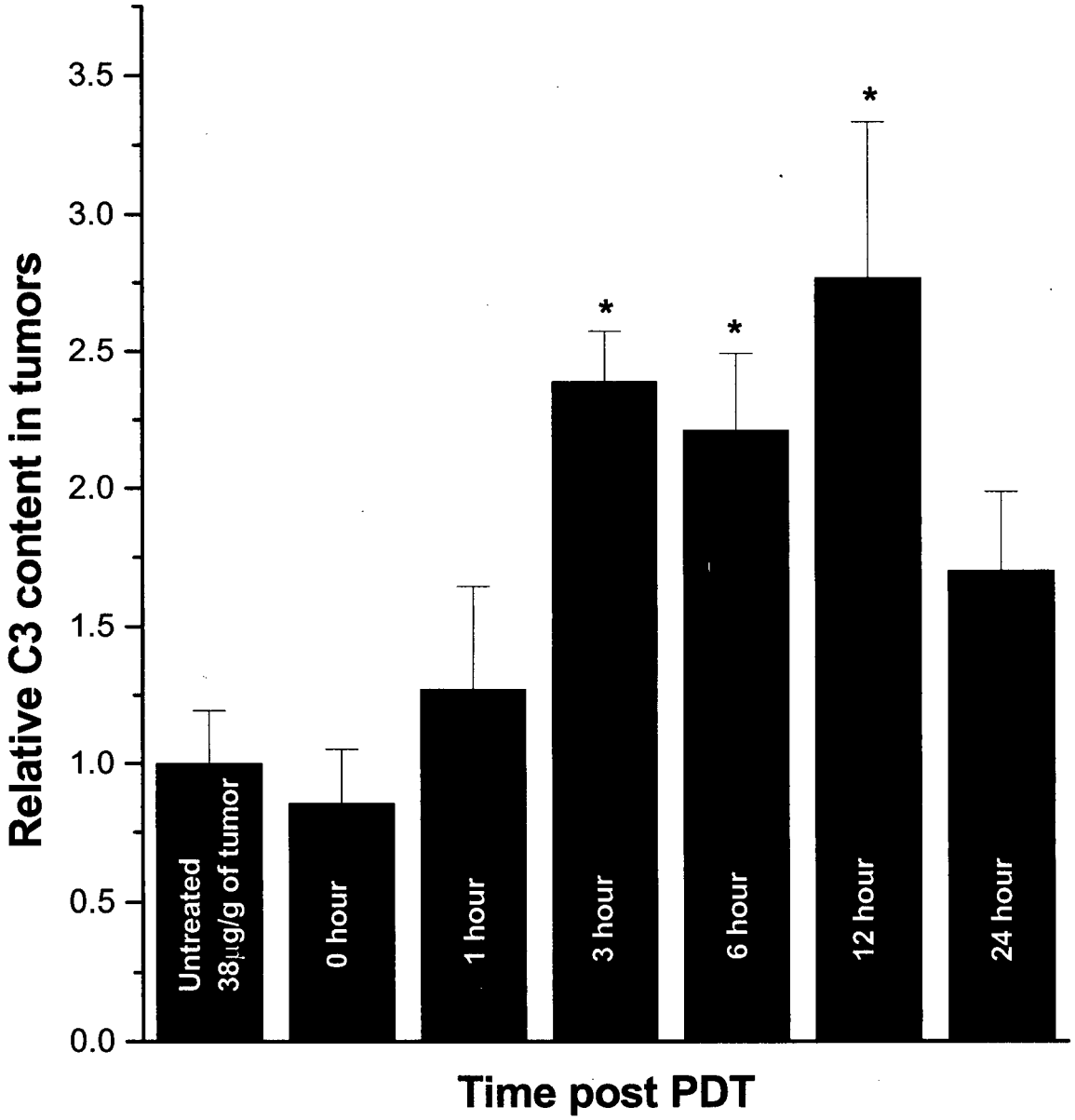

Figure 2.16 Complement C3 content increases in Lewis lung carcinoma tumors following PDT. Lewis lung carcinoma tumors were treated with PDT: Photofrin10 mg/kg and 150 J/cm^2, then excised at 0, 1, 3, 6, 12, and 24 hours following treatment (n=4 per time point). Immediately following excision tumors were homogenized. Tumor homogenate supernatants were analyzed by C3 ELISA. * $p<0.05$ compared to untreated control. Each column = Mean +/- SEM.

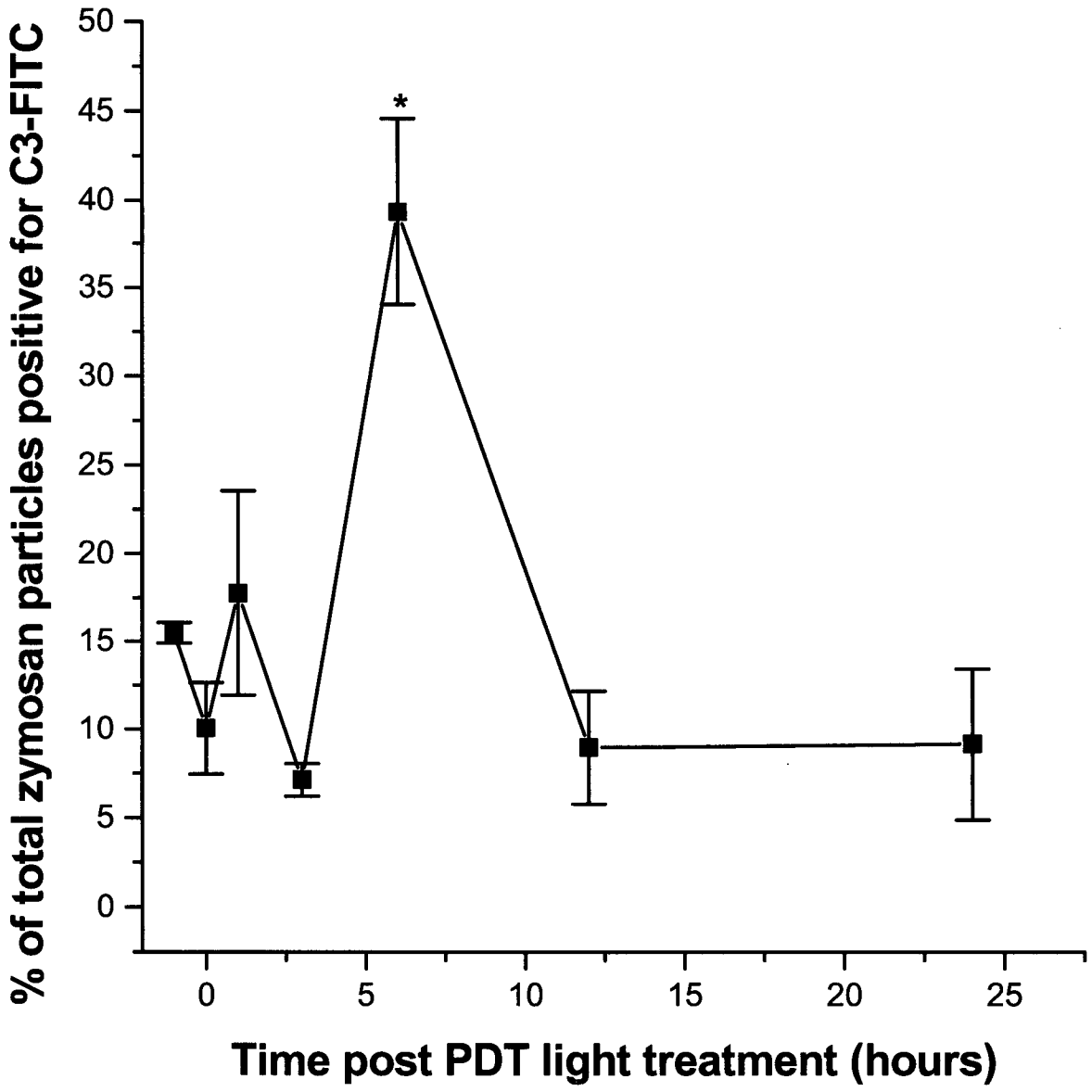

Figure 2.17 The alternative pathway of the complement system is activated in Lewis lung carcinoma tumors by PDT. Tumor homogenate supernatants collected at 0, 1, 3, 6, 12, and 24 hours following PDT: Photofrin 10 mg/kg and 150 J/cm^2, were exposed to heat-activated zymosan particles. In the presence of $MgCl_2$-EGTA the samples were incubated at 37°C for 1 hour at which time they were analyzed by C3 flow cytometry. * $p<0.01$ compared to untreated controls. Each column = MEan +/- SEM.

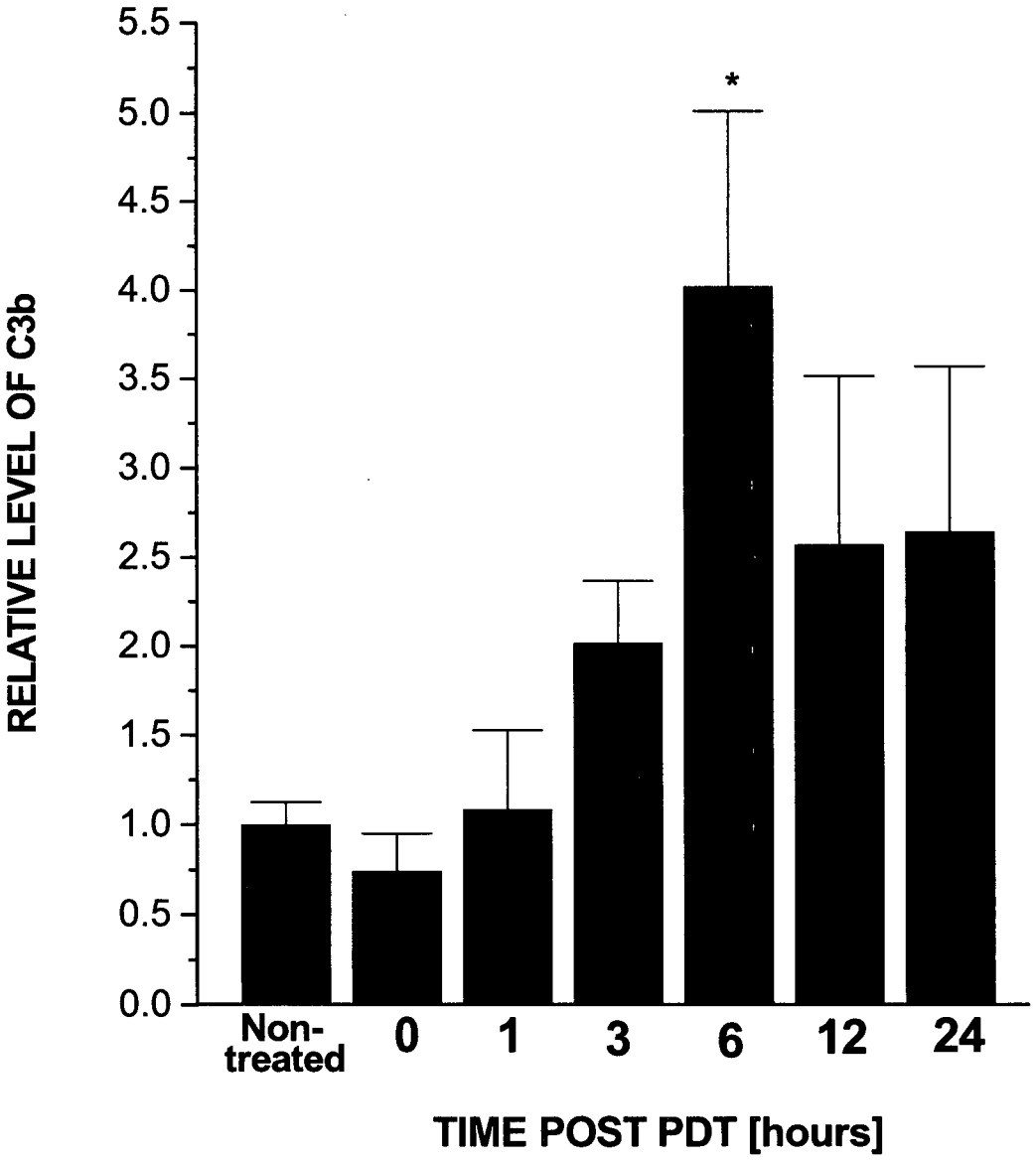

Figure 2.18 Complement C3b content increases in Lewis lung carcinoma tumors following PDT. Lewis lung carcinoma tumors were treated with PDT: Photofrin 10 mg/kg and 150 J/cm2, then excised at 0, 1, 3, 6, 12, and 24 hours following treatment (n=4 per time point). Immediately following excision tumors were homogenized. Tumor homogenate supernatants were analyzed by C3b ELISA. * $p<0.05$ compared to untreated control. Each column = Mean +/- SEM.

Chapter 3

The impact of complement activation on PDT-mediated tumor cures

3.1 INTRODUCTION

3.1.1 Tumor hypoxia and PDT

The outcome of photodynamic therapy applied in the treatment of solid tumors relies on the status of oxygen within the tumor at the time of photodynamic light delivery. Singlet oxygen, generally understood to be the main mediator of cytotoxicity in PDT, is generated by the transfer of energy from the excited photosensitizer to ground-state oxygen, therefore, any restriction of tissue oxygen supply during PDT light delivery will have negative consequences for treatment outcome. Furthermore, preexisting tumor hypoxia can play a major role in inhibiting the photodynamic process [Fingar *et al*, 1992].

Tumor hypoxia is the result of an inadequate supply of oxygen (O_2) compromising many biological functions due to a structurally and functionally disturbed microcirculation and the deterioration of diffusion conditions [Hockel and Vaupel, 2001]. It is becoming increasingly clear that hypoxia plays a fundamental role in tumor propagation and malignant progression. Furthermore, hypoxia increases tumor resistance to radiotherapy, chemotherapy, photodynamic therapy, and cytokine treatment, thus it has become a central issue in tumor physiology and cancer treatment [Hockel and Vaupel, 2001; Hockel *et al*, 1999; Henderson and Fingar, 1997; Teicher *et al*, 1990]. Sustained hypoxia in a growing tumor may cause cellular changes that can result in a more clinically aggressive phenotype [Brizel *et al*, 1996; Sundfor *et al*, 1998]. During the process of hypoxia-driven malignant progression, tumors may develop an increased

potential for local invasive growth and distant tumor cell spreading [Brizel *et al*, 1996; Sundfor *et al*, 1998; Young et al, 1990; Brizel *et al*, 1997; Jang *et al*, 1997].

PDT can itself lead to oxygen depletion. The consumption of molecular oxygen in the photochemical reaction during the formation and consumption of singlet oxygen is one mechanism [Sitnik *et al*, 1998]. Another is the halt in blood flow through vascular shutdown during and following light delivery. Although a reduction in blood flow can theoretically starve a tumor of oxygen and nutrients leading to cytotoxicity, an oxygen-deprived environment will hamper the effectiveness of the photodynamic process and lead to less tumor cytotoxicity. Together these events depend upon the accumulation, distribution, and the type of photosensitizer in the tumor at the time of light delivery. The issue of maintaining oxygen supply during PDT light delivery is therefore a matter of intense study.

3.1.2 Altering tumor oxygenation in the intent to improve PDT

Limitations to direct tumor cell photodamage by PDT include heterogeneous photosensitizer distribution, vascular occlusion, and a lack of ground state molecular oxygen during tumor illumination. Oxygen availability is always a concern during PDT light delivery. The direct effect that hypoxia has on the response of a tumor to PDT was demonstrated by Fingar *et al* in an experiment where they induced hypoxia in tumors using pharmacological and physical means [Fingar *et al*, 1988]. They discerned that 40% hypoxia in a tumor completely blocked tumor control by PDT. In order to improve PDT, both preclinical and clinical trials have indicated that adjuvant administration of

hyperbaric oxygen or carbogen significantly improve PDT efficacy [Schouwink *et al*, 2001; Jirsa *et al*, 1991]. Nicotinamide injection to overcome acute, perfusion-limited hypoxia, and carbogen breathing to overcome diffusion-limited hypoxia, have been combined with PDT to treat a human malignant mesothelioma (H-MESO-1) xenograft model with a significant increase in tumor oxygenation and tumor response [Schouwink *et al*, 2001]. In another study combining nicotinamide with PDT to treat a rat bladder tumor was, however, ineffective [Iinuma *et al*, 1999].

3.1.3 The effect of fluence rates on tumor oxygenation and the outcome of PDT

PDT efficiency in terms of tumor cures relies on combined effects of direct tumor cell damage and vascular response. The latter may depend upon fluence rates at which energy is delivered to the targeted lesion to excite the photosensitizer employed. The study of the impact of fluence rates began with the hypothesis that in combinations of both high photosensitizer and light doses, damage to the microvasculature in a tumor can be so acute and severe that it is actually counterproductive for the outcome of treatment. In some tumor models, PDT light treatment delivered at lowered fluence rates has been shown to improve tumor responses [Gibson *et al*, 1990; van Geel *et al*, 1996]. It has been proposed that in cases of high fluence rate applications, a temporary halt in blood flow starving tumor cells of nutrients occurs, however, reperfusion of the tumor following PDT shortly thereafter rescues cells and thus promotes re-growth of the tumor. The benefits of lowering fluence rates were demonstrated by Sitnik *et al* using an experimental RIF murine tumor model [Sitnik, 1998]. Oxygen levels in PDT-treated RIF

tumors can be maintained at higher levels using low fluence rate protocols (30mW/cm^2) with an overall significant improvement in tumor regrowth times compared to light delivery by high fluence rates (150 mW/cm^2) [Sitnik *et al*, 1998]. At high fluence rates, normal vasculature is nearly completely spared, yet low fluence rates can result in complete and total vascular collapse. Tumor vasculature collapses invariably regardless of fluence rate and seems slightly more susceptible to PDT damage compared to normal surrounding vasculature [Fingar *et al*, 1992]. Nonetheless, prolonging the time of light delivery to administer a particular dose of light energy may prolong vascular stability thereby ensuring at least basal levels of oxygen during photo-illumination. The mechanism of why this may be the case has not been fully described.

3.1.4 Ischemia-reperfusion injury and its significance in PDT

In addition to the primary, singlet oxygen-mediated oxidative stress, PDT-treated tumor tissue may sustain several forms of secondary stress, including hypoxic stress, oxidative stress mediated by superoxide, and nitrosative stress inflicted by the action of sequestered inflammatory cells [Korbelik and Cecic, 2003]. The underlying mechanism by which PDT leads to hypoxic and oxidative stress has been described a result of ischemia-reperfusion injury. Ischemia-reperfusion injury is responsible for microvascular and parenchymal cell dysfunction in a variety of common pathological conditions including myocardial infarction, stroke, acute kidney and liver failure, pulmonary and hemorrhagic shock, and organ transplant rejection [Zimmerman, 1994; De Greef, 1998; Hernandez, 1987]. A compilation of evidence for the induction of

ischemia-reperfusion injury in PDT-treated solid tumors has been published. In addition to an initial marked drop in tumor blood flow that recovers soon after PDT treatment, a buildup of the key enzyme xanthine oxidase in mouse tumors following treatment has been reported [Korbelik *et al*, 2003; Korbelik and Cecic, 2003]. Xanthine oxidase is an oxidant-producing enzyme that builds up during the ischemic period by conversion from xanthine dehydrogenase. Coinciding with this, the limited oxygen supply will drive the depletion of ATP with subsequent accumulation of its breakdown product hypoxanthine. During reperfusion, the newly introduced oxygen will interact with hypoxanthine in a reaction catalyzed by xanthine oxidase to produce superoxide [Zimmerman, 1994; De Greef, 1998].

The induction of ischemia-reperfusion injury by PDT in solid tumors is an important impact on overall tumor response to this therapy. The generation of ischemia in PDT-treated tumor tissue is due to the depletion of oxygen through its consumption in the photodynamic process [Foster, 1991; van Geel, 1996; Busch, 2000], decreased blood flow as a result of microvascular damage [Henderson, 1989; Korbelik *et al*, 2000], and vasoconstriction mediated by thromboxane [Fingar *et al*, 1990]. The reintroduction of oxygen to transient ischemic regions results in a massive generation of superoxide in the affected tumor vasculature [Parkins, 1997]. Using an experimental model of ischemia-reperfusion injury induced by transitory clamping of the feeding blood vessels to subcutaneous mouse tumors, Parkins and co-workers have demonstrated that this type of insult can produce significant generation of oxygen radicals, leading to anti-tumor effects [Parkins, 1995].

3.1.5 The role of inflammation mediated by complement activity in ischemia-reperfusion injury

Ischemia-reperfusion is accompanied with an inflammatory response, with the complement system described as the main mediator of this response [Chakraborti, 2000]. Interactions between the endothelium and plasma components particularly during reperfusion results in further damage to endothelium with increased vascular permeability, enhanced chemotaxis for neutrophils and platelets, events that parallel those described in the reperfusion of ischemic myocardium [Chakraborti, 2000]. The release of oxygen free radicals, cytokines, and other proinflammatory mediators activate both neutrophils and the affected endothelium [Chakraborti, 1998; O'Donnell, 1995]. Ischemia-reperfusion results in the activation of a pro-inflammatory host response. In particular the complement system has been shown to play a key role in mediating the events following ischemia and subsequent reperfusion in myocardial infarction for example [Chakraborti, 2000; Birnbaum *et al*, 1997]. Basement membrane exposure and ischemia-reperfusion injury, both PDT-instigated events, are known to prompt complement fixation [Kilgore et al, 2000; Hindmarsh *et al*, 1998]. Enhanced adhesion molecule expression, and the sequestering of neutrophils in PDT-treated tumors is significant toward the cure rate of PDT [de Vree, 1996; Sun *et al*, 2002; Gollnick *et al*, 2003; Menon *et al*, 2001]. Activated neutrophils induce further tissue damage with the production and release of reactive oxygen species (ROS), degranulation and secretion of proteases, and release of other proinflammatory mediators [Jordan, 1999; Lucchesi, 1997; Lucchesi, 1993; Montalescot, 1991]. The vascular endothelium is a particularly sensitive

target site of injury by ROS such as superoxide anions, hydrogen peroxide, and hydroxyl radicals [Jordan, 1999].

The role of the complement system in mediating these events is not yet fully described in PDT. It follows that the focal deposition of C3 and consequent assembly of the membrane attack complex may be pivotal in vascular damage in PDT-treated tumors. Therefore, with the use of a complement protein C3 knockout mouse, the following experiments were designed to characterize the significance of complement activation on the outcome of PDT as a cancer therapy, and its effect on oxygen status following treatment.

3.2 MATERIALS AND METHODS

3.2.1 Tumor model

Lewis lung carcinoma tumors (LLC) [Sugiura and Stock, 1955] were grown in syngeneic C57BL/6 and C3 knockout mice of the C57BL/6 strain, B6.129S6-*Cybb*^{tm1} (The Jackson Laboratory, Bar Harbor, Maine, USA). The cell line was maintained *in vivo* by biweekly intramuscular tumor brei inoculation. Mice were sacrificed by CO_2 inhalation and the tumors removed and minced using two #22 scalpel blades. Subsequently the tumor tissue was repeatedly passed through two 20-gauge needles, and diluted 5 times in phosphate buffered saline (PBS). 0.1 mL of tumor brei was inoculated into the thigh muscles of anesthetized mice. For experiments, the tumor was removed using aseptic technique, chopped using two #22 scalpel blades, suspended in 5 mL of PBS and enzymatically digested with gentle rotation at 37°C for 20 minutes. The three enzyme cocktail used for disaggregation contained: DNase (type I) 0.6 mg/ml, collagenase (type IV) 0.24 mg/mL and dispase (Boerhinger, Mannheim, Germany) 0.18 mg/mL, diluted in 5 mL of cold, sterile, PBS. The enzymes were added to the tumor just prior to incubation. The tumor cell suspension was then filtered through a 100 μm nylon mesh filter using a 6 cc syringe, and centrifuged at 600 rpm, then suspended in PBS. Cell concentration was determined by hemacytometer count. For experiments, 2 x 10^6 cells suspended in serum-free media were inoculated subcutaneously on the depilated backs of mice using a 26-gauge needle. MCA205 fibrosarcoma cells [Spiess *et al*, 1987] were grown adherent to the bottom of T80 cm^2 tissue culture flasks in alpha-MEM, 10% fetal bovine serum, 100μg/mL

streptomycin, and 100 Units/ml penicillin at 37°C, 5% CO_2, and 95% humidity. To harvest, a confluent monolayer of cells was treated with Trypsin-EDTA (ethylenediaminetetraacetic acid) solution (GIBCO) containing 0.25% trypsin and 1mM EDTA·4Na in HBSS (Hank's buffered salt solution), suspended in complete medium, washed once by centrifugation at 600 rpm, and re-suspended in serum-free DMEM. Two million cells were inoculated subcutaneously onto the depilated dorsal side of mice.

3.2.2 Tumor growth rate: C3 knockout vs C57BL/6

The growth rate of the Lewis lung carcinoma tumor was compared between the two strains of mice used: C57BL/6 background strain and its C3 knockout counterpart. Tumor volumes were measured every second day once the tumors became palpable using stainless steel dial caliper (Mitutoyo, USA). Tumor volume was calculated as (length)(width)(height)π/6.

3.2.3 Tumor cures: C3 knockout vs C57BL/6

Lewis lung carcinoma tumors and the MCA205 fibrosarcomas (chosen for their transplantability in the C57BL/6 mouse strain) at 7-8 mm diameter were treated by PDT in both the C57BL/6 and C3 knockout mice (n=8 per group). The Lewis lung carcinoma tumors were treated by either: Photofrin (Axcan, Canada) 10 mg/kg, followed 24 hours by 150 J/cm^2 630 nm red light, or BPD (QLT, Canada) 2.5 mg/kg, followed 3 hours later by 100 J/cm^2 690 nm red light delivered, at a fluence rate of about 100mW/cm^2. BPD is

delivered in <200nm unilamellar dimyristoyl phosphatidylcholine liposomes. Light was delivered to the tumors by a diode laser (SDL, Inc., San Jose, CA; model 7422) tuned to 690nm, through an 8mm diameter liquid light guide, model 77638 (Oriel Instruments, Stratford, CT). The MCA205 tumors were treated with Photofrin 7.5 mg/kg and 150 J/cm^2, at a fluence rate of about 100 mW/cm^2. The tumors were monitored for regrowth following PDT-light delivery and any mice remaining tumor-free 90 days post therapy were classified as cured. Statistical analysis was done by the Log-rank test and values $p<0.05$ were considered significantly different.

3.2.4 Varying Fluence rates: C3 knockout vs C57BL/6

Two groups of eight Lewis lung carcinoma tumors were grown subcutaneously on the dorsal sacral region on both the C3 knockout strain and their C57BL/6 wild-type counterparts. At 7-8 mm in largest diameter, all tumors were treated with 10mg/kg Photofrin followed by 150 J/cm^2. The light administered to the first group of tumors in each strain was delivered with a fluence rate of 100 mW/cm^2, whereas the second group was administered the same dose of light delivered at a fluence rate of 30 mW/cm^2. The power density was adjusted over a treatment field of one centimeter in diameter over the tumor to yield the fluence rates listed above. A sphere of aluminum foil was placed over the red-light filter to decrease the fluence rate from 100 mW/cm^2 to 30 mW/cm^2. Mice were monitored for tumor re-growth following treatment and were considered cured if free of tumor 90 days following treatment.

3.2.5 Cell survival assay

Lewis lung carcinoma tumors in both the C57BL/6 and C3 knockout strain of mice were treated with Photofrin 10 mg/kg and 150 J/cm^2 of 630 nm red light, then immediately excised following treatment and prompt sacrifice of the animal by CO_2 inhalation. The tumors were immediately placed on ice and processed into a single cell suspension as follows. The tumors were weighed then minced using two #22 scalpel blades and placed into 4 ml of alpha-MEM containing DNase (type I) 0.6 mg/ml, collagenase (type IV) 0.24 mg/ml and dispase (Boerhinger, Mannheim, Germany) 0.18 mg/ml. The suspensions were then rotated gently at 37°C for 15 minutes. The resulting cell suspensions were then filtered through a 100 μm nylon mesh and ~7 ml of alpha-MEM + 20% fetal bovine serum was added to each sample. The samples were centrifuged at 600 rpm and re-suspended in alpha-MEM + 20% fetal bovine serum, cell concentration determined by hemacytometer and plated for colony growth in prepared Falcon tissue culture plates. The cells were incubated at 37°C, 5% CO_2, 5%O_2, and balanced N_2. Ten days following, any colonies that formed from a single surviving tumor cell were stained with 0.5 g/L solution of Malachite Green-oxalate salt for 10 minutes, gently rinsed with running tap water, and counted.

3.2.6 Measurements of tumor oxygen tension values with needle electrodes

Un-anesthetized mice (5-6 per group) were restrained in lead holders, designed specifically to expose only their depilated backs bearing a subcutaneous Lewis lung carcinoma tumor. Immediately following PDT light treatment, the skin above the tumor

was pierced with a 26g hypodermic needle to allow ease of insertion of the microelectrode into the tumor below. Polarographic needle electrodes were used to measure tumor oxygen tension (pO_2) values. The microelectrode employed was the Eppendorf pO_2 histograph, Model KIMOC 6650 (Eppendorf-Netherler-Hinz GmbH, Hamburg, Germany). The needle sensor was calibrated using a chamber containing sterile saline (pH 7.4) that was bubbled alternately with room air and pure nitrogen (pO_2 = 0 mmHg) according to the manufacturer's instructions. Only sensors that conformed to the manufacturer's specifications regarding O_2 and N_2 currents and drift were used. Once the recordings stabilized, pO_2 measurements began with automatic probe advancement at 0.5 mm steps. In general, three radial electrode tracks were evaluated in each tumor, with 7-12 advancements per track (dependent of tumor size). At the end of a measurement the O_2 probe was automatically removed from the tissue and pO_2 frequency distributions were plotted on a histogram. Statistical analysis was performed using the non-parametric Wilcoxon matched pairs test where any values differing with a $p<0.05$ considered significantly different from untreated control tumors.

3.2.7 Human C3 and PDT cures

C3 knockout mice bearing 7-8 mm wide subcutaneous Lewis lung carcinoma tumors (n=8) were administered human complement C3 (RDI, New Jersey, USA) intravenously 30 minutes prior to PDT light delivery. PDT: Photofrin 10 mg/kg and 150 J/cm^2. Lyophilized powder containing 40-80% of C3 was reconstituted in 1.81 mL of ddH_2O

then diluted further so that each mouse was administered 1 mg per 200 μL volume in endotoxin free Dulbecco's PBS.

3.2.8 C5a receptor antagonist and PDT cures

The Lewis lung carcinoma tumor was grown subcutaneously on the backs of depilated C57BL/6 mice from bi-weekly intramuscular tumor brei maintenance. The tumors were treated with Photofrin 10 mg/kg and 200 J/cm^2 of 630 nm light as described above when they reached a diameter of no more than 7-8 mm. Two groups of eight mice were separated where one group was treated with PDT only and the second group was treated with PDT preceded by a bolus intravenous injection of 1 mg/kg C5a Receptor antagonist, a synthetic cyclic hexapeptide AcF-[OPdChaWR] [Mollnes *et al*, 2002b], generously provided by Dr. J.D.F. Lambris, University of Pennsylvania, Philadelphia, 30 minutes prior to light treatment. Following initial tumor ablation, the mice were monitored for tumor re-growth following treatment. Any mice surviving tumor-free up to 90 days following PDT were considered cured.

3.2.9 Statistical analysis

The significance in differences in tumor cures was tested by the log-rank test. The pO_2 measurements were assessed by the non-parametric Wilcoxon Matched pairs test on the advice of a biostatistics expert, Dr. Martial Guillaud. Statistical significant of tumor cell

survival between treatment groups was assessed by ANOVA and post-hoc comparison by the LSD test. $P<0.05$ was considered statistically significant. The statistical analyses were performed using the software program Statistica 6.1 (StatSoft, Inc.).

3. 3 RESULTS AND DISCUSSION

The inflammatory response plays an important role in mediating the secondary cytotoxic effects known to be associated with PDT eradication of solid tumors [Krosl *et al*, 1994; Dougherty *et al*, 1998; Korbelik *et al*, 2003]. However, inflammation can also lead to inadvertent damage to tumor and tumor-surrounding normal endothelium [Fingar, 1996]. Vascular shutdown and subsequent reperfusion by PDT-treated tumors can mimic ischemia-reperfusion injury, the latter being mediated by an activated complement system [Korbelik and Cecic, 2003]. We hypothesized complement activation leads to vascular occlusion hampering blood flow to the tumor during PDT light delivery and thereby diminishing oxygen delivery, limiting the efficiency of the photodynamic process.

Based on available evidence from PDT studies and general knowledge of complement, as a key mediator of inflammation and wound healing the activated complement system may hold a significant role in tumor response to PDT by participating in multiple events unfolding after treatment. Direct killing of cancer and endothelial cells can occur by assembly of the membrane attack complex. Promoting the release of arachidonic acid metabolites and chemokines attracts an influx of neutrophils and other inflammatory cells into PDT-treated sites. The release of a variety of other pro-inflammatory mediators such as histamine and cytokines and elevated production of leukocyte adhesion molecules by activated complement, further promotes leukocyte infiltration and retention in treated tissue. In general the complement system tags by opsonization cancer cell targets to be killed and/or phagocytized by mobilized phagocytes. Rounding off the result of complement activation by PDT is the promotion

and advancement of ischemia-reperfusion injury [Korbelik and Cecic, 2003] affecting the stability of tumor vessels.

The complement system is often described as a double-edged sword. Complement is a key in the induction of tolerance and clearance of immune complexes, and several other biological effects that contribute to the inflammatory reaction, mainly the activation of leukocytes and endothelial cells [Mollnes *et al*, 2002a]. Patients with genetic complement deficiencies are highly susceptible to infection and to diseases such as systemic lupus erythematosus. However, improper, enhanced or uncontrolled complement activation is disadvantageous to the host, mediating instead numerous pathological conditions. This thesis chapter begins to describe the double-edged impact of complement activation in PDT-treated solid tumors comparing tumor response in the C57BL/6 strain of mice and their complement C3 knockout counterpart.

3.3.1 Tumor cures: C3 knockout vs C57BL/6

In order to rule out any differences in the Lewis lung carcinoma tumor between the C57BL/6 wild-type strain of mice and the C3 knockout, tumor cells were inoculated subcutaneously into both strains and monitored for tumor formation and concomitant growth rate. Tumors formed in all mice in both strains and grew at the same rate, as shown in Figure 3.1. This observation was imperative in order to proceed with the following experiments determining a difference in response to PDT treatment. When Photofrin-based PDT was administered to the LLC model in both of these mouse strains, the initial tumor ablation was complete 24-48 hours following PDT light delivery. Figure 3.2 indicates that tumor regrowth began to occur quite soon after treatment in the

C57BL/6 mice, with 50% of the tumors re-appearing by 12 days after therapy and only 27% of the group being cured. In the C3 knockout model however, 75% of tumors were cured by the same dose of PDT. A second tumor model, the MCA205 fibrosarcoma, was treated with the same dose of Photofrin-based PDT, with a similar, significant result: a 50% cure rate is observed in the C3 knockout mouse strain compared to 25% cures in the C57BL/6 mouse strain (Figure 3.3). Treating the LLC tumor model with BPD-based PDT however, led to the opposite effect with significantly fewer cures in the C3 knockout group (Figure 3.4).

A higher cure rate in the C3 knockout model using Photofrin-based PDT was the opposite effect than that expected. Prior to the experiment, it was hypothesized that secondary tumor damage to all tumor components in particular the vasculature, inflicted by activated complement reactions in response to PDT would be beneficial to therapeutic outcome and therefore, the outcome of therapy would be worsened in the C3 knockout model. It was quite logical that vessel walls, and endothelial cells in particular are the first to be subjected to complement activity via interaction with circulation. Vascular collapse in PDT-treated tumors occurs due to a combination of effects: a) direct cytotoxicity induced by activated photosensitizer, and b) secondary effect of complement activity on the vasculature [Korbelik and Cecic, 2003]. In the knockout model, some vessel integrity is maintained due to the lack of a secondary effect of complement activity in response to Photofrin-based PDT ensuring a greater degree of oxygen availability during PDT light delivery. The potential for singlet oxygen production is enhanced in tumors treated by Photofrin-based PDT in the C3 knockout model compared to its C57BL/6 counterpart. A useful study would be to compare tumor uptake of

photosensitizer in the C57BL/6 and the C3 knockout mouse strains. A greater amount of photosensitizer retained in tumors prior to light activation may lead to increased number of cures. Although this was not addressed within this thesis project, it would be a highly critical future study.

BPD-based PDT results in an improved cure rate in the C57BL/6 model over the C3 knockout, as predicted. The mechanism of cell death by BPD differs from that of Photofrin. BPD-based PDT applied to *in vitro* cultures promotes cell death by apoptosis specifically and *in vivo*, this photosensitizer targets vasculature directly. Therefore, complement activity may play a more important role as opsonin of cells undergoing death by apoptosis, a role in wound healing and ultimately improved immune cell formation. Apoptotic cells in a BPD-PDT treated tumor may be labeled by complement proteins for uptake by phagocytes, carried to draining lymph nodes, where tumor antigens are then exposed and interact with T-cells leading to long-term tumor-specific memory. Therefore, the mechanism of action of a particular photosensitizer dictates how the complement system will affect tumor response to PDT.

3.3.2 Fluence rate changes and tumor cures: C3 knockout vs C57BL/6

There are many published works that demonstrate the benefits of lowering the fluence rate during light delivery to obtain higher PDT cure rates [Sitnik *et al*, 1998; Sitnik and Henderson, 1998; Busch *et al*, 2002]. During lower fluence rate applications or fractionated light delivery, oxygen levels are maintained at higher levels in tumors during and immediately following PDT. Therefore, it was hypothesized that an even

greater cure rate could be obtained in the C3 knockout model of the LLC tumor if fluence rates were dropped compared to original growth delay applications in Figure 3.2. Figure 3.6 however indicates that there was no overall difference in cure rates within the respective mouse strains when the LLC tumor was treated with either high fluence rates of 100 mW/cm^2 or low fluence rates of 30 mW/cm^2. The results were unchanged regardless of fluence rate applied, a higher number of LLC tumors are cured by Photofrin-mediated PDT in the C3 knockout mice compared to the C57BL/6 mice. No further hints for improving the cure rate of the LLC by Photofrin-based PDT by lowering the fluence rate of total light energy delivered were obtained in this experiment.

3.3.3 Tumor cell survival

A direct method for demonstrating cell survival in tumors following PDT is an *in vitro* survival assay. The ability of tumor cells that escape toxicity during treatment to form colonies on a Petri plate is an indication of their rate of survival. In order to determine the actual cell survival in LLC tumors treated with Photofrin-based PDT, tumors were excised immediately following PDT from both the C3 knockout and C57BL/6 strains of mice, processed into single cell suspensions and plated for colony formation. Figure 3.6 indicates that there is a log greater tumor cell killing effect by PDT when applied in the C3 knockout model. A significantly greater number of cells survive PDT phototoxicity in the C57BL/6 mice compared to the C3 knockout indicating improved/enhanced photodynamic process in the C3 knockout model. It is suggested

below that the reason for this is increased oxygen availability in the C3 knockout model compared to the C57BL/6 mouse strain.

3.3.4 Oxygen tension by Eppendorf pO_2 histograph

In order for the photodynamic process to proceed, the presence of molecular oxygen at the site of treatment during light delivery is imperative. Therefore, it was hypothesized that the differences in LLC tumor response between the two mouse strains C3 knockout and C57BL/6, is attributed to oxygen levels being maintained more efficiently in the C3 knockout model during Photofrin-based PDT yet not during BPD-based PDT. To test this theory partial pressure of oxygen in either untreated or PDT-treated tumor immediately following light delivery were delineated with the Eppendorf pO_2 histograph method of measuring tissue oxygen levels [Minchinton *et al*, 1999; Aquino-Parsons *et al*, 2000]. Table 3.1 and Figures 3.7 through 3.9 summarize all results collected. In Table 3.1 data is presented as Median pO_2, Mean pO_2, % of pO_2 values <2.5 mmHg, the number (No.) of values collected, and the No. of mice tested. Neither Photofrin nor BPD alone had any effect on the mean pO_2 value in the LLC tumors. In both Table 3.1 and Figure 3.7 it is shown that the partial pressure of oxygen does not differ between untreated LLC tumors grown in either the C3 knockout (Median=3.73 mmHg) or the C57BL/6 (Median=3.9mmHg) mouse strains. Although there is a drop in oxygen tension in the C3 knockout model immediately following Photofrin-PDT compared to untreated controls, Mean=5.42 $\pm$ 0.70 mmHg from 7.55 $\pm$ 0.84 mmHg, respectively, the drop in mean oxygen tension immediately following Photofrin-PDT is

significantly greater in the C57BL/6 model, 4.52 ± 0.56 mmHg from 13.34 ± 0.87 mmHg in untreated controls. Histograms presenting the distribution of pO_2 values in the Lewis lung carcinoma treated with Photofrin-based PDT in both the C57BL/6 and the C3 knockout mouse strains is depicted in Figure 3.8. This result suggests that tumor oxygen status is maintained during Photofrin-based PDT light delivery to a greater degree in the C3 knockout model compared to the C57BL/6. The LLC in the C3 knockout treated with BPD-PDT is slightly less oxygenated immediately following treatment compared to those tumors assessed in the C57BL/6 model, although this difference is not significant (Figure 3.9). There is less oxygen in BPD-PDT treated tumors, mean=4.7 ± 0.28 mmHg, in the C3 knockout strain compared to untreated control, 7.55 ± 0.84 and Photofrin-PDT 5.42 ± 0.70.

Light is delivered to a target tissue three hours following initial administration of BPD, during which time the photosensitizer accumulates along the vasculature inflicting vascular damage concentrated in previously highly oxygenated areas. This results in an overall decrease in tumor oxygenation, but not in an increase in severely anoxic tumor regions (<2.5mmHg). In contrast, Photofrin is administered and allowed to circulate and accumulate in tumors for a much longer period, 24 hours, prior to light delivery. Perhaps there is little influence of photosensitizer directly in the vessels due to most of it diffusing deeper into tissue, closer to anoxic regions and away from the vasculature. Further studies would have to be conducted to address this issue.

The hypothesis that in the C3 knockout model oxygen status in a tumor immediately following Photofrin-PDT light delivery is improved over the C57BL/6 model is backed by these observations. The status of oxygen in a tumor following BPD-

PDT in either the C3 knockout model or the C57BL/6 decreases at about the same rate immediately following treatment.

3.3.5 Effect of donor human C3 in the C3 knockout on PDT-mediated tumor cures

The next experiment in this series involved the administration of human C3 protein to the C3 knockout mice bearing PDT-treated LLC tumors. It was anticipated that by introducing C3 to C3 knockout mice to replace C3 function, the tumor cure rate of Photofrin-based PDT would equal that of the C57BL/6 model. The reverse effect was observed. Shown in Figure 3.10, 50% of mice were cured in the combination group, compared to 30% in the C3 knockout and 0% in the C57BL/6 background strain. This result suggests that the administration of human C3 protein into mice itself had an effect on the tumors. Unfortunately, this protein is costly and we were unable to test the effect of the protein on the growth rate of these mice alone in the absence of PDT. Since the protein is of the human species, the protein itself may have induced an immune response, enhancing then the inflammatory status following treatment in the tumor.

3.3.6 The role of C5aR in the treatment of PDT

The role of the anaphylatoxin C5a, a major inflammatory mediator of neutrophil trafficking and activation, in the ability of PDT to eradicate tumors was studied in a Lewis lung carcinoma tumor model. Figure 3.11 depicts how blocking C5a receptor (C5aR) 30 minutes prior to PDT light delivery worsens the cure rate in an already PDT-resistant tumor model. Blocking C5a-C5aR interactions and consequently C5aR-mediated signal transduction pathways, could inhibit neutrophil cytotoxic activity by decreased neutrophil aggregation, degranulation, and superoxide production, but may not necessarily decrease infiltration of neutrophils into PDT-treated lesions [Tofukuji, 1998]. This hypothesis was not investigated in this project. Further inhibiting the efficiency of PDT to cure the Lewis lung carcinoma tumor by blocking the C5aR around the time of light delivery, suggests the importance of the anaphylatoxin C5a in the cure rate of PDT. C5a acts specifically to activate neutrophils. The result of this experiment adds to the understanding of the mechanism of neutrophil trafficking and activation in response to PDT applied in the treatment of solid tumors.

3.3.7 Summary and conclusions

The data collected in this chapter highlight the complex involvement of the complement system in the anti-tumor effect of PDT. Oxygen status and delivery, dependent on oxygen consumption and vascular integrity during treatment, is a perpetual concern for the efficacy of the photodynamic process. Complement activity may hold a

prominent role in affecting vascular stability depending upon the mechanism of action of the photosensitizer used. It was observed that in the absence of complement activity, tumor response to PDT was abrogated when the treatment was mediated by Photofrin, yet if mediated by BPD, PDT response was slightly improved. This difference was attributed to higher levels of oxygen tension maintained immediately following Photofrin-PDT in LLC tumors grown and treated in the C3 knockout model compared to the C57BL/6 model. These data suggest that in the LLC model, a tumor resistant to Photofrin-PDT, combined damage to tumor endothelium inflicted by direct PDT-induced phototoxicity and secondary complement activity reduces treatment efficiency by severely compromising blood flow, limiting effectiveness of the photodynamic process in low oxygen conditions during Photofrin-PDT.

The C3 knockout model can be a useful tool in determining the role of C3 in PDT therapy, however, it should be taken into consideration that knockouts may have adapted to the loss of C3 function in an undefined manner. Unknown factor(s), perhaps an enhanced activity of another arm of inflammation other than complement may be playing an effect on the outcome of tumor cures outlined in this chapter. More direct means of temporarily blocking the effect of complement, such as the C5aR antagonist or inhibitors of more upstream complement cascade components, around the time of PDT light delivery could prove to be more specific and indicative of the overall effect that activated complement has on PDT.

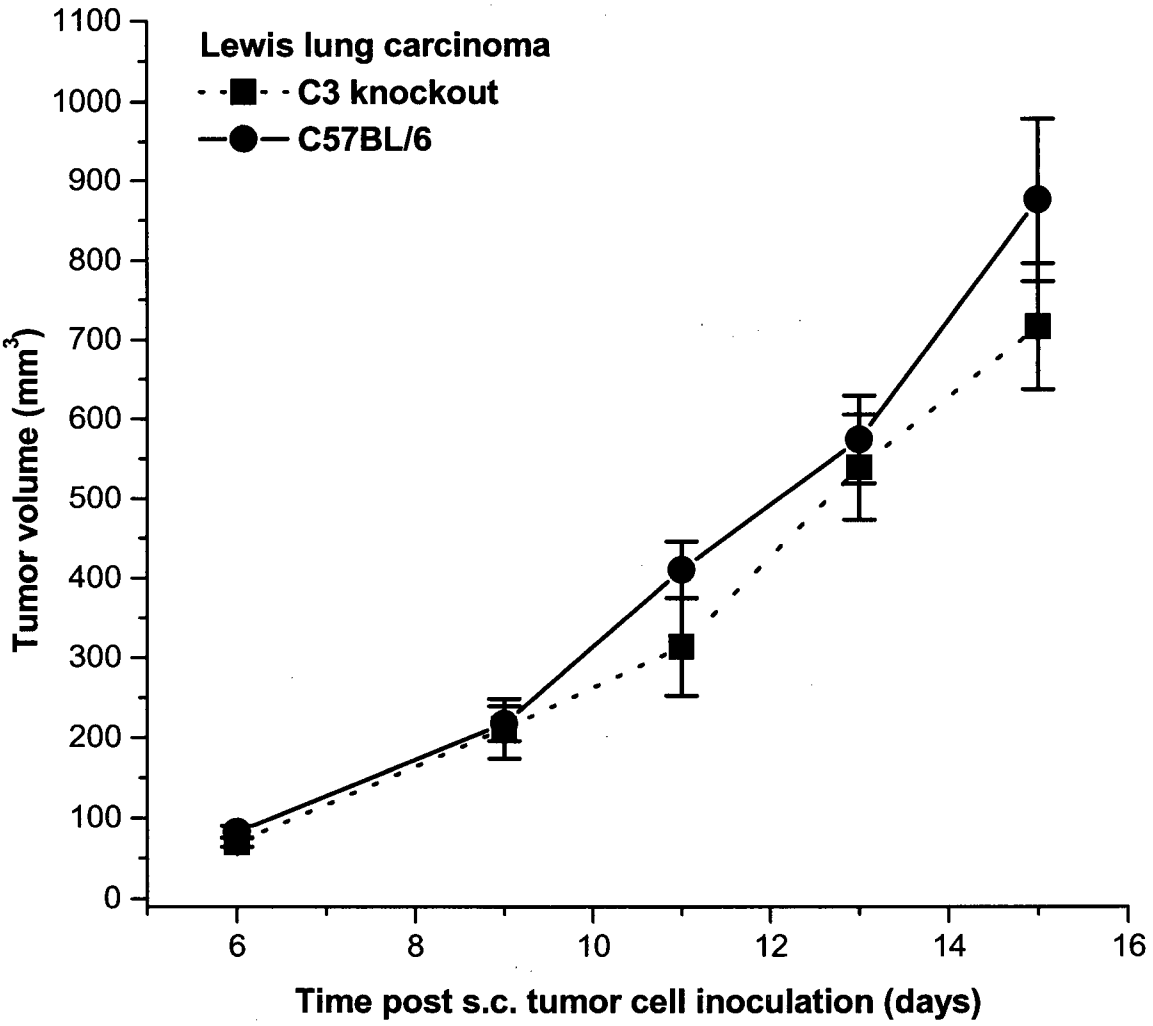

Figure 3.1 C3 knockout verses C57BL/6: Growth rate of the Lewis lung carcinoma tumor model. Lewis lung carcinoma cells were inoculated subcutaneous on the dorsal side of C3 knockout mice and also C57BL/6 mice. Animals were observed for tumor formation and subsequent growth rate. Data is presented as tumor volume (mm^3) plotted against time. No significant difference between the two strains of mice.

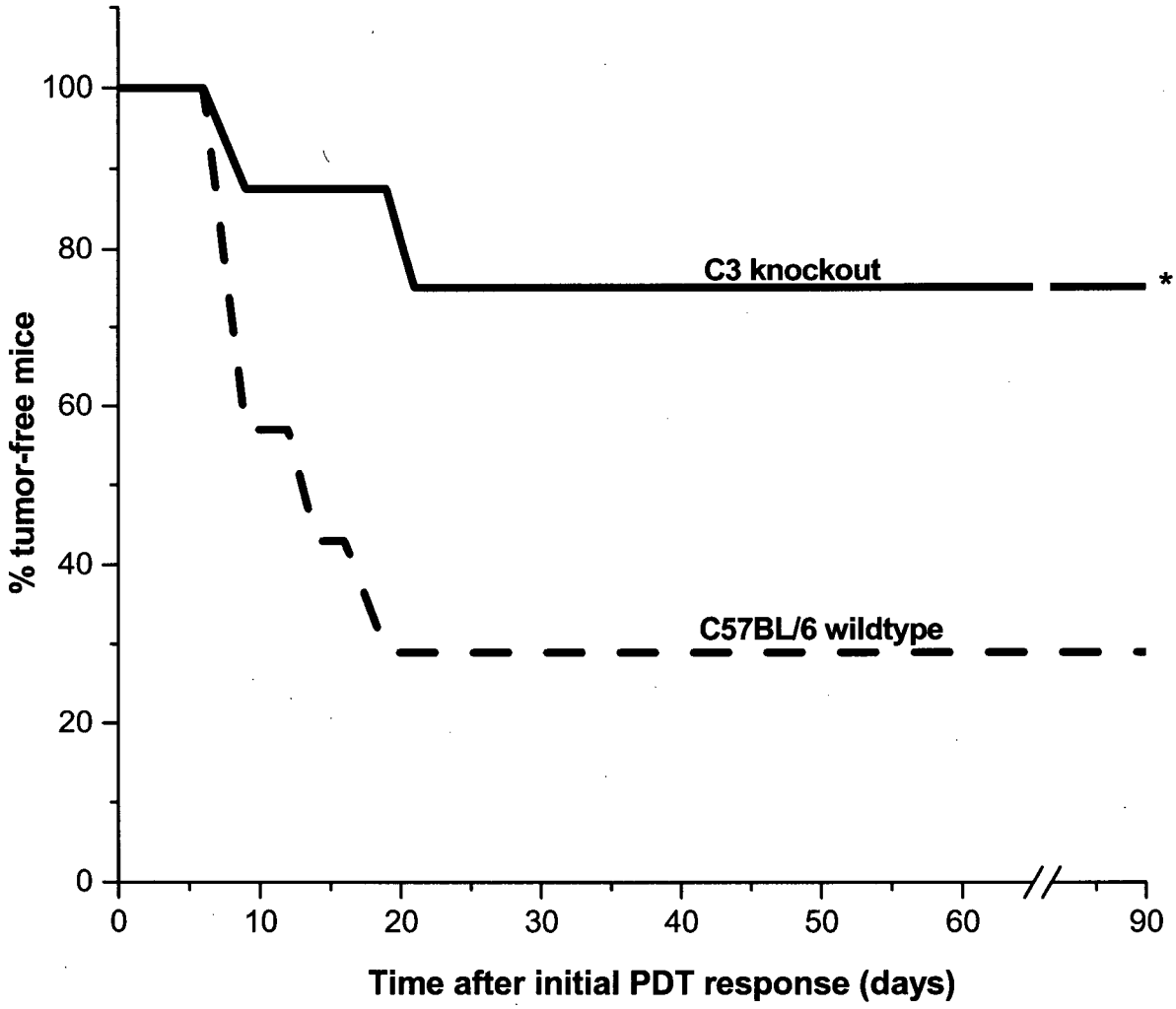

Figure 3.2 Lewis lung carcinoma tumor cures by Photofrin-based PDT in the C3 knockout compared to the C57BL/6 mouse strain. Lewis lung carcinoma tumors were grown subcutaneous on the C3 knockout and the C57BL/6 mice. Both groups of tumors were treated with Photofrin 10mg/kg and 200J/cm^2 then followed for tumor re-growth following treatment. * indicates significant increase in tumor cures compared to the C57BL/6 strain of mice. Statistical analysis was undertaken by the log-rank test.

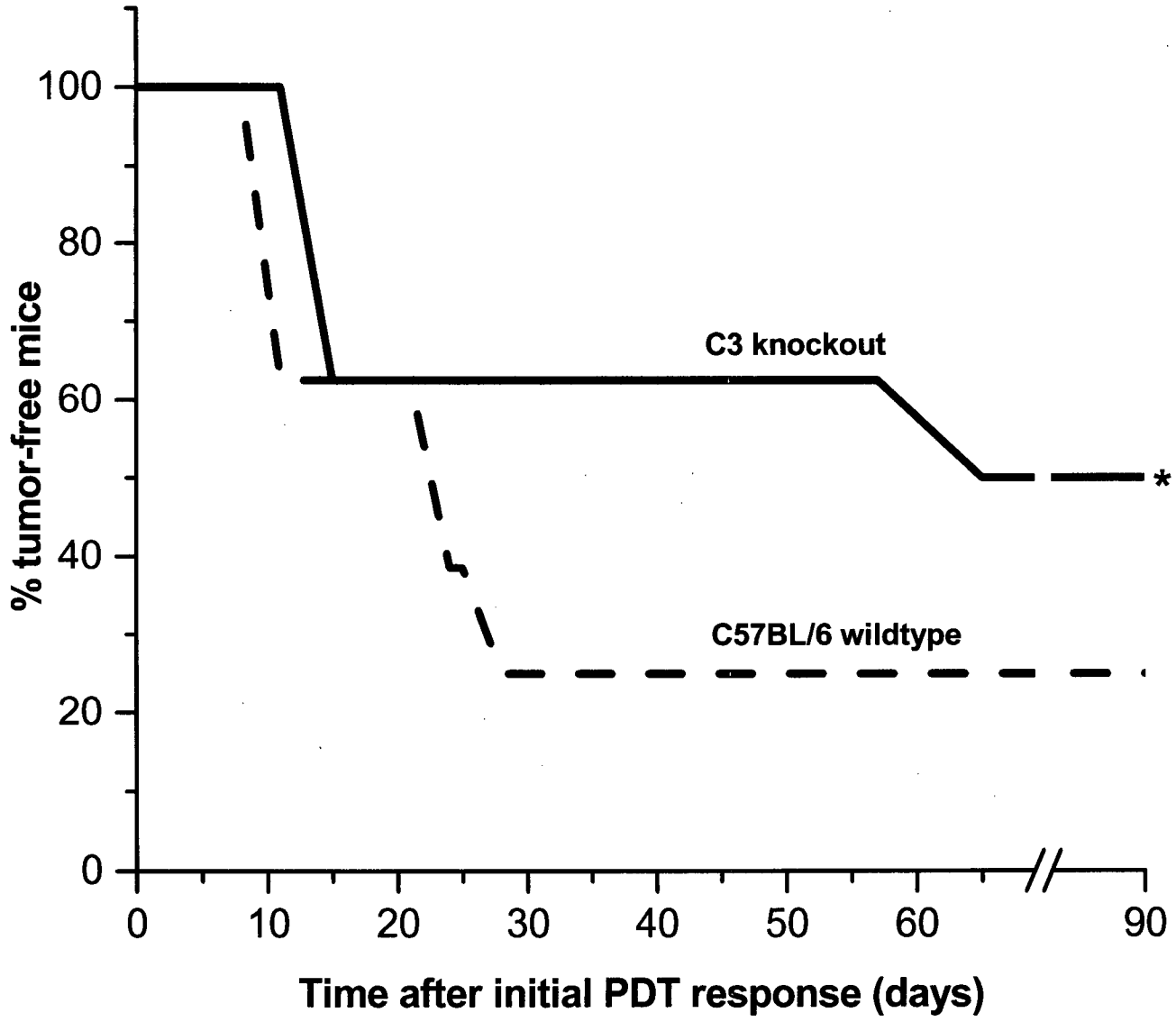

Figure 3.3 MCA205 fibrosarcoma tumor cures by Photofrin-based PDT in the C3 knockout compared to the C57BL/6 mouse strain. MCA205 fibrosarcoma tumors were grown subcutaneous on the C3 knockout and the C57BL/6 mice. Both groups of tumors were treated with Photofrin 10 mg/kg and 200 J/cm^2 then followed for tumor re-growth following treatment. * indicates significant increase in tumor cures compared to the C57BL/6 strain of mice. Statistical analysis was undertaken by the log-rank test.

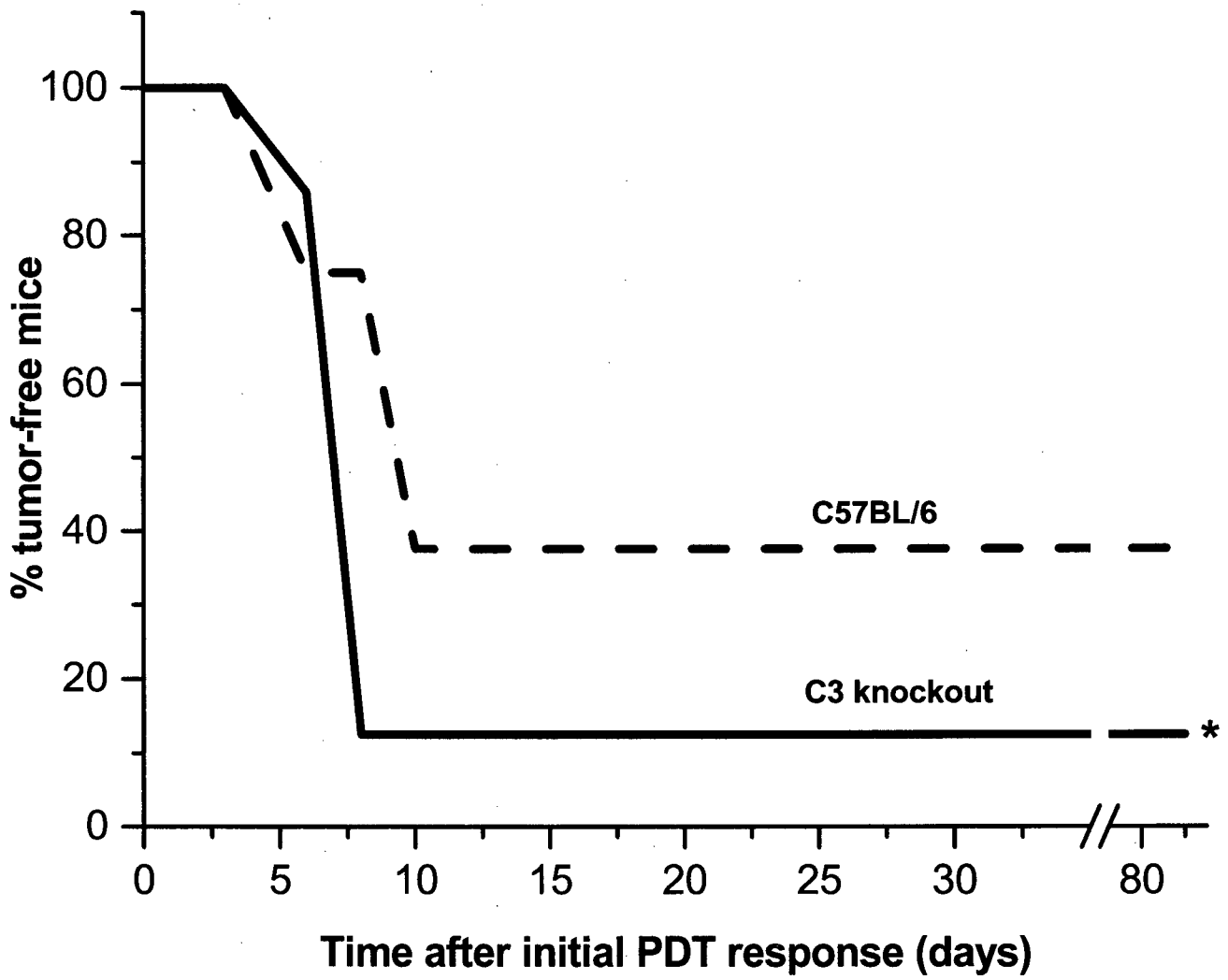

Figure 3.4 Lewis lung carcinoma tumor cure rate by BPD-based PDT comparing the C3 knockout and C57BL/6 mouse strains. The Lewis lung carcinoma tumor was grown subcutaneous on C3 knockout and C57BL/6 mice, treated with BPD 2.5 mg/kg and 100J/cm^2, then followed for signs of tumor re-growth over time in days. * $p<0.05$ indicates significant decrease in tumor cures compared to the C57BL/6 strain of mice. Statistical analysis was undertaken by the log-rank test. PDT response corresponds to de-bulking of tumors by 24 hours following PDT light delivery.

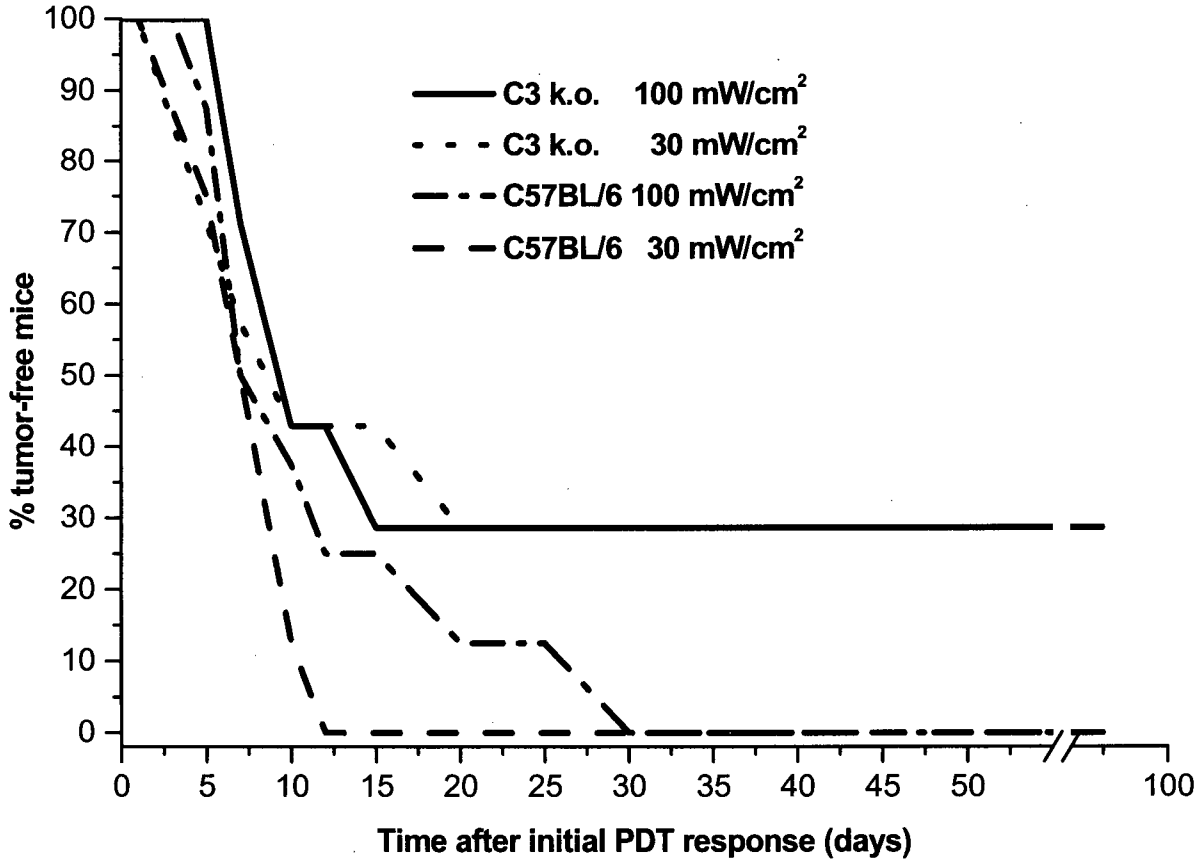

Figure 3.5 The effect of high verses low fluence rates on the cure rate of the Lewis lung carcinoma by Photofrin-based PDT in both the C3 knockout and the C57BL/6 mouse strains. Four groups of mice (n=8 per group), two group of C3 knockout (C3 k.o.) and two groups of C57BL/6 were inoculated subcutaneous with Lewis lung carcinoma tumors and treated with PDT: Photofrin 10 mg/kg and 150 J/cm^2. The total light dose was administered with either a high 100mW/cm^2 fluence rate (solid lines) or a low 30mW/cm^2 fluence rate (dotted lines). No statistical difference (log-rank test) between the fluence rates in either the C3 knockout or the C57BL/6 strains.

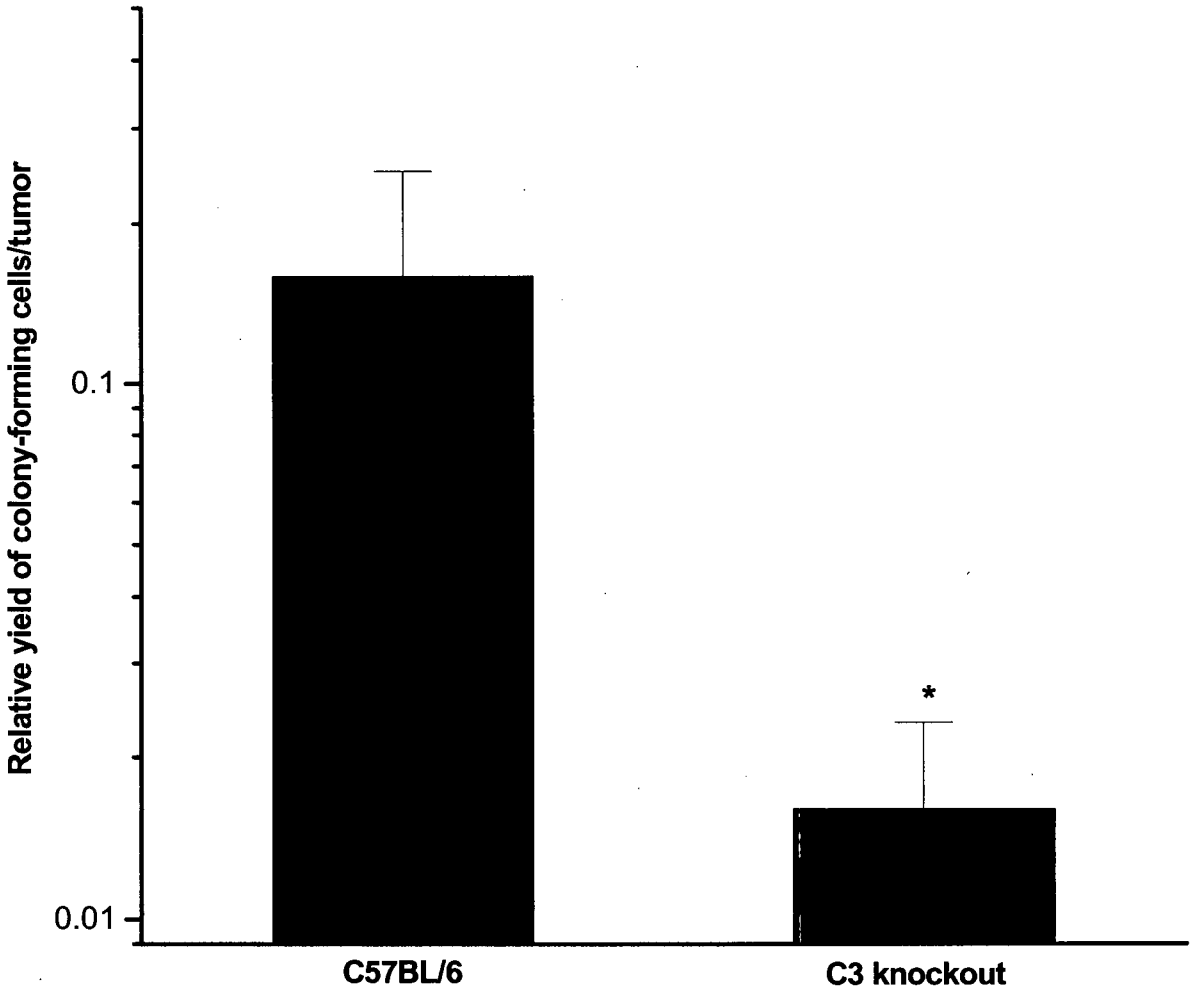

Figure 3.6 Cell survival assay: Lewis lung carcinoma response to Photofrin-based PDT in C57BL/6 and the C3 knockout mouse strains. Subcutaneous Lewis lung carcinoma tumors were treated with PDT: Photofrin 10 mg/kg and 150 J/cm^2 in both the C3 knockout and C57BL/6 mouse strains (n=4 per group), then excised immediately following illumination. The tumors were processed into a single cell suspension and plated onto petri dishes and incubated at 37 degrees celsius until visible colonies were formed from any tumor cells that may have survived treatment.

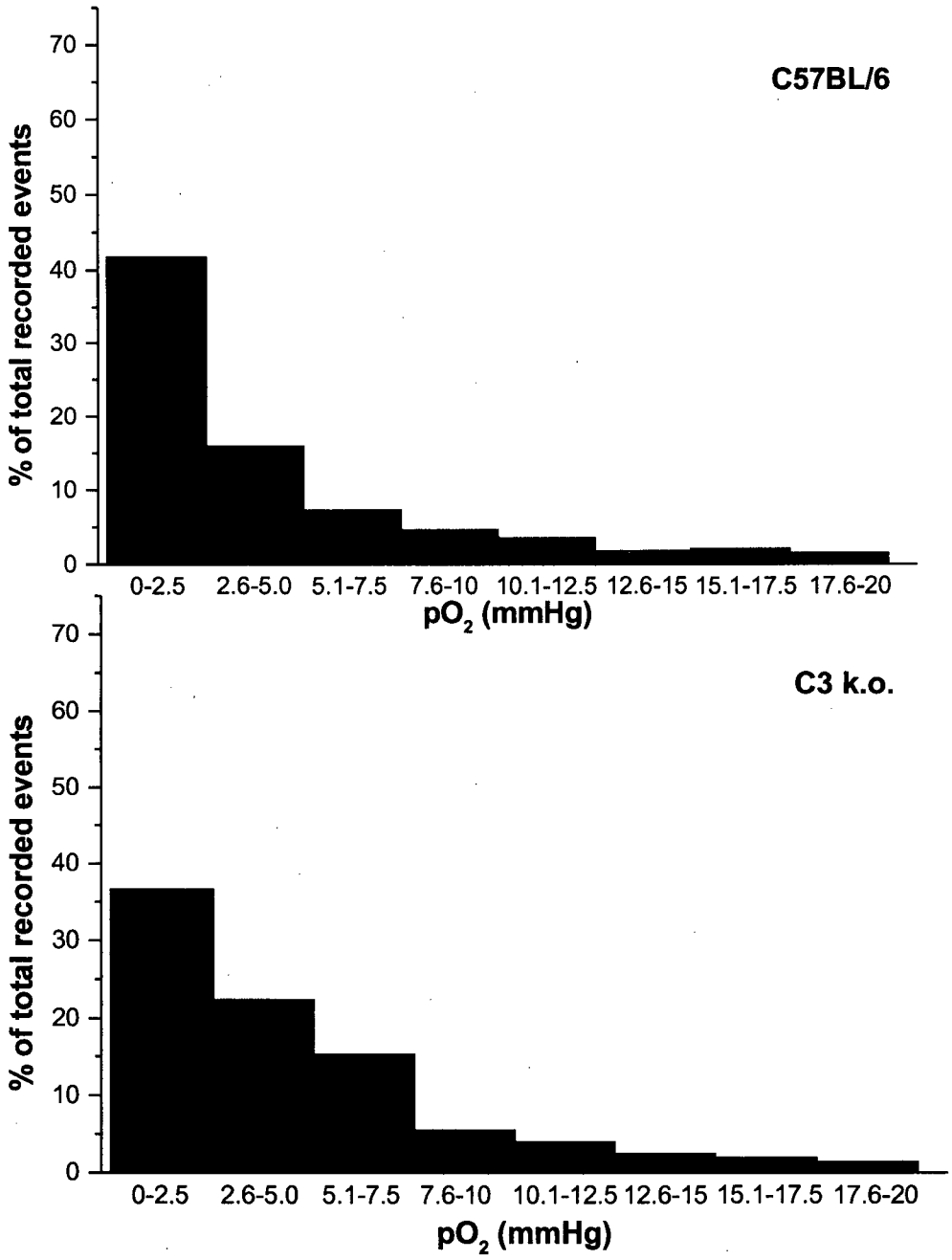

Figure 3.7 Histograms representing the distribution of partial pressure of oxygen in untreated Lewis lung carcinoma tumors in both the C57BL/6 and the C3 knockout mouse strains (C3 k.o.) as measured by the Eppendorf pO_2 needle probe. The data is represented as the percent of total events recorded and distributed into increments of 2.5 mmHg. The values of all tumors were pooled. No significance found between the C57BL/6 and C3 knockout by the non-parametric Wilcoxon Matched Pairs test.

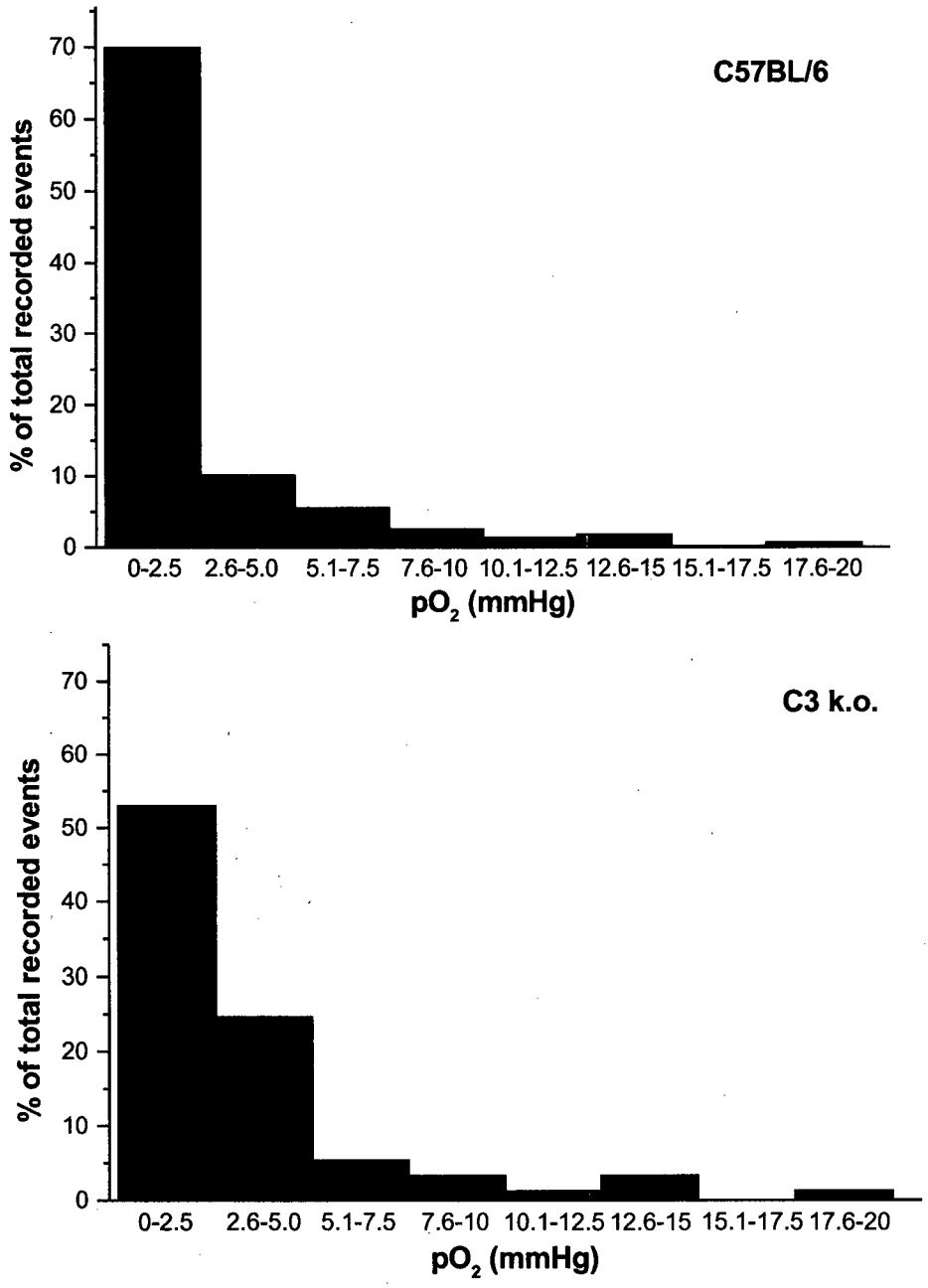

Figure 3.8 Histograms representing the distribution of partial pressure of oxygen in Photofrin-PDT treated Lewis lung carcinoma tumors in both the C57BL/6 and the C3 knockout mouse strains (C3 k.o.) as measured by the Eppendorf pO_2 needle probe. The data is presented as the percent of total events recorded and distributed into increments of 2.5 mmHg. The values of all tumors were pooled. A statistically significant increase in the incidence of pO2 measurements <5.0 mmHg in the C57BL/6 compared to the C3 knockout model was proven by the non-parametric Wilcoxon Matched pairs test.

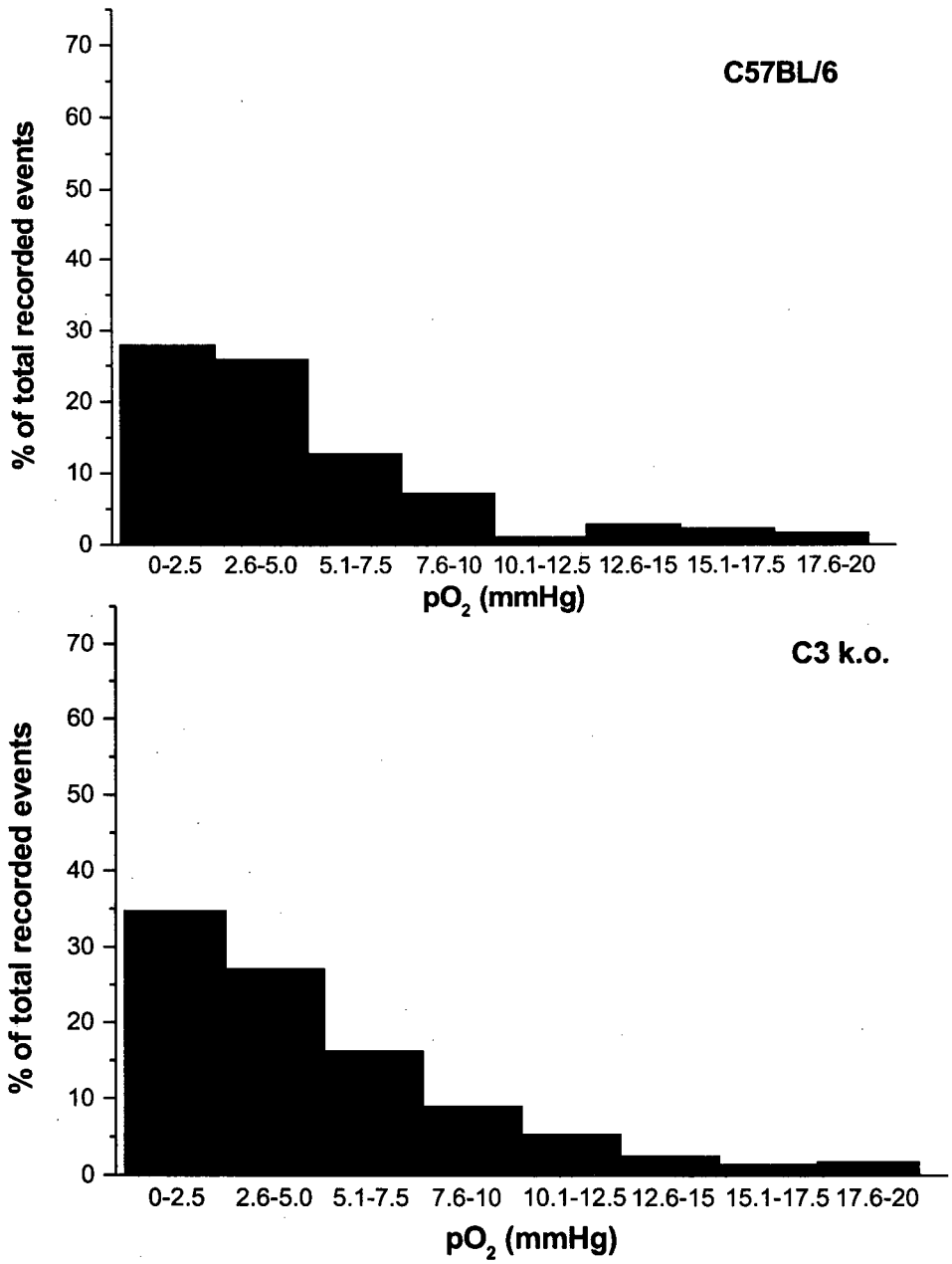

Figure 3.9 Histograms representing the distribution of partial pressure of oxygen in BPD-PDT treated Lewis lung carcinoma tumors in both the C57BL/6 and the C3 knockout mouse strains (C3 k.o.) as measured by the Eppendorf pO_2 needle probe. The data is presented as the percent of total events recorded and distributed into increments of 2.5 mmHg. The values of all tumors were pooled. Statistical analysis was undertaken by the non-parametric Wilcoxon Matched pairs test.

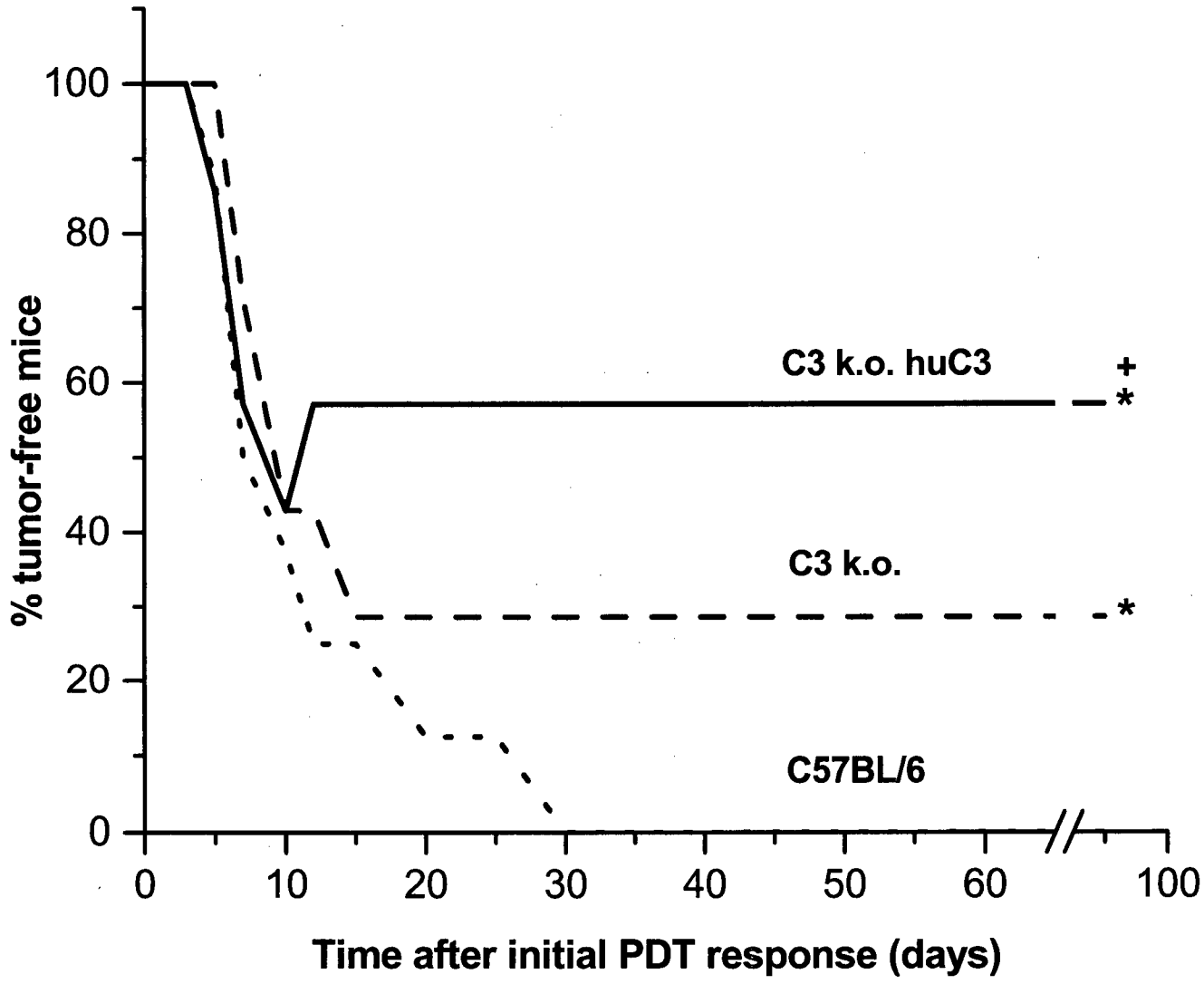

Figure 3.10 Human C3 administered to C3 knockout mice increases the PDT cure rate of the Lewis lung carcinoma. Two groups of C3 knockout mice and one group of C57BL/6 mice (n=8 per group) were inoculated with Lewis lung carcinoma tumors and treated with PDT: Photofrin 10 mg/kg and 150 J/cm^2. One of the two groups of C3 knockout mice were also administered a single dose of human C3 (huC3) 30 minutes prior to PDT light delivery. *$p<0.05$ statistical increase in cures compared to C57BL/6. + $p<0.05$ depicts significant difference between C3 k.o. huC3 group compared to C3 k.o. Statistical analysis performed by the log-rank test.

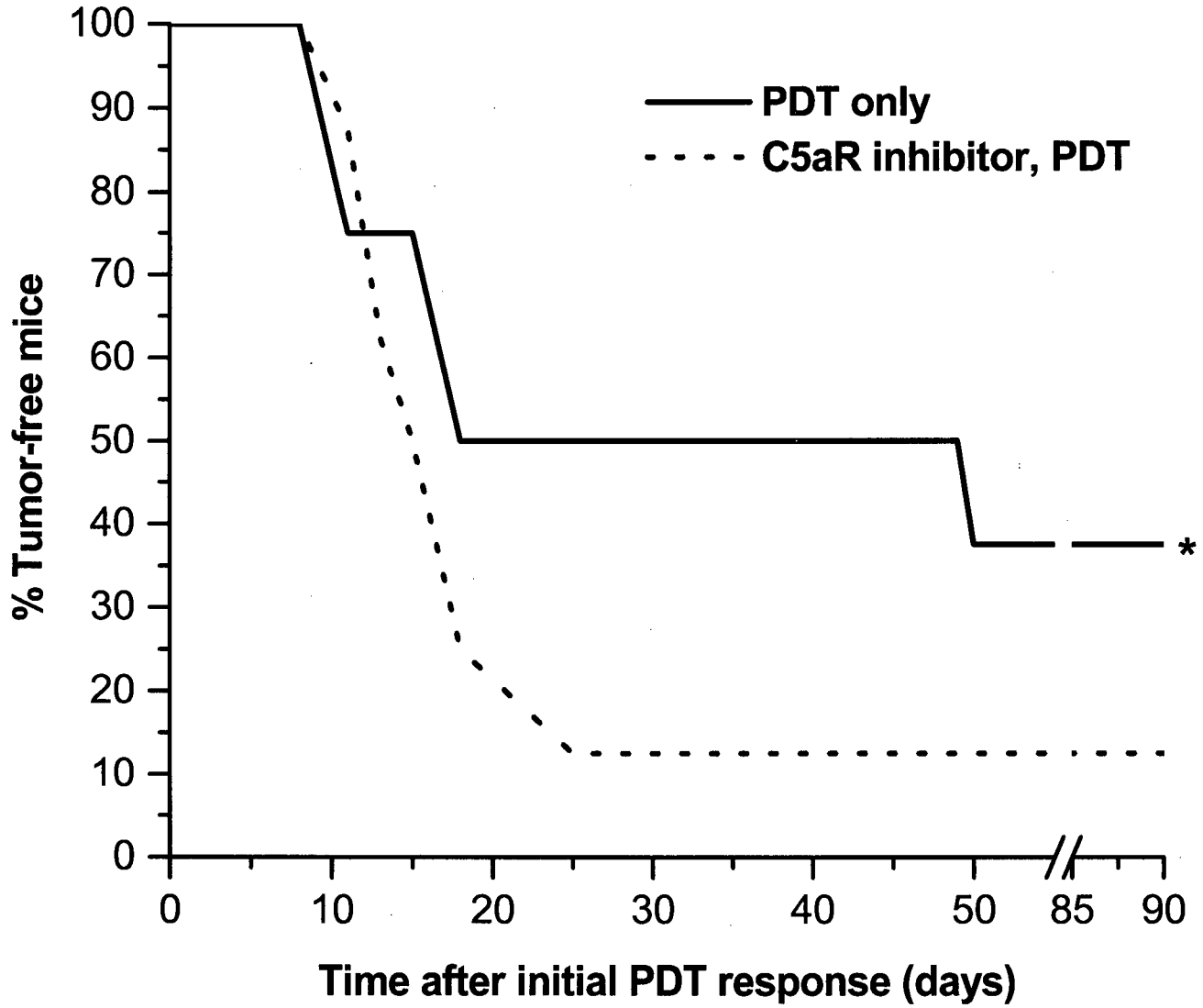

Figure 3.11 C5aR antagonist can decreases the cure rate of PDT applied in the treatment of Lewis lung carcinoma. C5aR antagonist was administered i.v. to one group (n=8) of LLC-tumor bearing mice 30 minutes prior to PDT light delivery. The second group of tumors (n=8) was treated by PDT alone. PDT: Photofrin 10 mg/kg and 150 J/cm2. Statistical analysis by log-rank test revealed a significant delay in tumor re-growth up to 30 days in the PDT only group compared to the C5aR inhibitor, PDT group. At 90 days post treatment there is significant difference in cures (log-rank test).

Table 3.1 Eppendorf pO_2 histograph values of Lewis lung carcinoma tumors treated by Photofrin- or BPD-based PDT in the C3 knockout and C57BL/6 mouse strains.

	Median (mmHg)	Mean ± s.e. (mmHg)	% ≤ 2.5 mmHg	No. of values	No. of mice
C57BL/6					
Untreated	3.75	13.34 ± 0.87	41.90	580	14
Photofrin-PDT	1.9	4.52 ± 0.56	70.45	264	7
BPD-PDT	3.8	7.10 ± 0.68	32.72	162	5
C3 knockout					
Untreated	3.9	7.55 ± 0.84	37.89	190	6
Photofrin-PDT	2.4	5.42 ± 0.70	54.61	141	4
BPD-PDT	3.4	4.70 ± 0.28	43.28	305	9
Drug alone:					
Untreated	3.75	13.34 ± 0.87	41.90	580	14
Photofrin	6.6	13.30 ± 1.72	26.73	101	3
Untreated	2.4	3.7 ± 0.32	49.15	118	3
BPD only	2.1	3.6 ± 0.40	54.00	106	3

GENERAL DISCUSSION

This dissertation is a comprehensive evaluation of PDT inflicted cell damage engaging the many effector functions of the complement system. The complement system is in a constant level of low activity in its primary role as the first line of defense against invading pathogens and maintenance of homeostasis. Importantly, it is also now well understood that when the complement system is unregulated, or balance in the system is disturbed, it can induce normal tissue damage. It has been labeled a major culprit in prolonging burn injury, transplant rejection, damage in renal and/or myocardial ischemia-reperfusion injury. Its ability to inflict damage to autologous tissue led to the finding that it also is engaged against tumor tissue altered by PDT-inflicted damage. Our aim was to define how. Schematic 2 offers a visual summary of our understanding of the role of complement based on the results collected in these studies. PDT leads to surface changes that can be described as altered self, engaging the many precarious functions of the complement system to the site of treatment. It may also play a beneficial role in the clearance of cells undergoing apoptosis and furthermore, mediating wound healing. Inadvertently, PDT damage may trigger multiple roles of the complement system to inflict further damage to tumor cells and also mop-up dead cells and debris.

Changes following PDT treatment on cells undergoing stress and death by apoptosis or necrosis include translocation of the HSP70 stress protein from the cytosol to the surface of cells. Such events lead to the deposition of complement C3, the pivotal protein in the centre of the complement cascade activated by all three activation pathways: alternative, classical, and lectin. Complement activity in response to PDT is

mainly initiated by antibody-independent alternative pathway activation in our Photofrin-based PDT solid tumor models. Once the alternative pathway is activated on cells, it branches out into a series of reactions leading to the fragmentation of C3 and C5 into their respective anaphylatoxins C3a and C5a, and progression toward the assembly of the membrane attack complex C5b-9. The function of these proteins and/or protein complexes includes mediating the many overlapping pathways of inflammation, neutrophil trafficking, and to promote immune cell activation.

A barrage of pro-inflammatory mediators is released from a site of PDT injury. Agents such as IL-1β, IL-6, TNF-α, histamine, and eicosanoids promote neutrophil trafficking to the PDT-treated site. The complement system mediates the many networks of inflammation that directly act on neutrophil chemotaxis and it was observed that blocking the complement system prior to PDT led to the greatest level of inhibition on PDT-specific neutrophilia. This suggests that the complement system recognizes the altered surfaces in a PDT-treated lesion and becomes engaged to trigger neutrophil trafficking at this site of inflammation. One particular complement protein, C5a anaphylatoxin was directly demonstrated to influence the outcome of therapy. C5a acts to promote neutrophil chemotaxis and activation, contributing to the success of PDT when applied in the treatment of experimental murine tumors.

The impact that the complement system may have on the success of PDT in the eradication of the Lewis lung carcinoma tumor was assessed in a C3 knockout mouse model of the C57BL/6 genetic background. The outcome clearly depends on the mechanism of action of the photosensitizer administered and subsequent effect on tumor oxygen levels. Photofrin-mediated PDT cured a significantly greater number of tumors

in the C3 knockout mice than in the background, complement-proficient strain, compared to a decrease in cures mediated by BPD-PDT. Immediately following Photofrin-based PDT tumor oxygen levels were higher than in BPD-PDT treated tumors. These results suggest that the photodynamic process is hampered in the presence of active complement. Endothelial cell damage by complement may hamper blood vessel integrity, and/or influence immune cell aggregation in vessels, creating an environment of low oxygen content. Hence, complement activity may play a dual, paradoxical, role in the outcome of PDT. Complement activity secondary to direct PDT damage may enhance tumor cell cytotoxicity, however, it may concomitantly disrupt the homeostasis in the tumor microenvironment specifically affecting oxygen delivery. Therefore, it is necessary to define the delicate balance of beneficial versus unwanted complement activity in a PDT-treated tumor. The impact of these findings on the overall clinical significance of PDT as a tumor therapy may lie in the development of methods to control local complement activity in combination with PDT to improve the success of PDT as an anti-cancer modality.

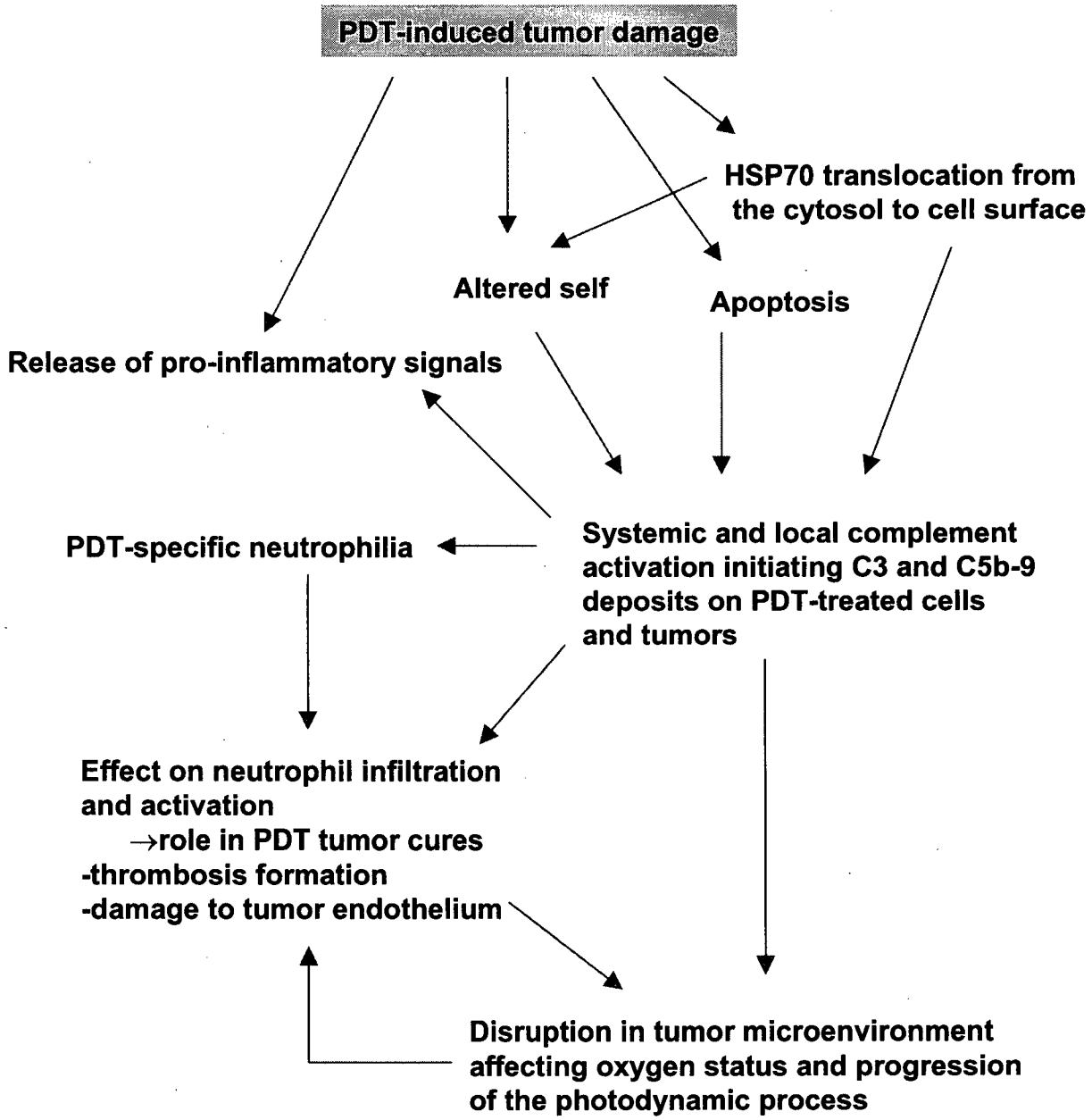

Schematic 2: Summary of events induced by PDT influencing a disruption in tumor microenvironment

REFERENCES

Agarwal, ML, Larkin, HE, Zaidi, SI, Mukhtar, H, Oleinick, NL, 1993, Phospholipase activation triggers apoptosis in photosensitized mouse lymphoma cells, Cancer Research, v. 53, p. 5897-902.

Allison, BA, Haydn-Pritchard, P, Richter, AM, Levy, JG, 1990, The plasma distribution of benzoporphyrin derivative and the effects of plasma lipoproteins on its biodistribution, Photochemistry and Photobiology, v. 52, p. 501-7.

Aquino-Parsons, C, Green, A, Minchinton, AI, 2000, Oxygen tension in primary gynaecological tumors: the influence of carbon dioxide concentration, Radiotherapy & Oncology, v. 57, p. 45-51.

Arvieux, J, Yssel, H, Colomb, MG, 1988, Antigen-bound C3b and C4b enhance antigen-presenting cell function in activation of human T-cell clones: Immunology, v. 65, p. 229-35.

Aslan, M, Freeman, BA, 2002, Oxidases and oxygenases in regulation of vascular nitric oxide signaling and inflammatory responses: Immunology Research, v. 26, p. 107-18.

Atkinson, JP, Oglesby, TJ, White, D, Adams, EA, Liszewski, MK, 1991, Separation of self from non-self in the complement system: a role for membrane cofactor protein and decay accelerating factor: Clinical & Experimental Immunology, v. 86, p. 27-30.

Auditore, JV, Olson, EJ, 1966, isolation, purification and probable structural configuration of N-acetyl-aspartyl glutamate in human brain, Archives of Biochemistry and Biophysics, v. 114, p. 452-63.

Babilas, P, Schacht, V, Liebsch, G, Wolfbeis, OS, Landthaler, M, Szeimies, RM, Abels, C, 2003, Effects of light fractionation and different fluence rates on photodynamic therapy with 5-aminolaevulinic acid in vivo: British Journal of Cancer, v. 88, p. 1462-9.

Bao, L, Haas, M, Boackle, SA, Kraus, DM, Cunningham, PN, Park, P, Alexander, JJ, Anderson, RK, Culhane, K, Holers, VM, Quigg, RJ, 2002, Transgenic expression of a soluble complement inhibitor protects against renal disease and promotes survival in MRL/lpr mice: Journal of Immunology, v. 168, p. 3601-7.

Barazzone-Argiroffo, C., A. Pagano, C. Juge, I. Metrailler, A. Rochat, C. Vesin, and Y. Donati, 2003, Glucocorticoids aggravate hyperoxia-induced lung injury through decreased nuclear factor-kappa B activity: American Journal of Physiology - Lung Cellular & Molecular Physiology, v. 284, p. L197-204.

Barel, A, Jori, G, Perin, A, Romandini, P, Pagnan, A, Biffanti, S, 1986, Role of high-, low-, and very low-density lipoproteins in the transport and tumor-delivery of hematoporphyrin in vivo, Cancer Letters, v. 32, p. 145-50.

Barr, H, Krasner, N, Boulos, PB, 1990, Photodynamic therapy for colorectal cancer: A quantitative study, British Journal of Surgery, v. 77, p. 93-6.

Basu, S, Binder, RJ, Ramalingam, Srivastava, PK, 2001, CD91 is a common receptor for heat shock proteins gp96, hsp90, hsp70, and calreticulin, Immunity, v. 14, p. 303-13.

Bellnier, DA, Ho, YK, Pandey, RA, Missert, JR, Dougherty, TJ, 1989, Photochemistry and Photobiology, v. 50, p. 221.

Bellnier, DA, Henderson, BW, 1992, Determinant for photodynamic tissue destruction, in: Photodynamic therapy, basic principles and clinical applications, Henderson, BW, Dougherty, TJ, eds, Dekker, New York, New York, p. 117.

Ben-Hur, E, Heldman, E, Crane, SE, Rosenthal, I, 1988, Release of clotting factors from photosensitized endothelial cells: A possible target for blood vessel occlusion by photodynamic therapy, FEBS Letter, v. 236, p. 105-8.

Benson, RC Jr, Farrow GM, Kinsey, JH, 1982, Detection and localization of in situ carcinoma of the bladder with hematoporphyrin derivative, Mayo Clinic Proceedings, v. 57, p. 548-55.

Berg, K, Moan, J, 1994, Lysosomes as photochemical targets, International Journal of Cancer, v. 59, p. 814-22.

Biel, M, 1998, Photodynamic therapy and the treatment of head and neck neoplasia, Laryngoscope, v. 108, p. 1259-68.

Birnbaum Y, Leor J, Kloner R, 1997, Pathobiology and clinical impact of reperfusion injury, Journals of Thrombosis and Thrombolysis, v. 4, p.185-95.

Bjorge L, Hakulinen, J, Wahlstrom, T, Matre, R, Meri, S, 1997, Complement-regulatory proteins in ovarian malignancies, International Journal of Cancer, v. 70, p. 14-25.

Bottger, EC, Bitter-Suermann, D, 1987, Complement and the regulation of humoral immune responses, Immunology Today, v. 8, p. 261-4.

Bouhlal H, Blondin C, Haeffner-Cavaillon N, Goldschmidt P, 2002, N-acetyl-aspartyl glutamic acid (NAAGA) inhibits the adhesion of leukocytes to activated endothelial cells and down-modulates the cytokine-induced expression of adhesion molecules, Journal Francais d Opthalmologie, v. 25, p. 993-1000.

Brizel, DM, Scully, SP, Harrelson, JM, Layfield, LJ, Bean, JM, Prosnitz, LR, Dewhirst, MW, 1996, Tumor oxygenation predicts for the likelihood of distant metastases in human soft tissue sarcoma: Cancer Research, v. 56, p. 941-3.

Brizel, DM, Sibley, GS, Prosnitz, LR, Scher, RL, Dewhirst, MW, 1997, Tumor hypoxia adversely affects the prognosis of carcinoma of the head and neck: International Journal of Radiation Oncology, Biology, Physics, v. 38, p. 285-9.

Busch, T M, Hahn, SM, Evans, SM, Koch, CJ, 2000, Depletion of tumor oxygenation during photodynamic therapy: detection by the hypoxia marker EF3 [2-(2-nitroimidazol-1[H]-yl)-N-(3,3,3-trifluoropropyl)acetamide]: Cancer Research, v. 60, p. 2636-42.

Busch, TM, Wileyto, EP, Emanuele, MJ, Del Piero, F, Marconato, L, Glatstein, E, Koch, CJ, 2002, Photodynamic therapy creates fluence rate-dependent gradients in the intratumoral spatial distribution of oxygen, Cancer Research, v. 62, p. 7273-9.

Campoli, M, Chang, CC, Ferrone, S, 2002, HLA class I antigen loss, tumor immune escape and immune selection, Vaccine, v. 20, p. A40-5.

Caragine, T A, Imai, M, Frey, AB, Tomlinson, S, 2002, Expression of rat complement control protein Crry on tumor cells inhibits rat natural killer cell-mediated cytotoxicity, Blood, v. 100, p. 3304-10.

Caragine, T A, Okada, N, Frey, AB, Tomlinson, S, 2002, A tumor-expressed inhibitor of the early but not late complement lytic pathway enhances tumor growth in a rat model of human breast cancer, Cancer Research, v. 62, p. 1110-5.

Carroll, MC, Fischer, MB, 1997, Complement and immune response, Current Opinions in Immunology, v. 9, p. 64-9.

Cecic, I., C. S. Parkins, and M. Korbelik, 2001, Induction of systemic neutrophil response in mice by photodynamic therapy of solid tumors: Photochemistry & Photobiology., v. 74, p. 712-20.

Cecic, I, Korbelik, M, 2002, Mediators of peripheral blood neutrophilia induced by photodynamic therapy of solid tumors, Cancer Letters, v. 183, p. 43-51.

Cerny, T, Borisch, B, Introna, M, Johnson, P, Rose, AL, 2002, Mechanism of action of rituximab, Anti-Cancer Drugs, 13 Supplement 2, p. S3-10.

Chabalgoity, JA, Dougan, G, Mastroeni, P, Aspinall, RJ, 2002, Live bacteria as the basis for immunotherapies against cancer, Expert Review of Vaccines, v. 1, p. 495-505.

Chakraborti, T, Ghosh, SK, Michael, JR, Batabyal, SK, Chakraborti, S, 1998, Targets of oxidative stress in cardiovascular system, Molecular & Cellular Biochemistry, v. 187, p. 1-10.

Chakraborti, T, Mandal,A, Mandal, M, Das, S, Chakraborti, S, 2000, Complement activation in heart diseases. Role of oxidants, Cellular Signalling, v. 12, p. 607-17.

Chen, Q, Huang, Z, Chen, H, Shapiro, H, Beckers, J, Hetzel, FW, 2002, Improvement of tumor response by manipulation of tumor oxygenation during photodynamic therapy, Photochemistry & Photobiology, v. 76, p. 197-203.

Chenoweth, D E, 1987, Complement activation in extracorporeal circuits: Annals of the New York Academy of Sciences, v. 516, p. 306-13.

Christensen, T, Moan, J, Smedshammer, L, 1985, Influence of hematoporphyrin derivative (HpD) and light on the attachment of cells to the substratum, Photochemistry and Photobiophysics, v. 10, p. 53.

Cole DS, Morgan, BP, 2003, Beyond lysis: how complement influences cell fate, Clinical Science, v. 104, p. 455-66.

Cooper, NR, 1999, Biology of the complement system, In: Inflammation: Basic principles and clinical correlations, Balin, JI, Snyderman, R, eds, Lippincott Williams & Wilkins, Philadelphia, p. 317-29.

Coutier, S, Bezdetnaya, LN, Foster, TN, Parache, RM, Guillemin, F, 2002, Effect of irradiation fluence rate on the efficacy of photodynamic therapy and tumor oxygenation in meta-tetra (hydroxyphenyl) chlorin (mTHPC)-sensitized HT29 xenografts in nude mice, Radiation Research, v. 158, p. 339-45.

Curti, BC, Ochoa, AC, Powers, GC, Kopp, WC, Alvord, WG, Janik, JE, Gause, BL, Dunn, B, Kopreski, MS, Fenton, R, Zea, A, Dansky-Ullman, C, Strobl, S, Harvery, L, Nelson, E, Sznol, M, Longo, DL, 1998, Phase I trial of anti-CD3-stimulated CD4+ T cells, infusional interleukin-2, and cyclophosphamide in patients with advanced cancer, Journal of Clinical Oncology, v. 16, p. 2752-60.

Davies, CL, Western, A, Lindmo, T, Moan, J, 1986, Changes in antigen expression on human FME melanoma cells after exposure to photoactivated hematoporphyrin derivatives, Cancer Research, v. 46, p. 6068-72.

De Greef, KE, Ysebaert, DK, Ghielli, M, Vercauteren, S, Nouwen, EJ, Eyskens, EJ, De Broe, ME, 1998, Neutrophils and acute ischemia-reperfusion injur, Journal of Nephrology, v. 11, p. 110-22.

De Vree, WJ, Essers, MC, de Bruijn, HS, Star, WM, Koster, JF, Sluiter, W, 1996, Evidence for an important role of neutrophils in the efficacy of photodynamic therapy in vivo, Cancer Research, v. 56, p. 2908-11.

De Vree, WJ, Fontijne-Dorsman ANRD, Koster, JF, Sluiter, W, 1996a, Photodynamic treatment of human endothelial cells promotes the adherence of neutrophils in vitro, British Journal of Cancer, v. 73, p. 1335-40.

De Vree, WJ, Essers, MC, Koster, JF, Sluiter, W, 1997, Role of Interleukin 1 and Granulocyte Colony-Stimulating Factor in Photofrin-based Photodynamic Therapy of Rat Rhabdomyosarcoma Tumors, Cancer Research, v. 57, p. 2555-8.

Dellian, M, Abels, C, Kuhnle, GE, Goetz, AE, 1995, Effects of photodynamic therapy on leucocyte-endothelium interaction: differences between normal and tumor tissue, British Journal of Cancer, v. 72, p. 1125-30.

Dempsey, PW, Allison, ME, Akkaraju, S, Goodnow, CC, Fearon, DT, 1996, C3d of complement as a molecular adjuvant: bridging innate and acquired immunity, Science, v. 271, p. 348-50.

Devine, D V, 1991, The regulation of complement on cell surfaces, Transfusion Medicine Reviews, v. 5, p. 123-31.

Dougherty TJ, 1974, Activated dyes as antitumor agents. Journal of the National Cancer Institute, v. 51, p. 1333-1336.

Dougherty TJ, Grindey GE, Fiel R, 1975, Photoradiation therapy. II. Cure of animal tumors with hematoporphyrin and light, Journal of the National Cancer Institute, v. 55, p. 115-21.

Dougherty TJ, Kaufman JE, Goldfarb A, 1978, Photoraditiontherapy for the treatment of malignant tumors, Cancer Research, v. 38, p. 2628-35.

Dougherty TJ, 1984, Photoradiation therapy, Urology Supplement, v. 23, p. 61.

Dougherty TJ, 1987, Photosensitizers: Therapy and detection of malignant tumors, Photochemistry and Photobiology, v. 45, p. 879-89.

Dougherty TJ, Gomer, CJ, Henderson, BW, Jori, G, Kessel, D, Korbelik, M, Moan, J, Peng, Q, 1998, Photodynamic therapy, Journal of the National Cancer Institute, v. 90, p. 889-905.

Dougherty, TJ, 2002, An update on photodynamic therapy applications, Journal of Clinical Laser Medicine & Surgery, v. 20, p. 3-7.

Dreyer, WJ, Michael, LH, West, MS, Smith, CW, Rothlein, R, Rossen, RD, Anderson, DC, Entman, ML, 1991, Neutrophil accumulation in ischemic canine myocardium. Insights into time course, distribution, and mechanism of localization during early reperfusion, Circulation, v. 84, p. 400-11.

Drouin, S, Kildsgaard, J, Haviland, J, Zabner, J, Jia, HP, McCray, PB Jr, Tack, BF, Wetsel, RA, 2001, Expression of the complement anaphylatoxin C3a and C5a receptors on bronchial epithelial and smooth muscle cells in models of sepsis and asthma, Journal of Immunology, v. 166, p. 2025-32.

Elward, K, Gasque, P, 2003, "Eat me" and don't eat me" signals govern the innate immune response and tissue repair in the CNS: emphasis on the critical role of the complement system, Molecular Immunology, v. 20, p. 85-94.

Ember, JA, Hugli, TE, 1997, Complement factors and their receptors, Immunopharmacology, v. 38, p. 3-15.

Entman, ML, Michael, L, Rossen, RD, Dreyer, RJ, Anderson, DC, Taylor, AA, Smith, CW, 1991, Inflammation in the course of early myocardial ischemia, FASEB Journal, v. 5, p. 2529-37.

Etievant, M, Leluc, B, David, B, 1988, In vitro inhibition of the classical and alternative pathways of activation of human complement by N acetyl aspartyl glutamic acid (NAAGA), Agents and Actions, v. 24, p. 137-44.

Evans, S, Matthews, W, Perry, R, Fraker, D, Norton, J, Pass, HI, 1990, Effect of photodynamic therapy on tumor necrosis factor production by murine macrophages, Journal of the National Cancer Institute, v. 82, p. 34-9.

Evenson, F, Moan, J, 1982, Photodynamic action and chromosomal damage: A comparison of haematoporphyrin derivative (HpD) and light with X-irradiation, British Journal of Cancer, v. 45, p. 456-65.

Fan, K, Hopper, C, Speigat, P, Buonaccursi, G, Bown, S, 1997, Photodynamic therapy using mTHPC for malignant disease in the oral cavity, International Journal of Cancer, v. 73, p. 25-32.

Fayyazi, A, Scheel, O, Werfel, R, Schqeyer, S, Oppermann, MO, Radzun, HJ, Zwirner, J, 2000, The C5a receptor is expressed in normal renal proximal tubular but not in normal pulmonary or hepatic epithelial cells, Immunology, v. 99, p. 38-45.

Fearon, DT, Carter, RH, 1995, The CD19/CR2/TAPA-1 complex of B lymphocytes: linking natural and acquired immunity, Annual Review of Immunology, v. 13, p. 127-49.

Ferrario, A, Von Tiehl, KF, Rucker, N, Schwarz, MA, Gill, PS, Gomer, CJ, 2000, Antiangiogenic treatment enhances photodynamic therapy responsiveness in a mouse mammary carcinoma, Cancer Research, v. 60, p. 4066-9.

Feuillard, J, Maillet, F, Goldschmidt, P, Weiss, L, Kazatchkine, MD, 1991, Comparative study of in vitro inhibition of activation of the classical and alternative pathways of human complement by the magnesium and sodium salts of the anti-inflammatory peptide N-acetyl-aspartyl-glutamic acid (NAAGA), Agents and Actions, v. 32, p. 343-6.

Fingar, VH, Mang, TS, Henderson, BW, 1988, Modification of photodynamic therapy-induced hypoxia by fluosol-DA (20%) and carbogen breathing in mice, Cancer Research, v. 48, p. 3350-4.

Fingar, VH, Wieman, TJ, Doak, KW, 1990, Role of thromboxane and prostacyclin release on photodynamic therapy-induced tumor destruction, Cancer Research, v. 50, p. 2599-603.

Fingar, VH, Wieman, TJ, Park, YJ, Henderson, BW, 1992, Implications of a pre-existing tumor hypoxic fraction on photodynamic therapy, Journal of Surgical Research, v. 53, p. 524-8.

Fingar, VH, Wieman, TJ, Wiehle, SA, Cerrito, PB, 1992, The role of microvascular damage in photodynamic therapy: the effect of treatment on vessel constriction, permeability, and leukocyte adhesion, Cancer Research, v. 52, p. 4914-21.

Fingar, V, Siegel, KA, Wieman, TJ, Doak, KW, 1993, The effect of thromboxane inhibitors on the microvascular response to photodynamic therapy, Photochemistry and Photobiology, v. 58, p. 393-9.

Fingar, VH, Wieman, TJ, Karavolos, PS, Doak, KW, Ouellet, R, van Lier, JE, 1993a, The effects of photodynamic therapy using differently substituted zinc phthalocyanines on vessel constriction, vessel leakage and tumor response, Photochemistry and Photobiology, v. 58, p. 251-8.

Fingar, VH, 1996, Vascular effects of photodynamic therapy, Journal of Clinical Laser Medicine and Surgery, v. 14, p. 323-8.

Fingar, VH, Haydon, PS, Wieman, TJ, 1996, Visualization of early microvascular damage after photodynamic therapy, Photochemistry and Photobiology, v. 63(S), p. 72(S).

Fingar, VH, Wieman, TJ, Haydon, PS, 1997, The effects of thrombocytopenia on vessel stasis and macromolecular leakage after photodynamic therapy using photofrin, Photochemistry & Photobiology, v. 66, p. 513-7.

Fingar, VH, Kik, PK, Haydon, PS, Cerrito, PB, Tseng, M, Abang, E, Wieman, TJ, 1999, Analysis of acute vascular damage after photodynamic therapy using benzoporphyrin derivative (BPD), British Journal of Cancer, v. 79, p. 1702-8.

Fisher, AMR, Murphee, AL, Gomer CJ, 1995, Clinical and preclinical photodynamic therapy, Lasers in Surgery and Medicine, v. 17, p. 2-31.

Foley, S, Li, B, Dehoff, M, Molina, H, Holers, VM, 1993, Mouse Crry/p65 is a regulator of the alternative pathway of complement activation, European Journal of Immunology, v. 23, p. 1381-4.

Foster, TH, Murant, RS, Bryant, RG, Knox, RS, Gibson, SL, Hilf, R, 1991, Oxygen consumption and diffusion effects in photodynamic therapy, Radiation Research, v. 126, p. 296-303.

Foster, TH, Murant, RS, Bryant, RG, Knox, RS, Gibson, SL, Hilf, R, 1991, Oxygen consumption and diffusion effects in photodynamic therapy, Radiation Research, v. 126, p. 296-303.

Francis, CW, Berkowitz, SD, Comp, PC, Lieberman, JR, Ginsberg, JS, Paiement, G, Peters, GR, Roth, AW, McElhattan, J, Colwell, CW, 2003, Comparison of Ximelagatran with Warfarin for the prevention of venous thromboembolism after total knee replacement, New England Journal of Medicine, v. 349, p. 1703-1712.

Frank, MM, Fries, LF, 1991, The role of complement in inflammation and phagocytosis, Immunology Today, v. 12, p. 322-325.

Frei, Y, Lambris, JD, Stockinger, B, 1987, Generation of a monoclonal antibody to mouse C5: application to an ELISA assay for detection of anti-C5 antibodies, Molecular and Cellular Probes, v. 1, p. 11-9.

Gabeler, EEE, Sluiter, W, van Hillegersberg, R, Edixhoven, A, Schoonderwoerd, K, van Eps, RGS, van Urk, H, 2003, Aminolevulinic Acid-induced Protoporphyrin IX Pharmacokinetics in Central and Peripheral Arteries of the Rat, Photochemistry and Photobiology, v. 78, p. 82-87.

Gasque, P, Chan, P, Fontaine, M, Ischenko, M, Lamacz, M, Gotze, O, Morgan, BP, 1995, Identification and characterization of the complement C5a anaphylatoxin receptor on human astrocytes, Journal of Immunology, v. 155, p. 4882-9.

Gasque, P, Singhrao SK, Neal, JW, Gotze, O, Morgan, BP, 1997, Expression of the receptor for complement C5a (CD88) is upregulated on reactive astrocytes, microglia, and endothelial cells in the inflamed human central nervous system, American Journal of Physiology, v. 150, p. 31-41.

Gelderman, KA, Blok, VT, Fleuren, GJ, Gorter, A, 2002, The inhibitory effect of CD46, CD55, and CD59 on complement activation after immunotherapeutic treatment of cervical carcinoma cells with monoclonal antibodies or bispecific monoclonal antibodies, Laboratory Investigation, v. 82, p. 483-93.

Gibson, SL, VanDerMeid KR, Murant RS, Raubertas, RF, Hilf, R, 1990, Effects of various photoradiation regimens on the antitumor efficacy of photodynamic therapy for R3230AC mammary carcinomas, Cancer Research v. 50, p. 7236-7241.

Gigli, I, Schothorst, AA, Soter, NA, Pathak, MA, 1980, Erythropoietic protoporphyria. Photoactivation of the complement system, Journal of Clinical Investigation, v. 66, p. 517-22.

Gluckman, JL, Waner, M, Shumrick, K, 1986, Photodynamic therapy. A viable alternative to conventional therapy for early lesions of the upper aerodigestive tract? Reflections on a 5-year experience, Laryngoscope, v. 191, p. 36-42.

Goldschmidt, PL, Vulliez-Le Normand, B, Briquet, I, Dray, F, 1990, Effects of *N*-acetyl-aspartyl-glutamic acid and sodium cromoglycate on leukotriene B4 secretion by human leukocytes,, Allergy, v. 45, p. 363-9.

Goldstein, IM, 1992, Complement: biologically active products, In: Inflammation: basic principles and clinical correlates, Gallin, JI, Goldstein, IM, Snyderman, R, eds, New York: Raven Press, p. 63-80.

Goldstein, JL, Brown, MS, 1977, The low-density lipoprotein pathway and its relation to atherosclerosis, Annual Review of Biochemistry, v. 46, p. 897-930.

Gollnick, SO, Liu, X, Owczarczak, B, Musser Da, Henderson, BW, 1997, Altered expression of interleukin 6 and interleukin 10 as a result of photodynamic therapy in vivo, Cancer Research, v. 57, p. 3904-9.

Gollnick, SO, Musser, DA, Oseroff, AR, Vaughan, L, Owczarczak, B, Henderson, BW, 2001, IL-10 does not play a role in cutaneous Photofrin photodynamic therapy-induced suppression of the contact hypersensitivity response, Photochemistry and Photobiology, v. 74, p. 811-6.

Gollnick, SO, Evans, SS, Baumann, H, Owczarczak, B, Maier, P, Vaughan, L, Wang, WC, Unger, E, Henderson, BW, 2003, Role of cytokines in photodynamic therapy-induced local and systemic inflammation, British Journal of Cancer, v. 88, p. 1772-9.

Gollnick, SO, Vaughan, L, Henderson, BW, 2002, Generation of effective antitumor vaccines using photodynamic therapy, Cancer Research, v. 62, p. 1604-8.

Gomer CJ, Luna M, Ferrario, A, Wong, S, Fisher, AM, Rucker, N, 1996, Cellular targets and molecular responses associated with photodynamic therapy, Journal of Clinical Laser Medicine & Surgery, v. 14, p. 315-21.

Gorter, A., and S. Meri, 1999, Immune evasion of tumor cells using membrane-bound complement regulatory proteins: Immunology Today., v. 20, p. 576-82.

Gragoudas, E, Schmidt-Erfurth, U, Sickenkey, M, 1997, Results and preliminary dosimetry of photodynamic therapy for choroidal neovascularization in age-related molecular degeneration in a phase I/II study, Association for Research in Vision Opthamology, v. 38, p. 73, Abstract.

Grosjean, P, Savary, J, Wagnieres, G, 1993, Tetra(m-hydroxyphenyl) chlorin clinical photodynamic therapy of the early bronchial and oseophageal cancer, Laser Medicine Science, v. 8, p. 235-43.

Gyongyossy, M. I., and S. N. Assimeth, 1977, Isolation of the third component of mouse complement: Journal of Immunology, v. 118, p. 1032-5.

Hakulinen, J, Meri, S, 1994, Expression and function of the complement membrane attack complex inhibitor protectin (CD59) on human breast cancer cells, Laboratory investigation, v. 71, p. 820-7.

Hasan, T, Parrish, JA, 1997, Photodynamic therapy of cancer, Cancer Medicine, V. 1, Holland JF, Bast RC Jr, Morton DL, Frei E III, Kufe DW, Weichselbaum RR, editors, Williams & Wilkins, Baltimore, p. 739-51.

Haviland, DL, McCoy, RL, Whitehead, QT, Akama, H, Molmenti, EP, Brown, A, Haviland, JC, Parks, WC, Perlmutter, DH, Wetsel, RA, 1995, Cellular expression of the C5a anaphylatoxin receptor (C5aR): demonstration of C5aR on non-myeloid cells of the liver and lung, Journal of Immunology, v. 154, p. 1861-9.

Hayata,Y, Kato H, Okitsu T, 1985, Photodynamic therapy with hematoporphyrin derivative in cancer of the upper gastrointestinal tract, Seminars in surgical oncology, v. 1, p. 1-11.

Henderson, BW, Waldow, SM, Mang, TS, Potter, WR, Malone, PB, Dougherty, TJ, 1985, Tumor destruction and kinetics of tumor cell death in two experimental mouse tumors following photodynamic therapy, Cancer Research, v. 45, p. 572-6.

Henderson, BW, Fingar, VH, 1987, Relationship of tumor hypoxia and response to photodynamic treatment in an experimental mouse tumor, Cancer Research, v. 47, p. 3110-4.

Henderson, BW, Donovan, JM, 1989, Release of prostaglandin E2 from cells by photodynamic treatment in vitro, Cancer Research, v. 49, p. 6896-6900.

Henderson, BW, Fingar, VH, 1989, Oxygen limitation of direct tumor cell kill during photodynamic treatment of a murine tumor model, Photochemistry & Photobiology, v. 49, p. 299-304.

Henderson, BW, Dougherty, TJ, 1992, How does photodynamic therapy work?, Photochemistry and Photobiology, v. 55, p. 145-57.

Henderson, BW, Sitnik-Busch, TM, Vaughan, LA, 1999, Potentiation of photodynamic therapy antitumor activity in mice by nitric oxide synthase inhibition is fluence rate dependent, Photochemistry & Photobiology, v. 70, p. 64-71.

Henderson, BW, Busch, TM, Vaughan, LA, Frawley, NP, Babich, D, Sosa, TA, Zollo, JD, Dee, AS, Cooper, MT, Bellnier, DA, Greco, WR, Oseroff, AR, 2000, Photofrin photodynamic therapy can significantly deplete or preserve oxygenation in human basal cell carcinomas during treatment, depending on fluence rate, Cancer Research, v. 60, p. 525-9.

Henderson BW, Gollnick, SO, 2002, Mechanistic principles of photodynamic therapy, in: Biochemical Photonics Handbook, Vo-Dinh, T, ed, CRC press, Boca Raton, FL.

Hernandez, LA, Grisham, MB, Twohig, B, Arfors, KE, Harlan, JM, Granger, DN, 1987, Role of neutrophils in ischemia-reperfusion-induced microvascular injury, American Journal of Physiology, v. 253, p. H699-703.

Hicklin, DJ, Wang, Z, Arienti, F, Rivoltini, L, Parmiani, G, Ferrone, S, 1998, beta2-Microglobulin mutations, HLA class I antigen loss, and tumor progression in melanoma, Journal of Clinical Investigation, v. 101, p. 2720-9.

Hilf, R, Smail, DB, Murant, RS, 1994, Hematoporphyrin derivative-induced photosensitivity of mitochondrial succinate dehydrogenase and selected cytosolic enzymes of R3230AC mammary adenocarcinoma of rats, Cancer Research, v. 44, p. 1483-8.

Hilf, R, Murant, RS, Narayanan, U, 1986, Relationship of mitochondrial function and cellular adenosine triphosphate levels to hematoporphyrin derivative-induced photosensitization in R3230AC mammary tumors, Cancer Research, v. 46, p. 211-7.

Hindmarsh, EJ, Marks, RM, 1998, Complement activation occurs on subendothelial extracellular matrix in vitro and is initiated by retraction or removal of overlying endothelial cells, Journal of Immunology, v. 160, p. 6128-36.

Hisazumi, H, Misaki, T, Miyoshi, N, 1983, Photoradiation therapy of bladder tumors, Journal of Urology, v. 130, p. 685-7.

Hockel, M, Schlenger, K, Hockel, S, Vaupel, P, 1999, Hypoxic cervical cancers with low apoptotic index are highly aggressive, Cancer Research, v. 59, p. 4525-8.

Hockel, M, Vaupel, P, 2001, Tumor hypoxia: definitions and current clinical, biologic, and molecular aspects, Journal of the National Cancer Institute, v. 93, p. 266-76.

Hofman, P, His, BL, Manie, S, Fenichel, P, Thyss, A, Rossi, B, 1994, High expression of the antigen recognized by the monoclonal antibody GB24 on human breast carcinomas: a preventive mechanism of malignant tumor cells against complement attack?, Breast Cancer Research and Treatment, v. 32, p. 213-9.

Hogasen, AK, Abrahamsen, TG, 1995, Polymyxin B stimulates production of complement components and cytokines in human monocytes, Antimicrobial Agents & Chemotherapy, v. 39, p. 529-32.

Hugli, TE, 1981, The structural basis for anaphylatoxin and chemotactic functions of C3a, C4a, and C5a, Critical Reviews in Immunology, v. 2., p. 321-66.

Iinuma, S, Schomacker, KT, Wagnieres, G, Rajadhyaksha, M, Bamberg, M, Momma, T, Hasan, T, 1999, In vivo fluence rate and fractionation effects on tumor response and photobleaching: photodynamic therapy with two photosensitizers in an orthotopic rat tumor model, Cancer Research, v. 59, p. 6164-70.

Janeway CA, Travers, P, 1996, Immunobiology, Current Biology Ltd./Garland Publishing Inc, London.

Jang, A, Hill, RP, 1997, An examination of the effects of hypoxia, acidosis, and glucose starvation on the expression of metastasis-associated genes in murine tumor cells, Clinical & Experimental Metastasis, v. 15, p. 469-83.

Jarvis, GA, Li, J, Hakulinen, J, Brady, KA, Nordling, S, Dahiya, R, Meri, S, 1997, Expression and function of the complement membrane attack complex inhibitor protectin (CD59) in human prostate cancer, International Journal of Cancer, v. 71, p. 1048-55.

Jesionek A, von Tappenier H, 1903, Zur behandlung der Hautkarcinome mit fluorescierenden stoffen, Munchen Med Wochenscher, v. 47, p. 2042-51.

Jirsa, M, Jr, Pouckova, P, Dolezal, J, Pospisil, J, Jirsa, M, 1991, Hyperbaric oxygen and photodynamic therapy in tumour-bearing nude mice, European Journal of Cancer, v. 27, p. 109.

Jordan, JE, Zhao, ZQ, Vinten-Johansen, J, 1999, The role of neutrophils in myocardial ischemia-reperfusion injury, Cardiovascular Research, v. 43, p. 860-78.

Jori, G, 1989, In vivo transport and pharmacokinetic behaviour of tumor photosensitizers, In: Photosensitizing compounds: Their chemistry, biology, and clinical use, Ciba Found Symposium, v. 146, p. 78-94.

Joshi, PG, Joshi, KJ, Mishra, S, Joshi, NK, 1994, Ca^{2+} influx induced by photodynamic action in human cerebral glioma (U-87MG) cells: Possible involvement of a calcium channel, Photochemistry and Photobiology, v. 60, p. 244-8.

Kalli, KR, Hsu, P, Fearon, DT, 1994, Therapeutic uses of recombinant complement protein inhibitors, Springer Seminars in Immunopathology, v. 15, p. 417-31.

Kamide, R, Gigli, I, Lim, HW, 1984, Participation of mast cells and complement in the immediate phase of hematoporphyrin-induced phototoxicity, Journal of Investigative Dermatology, v. 82, p. 485-90.

Kerdel, FA, Soter, NA, Lim, HW, 1987, In vivo mediator release and degranulation of mast cells in hematoporphyrin derivative-induced phototoxicity in mice, Journal of Investigative Dermatology, v. 88, p. 277-80.

Kerekes, K, Prechl, J, Bajtay, Z, Jozsi, M, Erdei, A, 1998, A further link between innate and adaptive immunity: C3 deposition on antigen-presenting cells enhances the proliferation of antigen-specific T cells, International Immunology, v. 10, p. 1923-30.

Kessel, D, 1986, Sites of photosensitization by derivatives of hematoporphyrin, Photochemistry and Photobiology, v. 44, p. 489-93.

Kessel, D, 1986b, Porphyrin-lipoprotein association as a factor in porphyrin localization, Cancer Letters, v. 33, p. 183-8.

Kessel, D, Castelli, M, 2001, Evidence that bcl-2 is the target of three photosensitizers that induce a rapid apoptotic response, Photochemistry and Photobiology, v. 74, p. 318-22.

Kessel, D, Luo, Y, 1996, Delayed oxidative photodamage induced by photodynamic therapy, Photochemistry and Photobiology, v. 64, p. 601-4.

Kick, G, Messer, G, Goetz, A, Plewig, G, Kind, P, 1995, Photodynamic therapy induces expression of interleukin 6 by activation of AP-1 but not NF-kappa B DNA binding, Cancer Research, v. 55, p. 2373-9.

Kilgore, KS, Ward, PA, Warren, JS, 1998, Neutrophil adhesion to human endothelial cells is induced by the membrane attack complex: the roles of P-selectin and platelet activating factor, Inflammation, v. 22, p. 583-98.

Kilgore, KS, Shwartz, CF, Gallagher, MA, Steffen, RP, Mosca, RS, Bolling, SF, 1999, RSR13, a synthetic allosteric modifier of hemoglobin, improves myocardial recovery following hypothermic cardiopulmonary bypass, Circulation, v. 100, p. II351-6.

Kilgore, KS, Todd, T III, Lucchesi, BR, 2000, Reperfusion Injury, In: Inflammation: Basic principles and Clinical Correlates, 3rd Ed., Gallin, JI, Snyderman, R, eds, Lippincott Williams & Wilkins, Philadelphia, USA.

Kocsis, J, Veres, A, Vatay, A, Duba, J, Karadi, I, Fust, G, Prohaszka, Z, 2002, Antibodies against human heat shock protein hsp70 in patients with severe coronary artery disease, Immunological Investigations, v. 31, p. 219-31.

Korbelik, M, Krosl, G, Chaplin, DJ, 1991a, Photofrin uptake by murine macrophages, Cancer Research, v. 51, p. 2251-5.

Korbelik, M, Krosl, G, Olive, PL, Chaplin, DJ, 1991b, Distribution of photofrin between tumor cells and tumor associated macrophages, British Journal of Cancer, v. 64, p. 508-12.

Korbelik, M, Krosl, G, 1994a, Enhanced macrophage cytotoxicity against tumor cells treated with photodynamic therapy, Photochemistry & Photobiology, v. 60, p. 497-502.

Korbelik, M, Krosl, G, 1994b, Cellular levels of photosensitizers in tumors: the role of proximity to blood supply, British Journal of Cancer, v. 70, p. 604-10.

Korbelik, M, 1996, Induction of tumor immunity by photodynamic therapy, Journal of Clinical Laser Medicine & Surgery, v. 14, p. 329-34.

Korbelik, M, Krosl G, 1996, Photofrin accumulation in malignant and host cells populations of various tumors, British Journal of Cancer, v. 73, p. 506-513.

Korbelik, M, Cecic, I, Shibuya H, 1997, The role of nitric oxide in the response of cancerous lesions to photodynamic therapy, Recent research developments in photochemistry and photobiology, v. 1, p. 267-76.

Korbelik, M, Cecic, I, 1998, Enhancement of tumor response to photodynamic therapy by adjuvant mycobacterium cell-wall treatment, Journal of Photochemistry and Photobiology, B: Biology, v. 44, p. 151-8.

Korbelik, M, Cecic, I, 1999, Contribution of myeloid and lymphoid host cells to the curative outcome of mouse sarcoma treatment by photodynamic therapy, Cancer Letters, v. 137, p. 91-8.

Korbelik, M, Parkins, CS, Shibuya, H, Cecic, I, Stratford, MR, Chaplin, DJ, 2000, Nitric oxide production by tumour tissue: impact on the response to photodynamic therapy, British Journal of Cancer, v. 82, p. 1835-43.

Korbelik, M, Cecic, I, Sun, J, 2001, Relevance of PDT-induced inflammatory response for the outcome of photodynamic therapy, SPIE proceedings, v. 4257, p. 19-24.

Korbelik, M, 2002, Generation of anti-cancer vaccine by photodynamic therapy, American Association of Cancer Research Proceedings, v. 43, p. 979.

Korbelik, M, Cecic, I, 2003, Mechanism of tumor destruction by photodynamic therapy, in: Handbook of Photochemistry and Photobiology, Vol. 4 Photobiology, Abdel-Mottaleb, MSA, Nalwa, HS, eds, American Scientific Publishers, Stevenson Ranch, CA, p. 39-71.

Korbelik, M, Sun, J, Zeng, H, 2003, Ischaemia-reperfusion injury in photodynamic therapy-treated mouse tumours, British Journal of Cancer, v. 88, p. 760-6.

Korbelik, M, Sun, J, 2003, Progress in the development of photodynamic therapy-generated cancer vaccines, Proceedings of SPIE, v. 4961, p. 10-17.

Korbelik M, Sun, J, Payne, PW, 2003b, Activation of Poly(adenosine diphosphate-ribose) Polymerase in Mouse Tumors treated by Photodynamic Therapy, Photochemistry and Photobiology, v. 78, p. 400-406.

Koretz, K, Bruderlein, S, Henne, C, Moller, P, 1992, Decay-accelerating factor (DAF, CD55) in normal colorectal mucosa, adenomas and carcinomas, British Journal of Cancer, v. 66, p. 810-4.

Koretz, K, Bruderlein, S, Henne, C, Moller, P, 1993, Expression of Cd59, a complement regulator protein and a second ligand of the CD2 molecule, and CD46 in normal and neoplastic colorectal epithelium, British Journal of Cancer, v. 68, p. 926-31.

Koukourakis, MI, Giatromanolaki, A, Skarlatos, J, Corti, L, Blandamura, S, Piazza, M, Gatter, KC, Harris, AL, 2001, Hypoxia inducible factor (HIF-1a and HIF-2a) expression in early esophageal cancer and response to photodynamic therapy and radiotherapy, Cancer Research, v. 61, p. 1830-2.

Krosl, G, Korbelik, M, 1994, Potentiation of photodynamic therapy by immunotherapy: the effect of schizophyllan (SPG), Cancer Letters, v. 84, p. 43-9.

Krosl, G, Korbelik, M, Dougherty, GJ, 1995, Induction of immune cell infiltration into murine SCCVII tumour by photofrin-based photodynamic therapy, British Journal of Cancer, v. 71, p. 549-55.

Lam, S, Palcic, B, McLean, D, 1990, Detection of early lung cancer using low dose Photofrin II, Chest, 97, 333-7.

Lam, S, Crofton, C, Cory, P, 1991 Combined photodynamic therapy (PDT) using photofrin and radiotherapy (XRT) versus radiotherapy alone in patients with inoperable distribution non-small cell bronchogenic cancer, SPIE proceedings, p. 20-28.

Lam, S, Kennedy T, Unger, M, 1998, Localization of bronchial intraepithelial neoplastic lesions by fluorescence bronchoscopy, Chest, v. 113, p. 696-702.

Laufer, J, Boichis, H, Farzam, N, Passwell, JH, 1995, IgA and IgG immune complexes increase human macrophage C3 biosynthesis, Immunology, v. 84, p. 207-12.

Lehrer RI, Ganz, T, Selsted, ME, Babior, BM, Curnette, JT, 1988, Neutrophils and host defense, Annals of Internal Medicine, v. 109, p. 127-42.

Leung, J, 1994, Photosensitizers in photodynamic therapy, Seminars in Oncology, v. 21, p. 4-10.

Li, L, Spendlove, I, Morgan, J, Durrant, LG, 2001, CD55 is over-expressed in the tumour environment, British Journal of Cancer, v. 84, p. 80-6.

Li, Q, Furman, SA, Bradford, CR, Chang, AE, 1999, Expanded tumor-reactive CD4+ T-cell responses to human cancers induced by secondary anti-CD3/anti-CD28 activation, Clinical Cancer Research, v. 5, p. 461-9.

Liaudet, L, Soriano, FG, Szabo, E, Virag, L, Mabley, JG, Salzman, AL, Szabo, C, 2000, Protection against hemorrhagic shock in mice genetically deficient in poly(ADP-ribose)polymerase, Proceedings of the National Academy of Sciences of the United States of America, v. 97, p. 10203-8.

Lim, HW, Perez, HD, Poh-Fitzpatrick, M, Goldstein, IM, Gigli, I, 1981, Generation of chemotactic activity in serum from patients with erythropoietic protoporphyria and porphyria cutanea tarda, New England Journal of Medicine, v. 304, p. 212-6.

Lipson RL, Blades EJ, 1960, The photodynamic properties of a particular hematoporphyrin derivative, Archives of Dermatology, v. 82, p. 508-16.

Liszewski, M. K., T. C. Farries, D. M. Lublin, I. A. Rooney, and J. P. Atkinson, 1996, Control of the complement system: Advances in Immunology., v. 61, p. 201-83.

Liszewski, MK, Farries, TC, Lublin, DM, Rooney, IA, Atkinson, JP, 1996, Control of the complement system, Advances in Immunology, v. 61, p. 201-83.

Lucchesi, BR, 1993, Complement activation, neutrophils, and oxygen radicals in reperfusion injury, Stroke, v. 24, p. I41-7; discussion I38-40.

Lucchesi, BR, Kilgore, KS, 1997, Complement inhibitors in myocardial ischemia/reperfusion injury, Immunopharmacology, v. 38, p. 27-42.

Luna, MC, Ferrario, A, Rucker, N, Gomer, CJ, 1995, Decreased expression and function of α-2 macroglobulin receptor/low density lipoprotein receptor-related protein in photodynamic therapy-resistant mouse tumor cells, Cancer Research, v. 55, p. 1820-3.

Ma, LW, Moan, J, Peng, Q, 1992, International Journal of Cancer, v, 52, p. 120.

Maenpaa, A, Junnikkala, S, Hakulinen, J, Timonen, T, Meri, S, 1996, Expression of complement membrane regulators membrane cofactor protein (CD46), decay accelerating factor (CD55), and protectin (CD59) in human malignant gliomas, American Journal of Pathology, v. 148, p. 1139-52.

Malech, HL, Gallin, JI, 1988, Current concepts: immunology. Neutrophils in human disease, New England Journal of Medicine, v. 317, p. 687-94.

Marincola, FM, Wang, E, Herlyn, M, Seliger, B, Ferrone, S, 2003, Tumors as elusive targets of T-cell-based active immunotherapy, Trends in Immunology, v. 24, p. 335-42.

Maziere, JC, Morliere, P, Santus, R, 1991, The role of the low density lipoprotein receptor pathway in the delivery of lipophilic photosensitizers in the photodynamic therapy of tumors, Journal of Photochemistry and Photobiology. B-Biology, v. 8, p. 351-60.

McBride, G, 2002, Studies expand potential uses of photodynamic therapy, Journal of the National Cancer Institute, v. 94, p. 1740-2.

Medzhitov, R, Janeway, CA Jr., 1999, Innate immune induction of the adaptive immune response, Cold Spring Harbor Symposia on Quantitative Biology, v. 64, p. 429-35.

Medzhitov, R, Janeway, C Jr, 2000, Innate Immunity, New England Journal of Medicine, v. 343, p. 338-44.

Menon, C, Kutney, SN, Lehr, SC, Hendren, SK, Busch, TM, Hahn, SM, Fraker, DL, 2001, Vascularity and uptake of photosensitizer in small human tumor nodules, implications for intraperitoneal photodynamic therapy: Clinical Cancer Research, v. 7, p. 3904-11.

Meyer-Betzz F, 1913, Untersuchungen uber die biologische (photodynamische) Wirkung des Hamatoporphyrins und anderer Derivative des Blut- und Gallenfarbstoffs, Dtsch Arch Klin Med Wochenschr, v. 112, p. 476-503.

Miadonna, A, Cottine, M, Candiani, C, Tedeschi, A, 1994, Modulation of allergen-induced nasal symptoms and mediator release by treatment with *N*-acetyl-aspartyl-glutamate (ZY15106), European Journal of Clinical Pharmacology, v. 46, p. 127-31.

Miadonna, A, Milazzo, N, Salmaso, C, Cottini, M, Lorini, M, Tedeschi, A, 1998, *N*-acetyl-aspartyl-glutamic acid inhibits cellular recruitment and mediator release during the late allergen-induced nasal reaction, European Journal of Clinical Pharmacology, v. 54, p. 515-20.

Milas, L, Wike, J, Hinter, N, Volpe, J, Basic, I, 1987, Macrophage content of murine sarcomas and carcinomas: association with tumor growth parameters and tumor radiocurability, Cancer Research, v. 47, p. 1069-75.

Minchinton, AI, Fryer, KH, Lim, P, Aquino-Parsons, C, 1999, Effect of breathing carbogen on the oxygen tension of murine and human tumors measured using an Eppendorf pO2 histograph, Advances in Experimental Medicine & Biology, v. 471, p. 507-13.

Moan, J, Pettersen, EO, Christensen, T, 1979, The mechanism of photodynamic inactivation of human cells *in vitro* in the presence of hematoporphyrin, British Journal of Cancer, v. 39, p. 398-407.

Moan, J, Christensen, T, 1981, Cellular uptake and photodynamic effect of hematoporphyrin, Photochemistry and Photobiophysics, v. 2, p. 291-9.

Moan, J, McGhie, J, Jacobsen, PB, 1983, Photodynamic effects on cells in vitro exposed to hematoporphyrin derivative and light, Photochemistry and Photobiology, v. 37, p. 599-604.

Mollnes, TE, Song, WC, Lambris, JD, 2002a, Complement in inflammatory tissue damage and disease, Trends in Immunology, v. 23, p. 61-4.

Mollnes, TEW, Brekke, O, Fung, M, Fure, H, Christiansen, D, Bergseth, G, Videm, V, Lappegard, KT, Kohl, J, Lambris, JD, 2002b, Essential role of the C5a receptor in *E coli*-induced oxidative burst and phagocytosis revealed by a novel lepirudin-based human whole blood model of inflammation, Blood, v. 100, p. 1869-77.

Monsinjon, T, Richard, V, Fontaine, M, 2001, Complement and its implications in cardiac ischemia/reperfusion: strategies to inhibit complement, Fundamental & Clinical Pharmacology, v. 15, p. 293-306.

Monsijohn, T, Gasque, P, Chan, P, Ischenko, A, Brady JJ, Fontaine, M, 2003, Regulation by complement C3a and C5a anaphylatoxins of cytokine production in human umbilical vein endothelial cells, FASEB Journal, v. 17, p. 1003-14.

Montalescot, G, Drobinski, G, Maclouf, J, Maillet, F, Salloum, J, Ankri, A, Kazatchkine, M, Eugene, L, Thomas, D, Grosgogeat, Y, 1991, Evaluation of thromboxane production and complement activation during myocardial ischemia in patients with angina pectoris, Circulation, v. 84, p. 2054-62.

Morgan, BP, Gasque, P, 1997, Extrahepatic complement biosynthesis: where, when and why?, Clinical Experimental Immunology, v. 107, p. 1-7.

Muller, P, Wilson, B, 1995, Photodynamic therapy for recurrent supratentorial gliomas, Seminars in Surgical Oncology, v. 11, p. 346-54.

Muller, P, Wilson B, 1996, Photodynamic therapy for malignant newly diagnosed supratentorial gliomas, Journal of Clinical Laser Medicine & Surgery, v. 14, p. 263-70.

Musser, DA, Camacho, SH, Manderscheid, PA, Oseroff, AR, 1999, The anatomic site of photodynamic therapy is a determinant for immunosuppression in a murine model, Photochemistry & Photobiology, v. 69, p. 222-5.

Nelson JS, Liaw, LH, Berns, MW, 1987, Tumor destruction in photodynamic therapy, Photochemistry and Photobiology, v. 46, p. 829-35.

Nseyo, UO, Dehaven, J, Dougherty, TJ, Potter, WR, Merrill, DL, Lundahl, SL. Lamm, DL, 1998, Photodynamic therapy (PDT) in the treatment of patients with resistant superficial bladder cancer: a long-term experience, Journal of Clinical Laser Medicine & Surgery, v. 16, p. 61-8.

O'Donnell, VB, Spycher, S, Azzi, A, 1995, Involvement of oxidants and oxidant-generating enzyme(s) in tumour-necrosis-factor-alpha-mediated apoptosis: role for lipoxygenase pathway but not mitochondrial respiratory chain, Biochemical Journal, v. 310, p. 133-41.

Ochsner, M, 1997, Photophysical and photobiological processes in the photodynamic therapy of tumors, Journal of Photochemistry and Photobiology B: Biology, v. 39, p. 1-18.

Ogden, CA, deCathelineau, A, Hoffman, PR, Bratton, D, Ghebrehiwet, B, Fadok, VA, Henson, PM, 2001, C1q and mannose binding lectin engagement of cell surface calreticulin and CD91 initiates macropinocytosis and uptake of apoptotic cells, Journal of Experimental medicine, v. 194, p. 781-95.

Okamura, T, Akita, H, Tozawa, K, Kawai, N, Nagata, D, Kohri, K, 2003, Bacillus Calmette-Guerin-refractory superficial bladder cancers: focus on pretreatment episodes, International Journal of Clinical Oncology, v. 8, p. 168-73.

Oleinick, N, 1998, Apoptosis in response to photodynamic therapy, Photodynamic News, v.1, #2.

Parkins, CS, Dennis, MF, Stratford, MR, Hill, SA, Chaplin, DJ, 1995, Ischemia reperfusion injury in tumors: the role of oxygen radicals and nitric oxide, Cancer Research, v. 55, p. 6026-9.

Pass, HI, Pogrebniak HW, 1992, Photodynamic therapy for thoracic malignancies, Seminars in Surgical Oncology, v. 8, p. 217-25.

Pass, HI, 1993, Photodynamic therapy in oncology: Mechanisms and clinical use, Journal of the National Cancer Institute, v. 85, p. 443-56.

Pass H, Delaney T, Tochner Z, 1994, Intrapleural photodynamic therapy: Results of a Phase I trial, Annals of Surgical Oncology, v. 1, p. 28-37.

Parkins, CS, Hill, SA, Stratford, MR, Dennis, MF, Chaplin, DJ, 1997, Metabolic and clonogenic consequences of ischaemia reperfusion insult in solid tumours, Experimental Physiology, v. 82, p. 361-8.

Pathak MA, Kramer DM, Fitzpatrick TB, 1974, Photobiology and photochemistry of furocoumarins (psoralens) In: Fitzpatrick TB, Pathak MA, Harber LC, Seiji M, Kukita A, editors. Sunlight and man. Tokyo: University of Tokyo Press, p. 335-68.

Peyman, GA, Kazi, AA, Unal, M, Khoobehi, B, Yoneya, S, Mori, K, Moshfeghi, DM, 2000, Problems with and pitfalls of photodynamic therapy, Ophthalmology, v. 107, p. 29-35.

Popovic, E, Kaye, A, Hill, A, 1996, Photodynamic therapy for brain tumors, Journal of Clinical Lasers in Medicine & Surgery, v. 14, p. 251-61.

Projaszka, A, Singh, M, Nagy, K, Kiss, E, Lakos, G, Duba, J, Fust, G, 2002, Heat shock protein 70 is a potent activator of the human complement system, Cell Stress & Chaperones, v. 7, p. 17-22.

Quigg, RJ, He, C, Lim, A, Berthiaume, D, Alexander, JJ, Kraus, D, Holers, VM, 1998, Transgenic mice overexpressing the complement inhibitor crry as a soluble protein are protected from antibody-induced glomerular injury, Journal of Experimental Medicine, v. 188, p. 1321-31.

Quigg, RJ, Kozono, Y, Berthiaume, D, Lim, A, Salant, DJ, Weinfeld, A, Griffin, P, Kremmer, E, Holers, VM, 1998, Blockade of antibody-induced glomerulonephritis with Crry-Ig, a soluble murine complement inhibitor, Journal of Immunology, v. 160, p. 4553-60.

Raab C, 1900, Uber die Wirkung Fluoreszierenden Stoffe auf Infusoria. Z Biol, v. 39, p. 524-6.

Razum, N, Snyder, A, Doiron, D, 1996, SnET2: Clinical update, SPIE proceedings, v. 2675, p. 43-6.

Rettenmaier, MA, Berman, ML, Disaia, PJ, 1984, Gynecologic uses of photoradiation therapy, In: Porphyrin Localization and Treatment of Tumors, Doiron, DT, Gomer, CJ, editors, Alan R Liss, New York.

Robinson, DJ, de Bruijn, HS, Star, WM, Sterenborg, HJ, 2003, Dose and timing of the first light fraction in two-fold illumination schemes for topical ALA-mediated photodynamic therapy of hairless mouse skin, Photochemistry & Photobiology, v. 77, p. 319-23.

Rockwell, S, Kallman, RF, Fajardo, LF, 1972, Characteristics of a serially transplanted mouse mammary tumor and its tissue-culture-adapted derivative, Journal of the National Cancer Institute, v. 49, p. 735-49.

Roitt, I, Brostoff, J, Male, D, 2001, Immunology, Sixth Ed., Harcourt Publishers Limited, Toronto.

Ryter, SW, Gomer, CJ, 1993, Nuclear factor kappa B binding activity in mouse L1210 cells following photofrin II-mediated photosensitization, Photochemistry and Photobiology, v. 58, p. 753-6.

Saleh, M, Monoclonal antibody therapy of non-Hodgkin's lymphoma: the Rituximab story, Journal of the Medical Association of Georgia, v. 92, p. 39-46.

Santoro, O, Bandieramonte, G, Melloni, E, 1990, Photodynamic therapy by topical mesotetraphenylporphinesulfate tetrasodium salt administration in superficial basal cell carcinomas, Cancer Research, v. 50, p. 4501-3.

Schouwink, H, Ruevekamp, M, Oppelaar, H, van Veen, R, Baas, P, Stewart, FA, 2001, Photodynamic therapy for malignant mesothelioma: preclinical studies for optimization of treatment protocols, Photochemistry & Photobiology, v. 73, p. 410-7.

Schouwink, H, Ruevekamp, M, Oppelaar, H, van Veen, R, Baas, P, Stewart, FA, 2001, Photodynamic therapy for malignant mesothelioma: preclinical studies for optimization of treatment protocols, Photochemistry & Photobiology, v. 73, p. 410-7.

Seliger, B, Maeurer, MJ, Ferrone, S, 1997, TAP off--tumors on, Immunology Today, v. 18, p. 292-9.

Shapiro, S, 2003, Treating thrombosis in the 21st century, New England Journal of Medicine, v. 349, p. 1762-1764.

Shikowitz MJ, Steinberg, BM, Abramson, AL, 1986, Hematoporphyrin derivative therapy of papillomas: Experimental study, Archives of Otolaryngology Head & Neck Surgery, v. 118, p. 25-9.

Simpson, KL, Jones, A, Norman, S, Holmes, CH, 1997, Expression of the complement regulatory proteins decay accelerating factor (DAF, CD55), membrane cofactor protein (MCP, CD46) and CD59 in the normal human uterine cervix and in premalignant and malignant cervical disease, American Journal of Pathology, v. 151, p. 1455-67.

Sindelar, WF, DeLaney, TF, Tochner, Z, 1991, Technique of photodynamic therapy for disseminated intraperitoneal malignancies Phase I study, Archives of Surgery, v. 126, p. 318-24.

Sitnik, TM, Hampton, JA, Henderson, BW, 1998, Reduction of tumour oxygenation during and after photodynamic therapy in vivo: effects of fluence rate, British Journal of Cancer, v. 77, p. 1386-94.

Sitnik, TM, Henderson, BW, 1998, The effect of fluence rate on tumor and normal tissue responses to photodynamic therapy, Photochemistry & Photobiology, v. 67, p. 462-6.

Soncin, M, Polo, L, Reddi, E, Jori, G, Kenney, ME, Cheng, G, Rodgers, MAJ, 1995, Effect of axial ligation and delivery system on the tumor-localizing and photosensitizing properties of Ge(IV)-octabutoxy-phthalocyanines, British Journal of Cancer, v. 71, p. 727-32.

Song, WC, Sarrias, MR, Lambris, JD, 2000, Complement and innate immunity, Immunopharmacology, v. 49, p. 187-98.

Spiess, PJ, Uang J, Rosenberg, SA, 1987, *In vivo* antitumor activity of tumor-infiltrating lymphocytes expanded in recombinant IL-2, Journal of the National Cancer Institute, v. 79, p. 1067-75.

Sugiura, K, Stock, CC, 1955, The effect of phosphoramides on the growth of a variety of mouse and rat tumors, Cancer Research, v. 15, p. 38-51.

Suit, HD, Sedlacek, RS, Silver, G, Dosoretz, D, 1985, Pentobarbital anesthesia and response of tumor and normal tissue in the C3Hf/Sed mouse to radiation, Radiation Research, v. 104, p. 47-65.

Sun, J, Cecic, I, Parkins, CS, Korbelik, M, 2002, Neutrophils as inflammatory and immune effectors in photodynamic therapy-treated mouse SCCVII tumours, Photochemical & Photobiological Sciences, v. 1, p. 690-5.

Sundfor, K, Lyng, H, Rofstad, EK, 1998, Tumour hypoxia and vascular density as predictors of metastasis in squamous cell carcinoma of the uterine cervix, British Journal of Cancer, v. 78, p. 822-7.

Specht, KG, Rodgers, MAJ, 1990, Depolarization of mouse myeloma cell membrane during photodynamic action, Photochemistry and Photobiology, v. 51, p. 319-24.

Struyf, S, Proost, P, Lenaerts, JP, Stoops, G, Wuyts, A, van Damme, J, 2001, Identification of a blood-derived chemoattractant for neutrophils and lymphocytes as a novel CC chemokine, Regakine-1, Blood, V. 97, p. 2197-2204.

Szabo, G, Bahrle, S, Stumpf, N, Sonnenberg, K, Szabo, EE, Pacher, P, Csont, T, Schulz, R, Dengler, TJ, Liaudet, L, Jagtap, PG, Southan, GJ, Vahl, CF, Hagl, S, Szabo, C, 2002, Poly(ADP-Ribose) polymerase inhibition reduces reperfusion injury after heart transplantation, Circulation Research., v. 90, p. 100-6.

Taber, SW, Wieman, TJ, Fingar, VH, 1993, The effects of aspirin on microvasculature after photodynamic therapy, Photochemistry & Photobiology, v. 57, p. 856-61.

Taktak, YS, Stenning, B, 1992, Solid phase enzyme immunoassays for the quantification of serum amyloid P (SAP) and complement component 3 (C3) proteins in acute-phase mouse sera, Hormone & Metabolic Research, v. 24, p. 371-4.

Teicher, BA, Holden, SA, al-Achi, A, Herman, TS, 1990, Classification of antineoplastic treatments by their differential toxicity toward putative oxygenated and hypoxic tumor subpopulations in vivo in the FSaIIC murine fibrosarcoma, Cancer Research, v. 50, p. 3339-44.

Thomas, JP, Girotti, AW, 1989, Role of lipid peroxidation in hematoporphyrin derivative-sensitized photokilling of tumor cells: protective effects of glutathione peroxidase, Cancer Research, v. 49, p. 1682-6.

Tofukuji, M., G. L. Stahl, A. Agah, C. Metais, M. Simons, and F. W. Sellke, 1998, Anti-C5a monoclonal antibody reduces cardiopulmonary bypass and cardioplegia-induced coronary endothelial dysfunction: Journal of Thoracic & Cardiovascular Surgery, v. 116, p. 1060-8.

Tralau, CJ, Barr, H, MacRobery, J, Bown SG, 1990, Photodynamic therapy of neoplastic disease, Kessel, D, ed, CRC Press, Boca Raton, Florida, p. 263.

Tsuji, RF, Kawikova, I, Ramabhadran, R, Akahira-Azuma, M, Taub, D, Hugli, TE, Gerard, C, Askenase, PW, 2000, Early local generation of C5a initiates the elicitation of contact sensitivity by leading to early T cell recruitment, Journal of Immunology, v. 165, p. 1588-98.

Vakeva, A, Meri, S, 1998, Complement activation and regulator expression after anoxic injury of human endothelial cells, Apmis, v. 106, p. 1149-56.

Van Geel, IP, Oppelaar, H, Marijnissen, JP, Stewart, FA, 1996, Influence of fractionation and fluence rate in photodynamic therapy with Photofrin or mTHPC, Radiation Research, v. 145, p. 602-9.

Van Geel, IP, Oppelaar, H, Rijken, PF, Bernsen, HJ, Hagemeier, NE, van der Kogel, AJ, Hodgkiss, RJ, Stewart, FA, 1996, Vascular perfusion and hypoxic areas in RIF-1 tumours after photodynamic therapy, British Journal of Cancer, v. 73, p. 288-93.

Vandivier, RW, Ogden, CA, Fadok, VA, Hoffman, PR, Brown, KK, Botto, M, Walport, MJ, Fisher, JH, Henson PM, Greene, KE, 2002, Role of surfactant proteins A, D, and C1q in the clearance of apopototic cells in vivo and in vitro: calreticulin and CD91 as a common collectin receptor complex, Journal of Immunology, v. 169, p. 3978-86.

Vaporciyan, AA, Ward, PA, 1993, Enhanced generation of O2- by human neutrophils via a complement iC3b/Mac-1 interaction, Biological Signals, v. 2, p. 126-35.

Vilella, R, Benitez, D, Mila, J, Vilalta, A, Rull, R, Cuellar, F, Conill, C, Vidal-Sicart, S, Costa, J, Yachi, E, Palou, J, Malvehy, J, Puig, S, Marti, R, Mellado, B, Castel, T, 2003, Treatment of patients with progressive unresectable metastatic melanoma with a heterologous polyvalent melanoma whole cell vaccine, International Journal of Cancer, v. 106, p. 626-31.

Volden, G, Christensen, T, Moan, J, 1981, Photodynamic membrane damage of hematoporphyrin derivative-treated NHIK 3025 cell in vitro, Photochemistry and Photobiophysics, v. 3, p. 105-11.

Volpe, JP, Hunter, N, Basic, I, Milas, L, 1985, Metastatic properties of murine sarcomas and carcinomas. I. Positive correlation with lung colonization and lack of correlation with s.c. tumor take, Clinical & Experimental Metastasis, v. 3, p. 281-94.

Waldow, SM, Lobraico, RV, Kohler, IK, 1987, Photodynamic therapy for treatment of malignant cutaneous lesions, Lasers in Surgery & Medicine, v. 7, p. 451-6.

Walport, MJ, 2001, Complement, In: Advances in Immunology, The New England Journal of Medicine, v. 344.

Warren, JS, Ward, PA, Johnson, KJ, 1990, Hematology, McGraw-Hill, New York.

Weiser, MR, Williams, JP, Moore, FD Jr., Kobzik, L, Ma, M, Hechtman, HB, Carroll, MC, 1996, Reperfusion injury of ischemic skeletal muscle is mediated by natural antibody and complement, Journal of Experimental Medicine, v. 183, p. 2343-8.

Weiss, SJ, 1989, Tissue destruction by neutrophils, New England Journal of Medicine, v. 320, p. 365-76.

White, CA, Weaver, RL, Grillo-Lopez, AJ, 2001, Antibody-targeted immunotherapy for treatment of malignancy, Annual Review of Medicine, v. 52, p. 125-45.

Wieman, TJ, Mang, TS, Fingar, VH, Hill, TG, Reed, MW, Corey, TS, Nguyen, VQ, Render, ER Jr., 1988, Effect of photodynamic therapy on blood flow in normal and tumor vessels, Surgery, v. 104, p. 512-7.

Wieman, TJ, Doak, KD, Fingar, VH, 1991, Effects of PDT on cytoskeletal F-actin structures, Photochemistry and Photobiology, v. 53(S), p. 96S-97S.

Woodburn, KW, Fan, Q, Kessel, D, Luo, Y, Young, SW, 1998, Photodynamic therapy of B16F10 murine melanoma with lutetium texaphyrin, Journal of Investigative Dermatology, v. 110, p. 746-51.

Xia Y, Ross, GD, 2000, Roles of Integrins CR3 and CR4 in Disease and Therapeutic Strategies, In: Therapeutic Interventions of the Complement System, Lambris, JD, Holers, VM, eds, Humana Press Inc, Totowa, NJ.

Xu, C, Mao, D, Holers, MV, Palanca, B, Cheng, A, Molina, H, 2000, A critical role for murine complement regulator Crry in fetomaternal tolerance, Science, v. 287, p. 498-501.

Xue, LY, Chiu, SM, Oleinick, NL, 2001, Photochemical destruction of the Bcl-2 oncoprotein during photodynamic therapy with the phthalocyanine photosensitizer Pc 4, Oncogene, v. 20, p. 3420-7.

Yamakawa, M, Yamada, K, Tsuge, T, Ohrui, H, Ogata, T, 1994, Protection of thyroid cancer cells by complement-regulatory factors, Cancer, v. 73, p. 2808-17.

Yamamoto, N., and S. Homma, 1991, Vitamin D3 binding protein (group-specific component) is a precursor for the macrophage-activating signal factor from lysophosphatidylcholine-treated lymphocytes: Proceedings of the National Academy of Sciences of the United States of America, v. 88, p. 8539-43.

Young, SD, Marshall, RS, Hill, RP, 1988, Hypoxia induces DNA overreplication and enhances metastatic potential of murine tumor cells, Proceedings of the National Academy of Sciences of the United States of America, v. 85, p. 9533-7.

Zeitouni, NC, Oseroff, AR, Shieh, S, 2003, Photodynamic therapy for nonmelanoma skin cancers. Current review and update, Molecular Immunology, v. 39, p. 1133-6.

Zhang, B, Hirahashi, J, Cullere, X, Mayadas, TN, 2003, Elucidation of molecular events leading to neutrophil apoptosis following phagocytosis: cross-talk between caspase 8, reactive oxygen species, and MAPK/ERK activation, Journal of Biological Chemistry, v. 278, p. 28443-54.

Zimmerman, BJ, Granger, DN, 1994, Mechanisms of reperfusion injury, American Journal of the Medical Sciences, v. 307, p. 284-92.

Zhou, W, Farrar, CA, Abe, K, Pratt, JR, Marsh, JE, Wang, Y, Stahl, GL, Sacks, SH, 1999, Predominant role for C5b-9 in renal ischemia/reperfusion injury, Journal of Clinical Investigation, v. 105, p. 1363-71.